

PALEOMAGNETIC STUDIES OF VOLCANIC ROCKS IN  
IRELAND, NEWFOUNDLAND AND LABRADOR

CENTRE FOR NEWFOUNDLAND STUDIES

**TOTAL OF 10 PAGES ONLY  
MAY BE XEROXED**

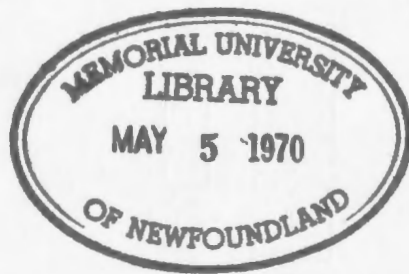
(Without Author's Permission)

CHAVALI R. SOMAYAJULU



205538

C.1





PALEOMAGNETIC STUDIES OF VOLCANIC ROCKS IN  
IRELAND, NEWFOUNDLAND AND LABRADOR

BY

CHAVALI R. SOMAYAJULU, M.Sc (Tech)

"Submitted in partial fulfilment of the  
requirements for the degree of Master of Science,  
Memorial University of Newfoundland,  
April, 1969".

## CONTENTS

ABSTRACT

CONTENTS

CHAPTER 1	INTRODUCTION	
1.1	Purpose and scope	1
1.2	Significance of paleomagnetic studies	1
1.3	Process of magnetization of rocks	5
1.4	Lower Paleozoic paleomagnetism	6
CHAPTER 2	GEOLOGY AND NATURAL REMANENT MAGNETISM OF THE KILLARY HARBOUR IGNIMBRITES	
2.1	Geological setting	8
2.2	Tectonics and petrology of the ignimbrites	8
2.3	Paleomagnetic sampling at Killary Harbour	12
2.4	Measurement of the natural remanent magnetization of the ignimbrites	13
2.5	Stability criteria in the present study	16
CHAPTER 3	ALTERNATING-FIELD DEMAGNETIZATION OF THE IGNIMBRITES	
3.1	Definitions of stability	18
3.2	Field and laboratory procedures for assessing stability	19
3.2.1	Field tests	20
3.2.2	Laboratory tests	20
3.3	Alternating-field demagnetization of the Killary Harbour ignimbrites	22
3.3.1	Pilot study	23
3.3.2	Systematic a.c. demagnetization	30

3.4	Separation of bands 3 and 4	39
3.4.1	Test for non-randomness	39
3.4.2	F-test for similar variances	41
3.4.3	F-test for significantly different band-directions	41
3.5	Application of the fold test	43
CHAPTER 4	DESIGN AND CALIBRATION OF THE THERMAL DEMAGNETIZATION UNIT	
4.1	Magnetic environment	47
4.2	Design of the thermal demagnetization unit	50
4.3	Description of the unit	52
4.3.1	The oven	52
4.3.2	The field nulling and control assemblies	52
4.3.3	Measurement of temperature	54
4.4	The fluxgate monitoring system	55
4.4.1	Nulling of helmholtz coil fields	58
4.4.2	Calibration of the fluxgate elements	58
4.5	Fluxgate survey of the oven area	59
4.6	Field monitoring outside the oven	63
4.7	Procedure for demagnetization	64
4.8	First test of the oven	67
4.9	Second test of the oven	87
CHAPTER 5	THERMAL DEMAGNETIZATION OF THE KILLARY HARBOUR IGNIMBRITES	
5.1	Introduction	94
5.2	Polished section study	95
5.3	Preliminary study of the ignimbrites	96

5.4	Extended demagnetization of the ignimbrites	105
5.5	Fold test	112
5.6	Comparison of alternating-field with thermal demagnetization	114
5.6.1	Comparison of pilot studies	114
5.6.2	Comparison of extended demagnetizations	117
5.6.3	Optimum demagnetization	118
5.7	The fold test and secular variation	120
5.8	Ordovician pole positions	121
CHAPTER 6	DEMAGNETIZATION STUDY OF SINGLE LAVAS FROM NEWFOUNDLAND AND LABRADOR	
6.1	Previous work	127
6.2	Geological setting	128
6.3	Earlier measurements of the Labrador basalts	131
6.4	The basalts from southern Labrador	133
6.4.1	Table Head	140
6.4.2	Henley Harbour	144
6.5	Cloud Mountain	150
APPENDIX 1	EXISTING APPARATUS	
A1.1	Astatic magnetometer	162
A1.2	Alternating-field demagnetization unit	162
APPENDIX 2	AUXILIARY EQUIPMENT FOR THERMAL DEMAGNETIZATION	
A2.1	Thermocouple	168
A2.2	Thermostat	168
A2.3	Thermal gradient measurement	173

APPENDIX 3	POLISHED SECTION STUDY OF KILLARY HARBOUR IGNIMBRITES AND BASALTS FROM NEWFOUNDLAND AND LABRADOR	177
APPENDIX 4	INITIAL NRM AND DEMAGNETIZATION MEASUREMENTS OF THE LABRADOR BASALTS	180
APPENDIX 5	MAGNETIC SHIELDING	184
	ACKNOWLEDGEMENTS	191
	REFERENCES	192

## ABSTRACT

Twenty-five samples from four bands of Ordovician ignimbrite exposed near Killary Harbour, Eire, were studied in detail, yielding strong evidence for magnetic stability: (1) At two collection sites, the natural remanent magnetization was significantly misaligned with the present field. At all three sites its direction was substantially stable against (2) a.c. demagnetizing fields up to 795 oe (peak), and (3) heating to 400-550°C; both treatments tended to reduce directional scatter. (4) A positive fold test suggests that the stable magnetization is primary. Assuming a "reversed" axial dipole field, a geographic north pole in the Pacific Ocean (9°N, 146°W;  $dp = 12^\circ$ ,  $dm = 22^\circ$ ) was calculated from the resultant of the four band mean directions relative to bedding planes, after a.c. treatment of all samples to 540 oe. Allowing for possible incomplete averaging of the secular variation, this result is compatible with the few published Ordovician poles relative to Europe.

An oven for stepwise demagnetization, used in the present study, was calibrated. Various tests showed that field-nulling errors would be within 50 -100 $\gamma$  during runs. Systematic directional errors from this cause can be greatly reduced by random specimen grouping.

Basalts from three Lower or Middle Paleozoic single flows in southern Labrador (Henley Harbour, Table Head), and at Cloud Mountain in northern Newfoundland, were thermally tested for stability. Like the Irish ignimbrites, these rocks tend to be highly oxidized, with hematite partly replacing the primary titanomagnetite. The three lavas showed comparable thermomagnetic behaviour, with blocking temperatures

mostly in a 100-200°C range below 450°C. Treatment to 350-450°C destroyed some secondary components, yielding new mean directions that were similar at the three sites, though with poor vector grouping. Being spot readings of the ancient field, these directions agree broadly with published directions from Lower Paleozoic rocks.

## CHAPTER 1

### INTRODUCTION

#### 1.1. Purpose and scope.

The subject of this thesis is a paleomagnetic investigation of some volcanic rocks in Ireland, Newfoundland and Labrador. Samples of Ordovician ignimbrites from western Eire have been subjected to systematic magnetic and thermal demagnetization and a fold test. Several stability criteria were satisfied, yielding a new, paleomagnetically useful result which is discussed with reference to some geophysical hypotheses. Samples from single basaltic lavas comprising one flow each at two sites on the southern Labrador coast and at one site on the Great Northern Peninsula of Newfoundland, were also tested for stability. These basalts, of Cambrian to Devonian age, were probably contemporaneous at the three sites, but since only single flows were exposed at any one site, the data in this case represents only spot readings of the ancient field and cannot be used for paleomagnetic interpretations. However, interesting results regarding the magnetic stability of these lavas were obtained and are compared with the results of the ignimbrite study. In the course of this investigation a thermal demagnetization unit was constructed and tested. A description of the furnace and associated equipment is given, along with an account of some experiments to estimate the errors associated with the thermal demagnetization technique.

#### 1.2. Significance of paleomagnetic studies.

During the last two decades paleomagnetic studies have been carried out on all continents in an attempt to shed light on certain

controversial geophysical hypotheses such as continental drift, expansion of the earth, and polar wandering. The word "paleomagnetism" means "ancient magnetism", but specifically it refers to the magnetic record acquired by certain rocks in ancient field at or since their time of formation. Ideally, the measurement of a vector remanent magnetization in rocks should provide evidence on (1) the direction of the Earth's magnetic field at one or more times during the history of the rocks; (2) the strength of the field in which the remanence was acquired.

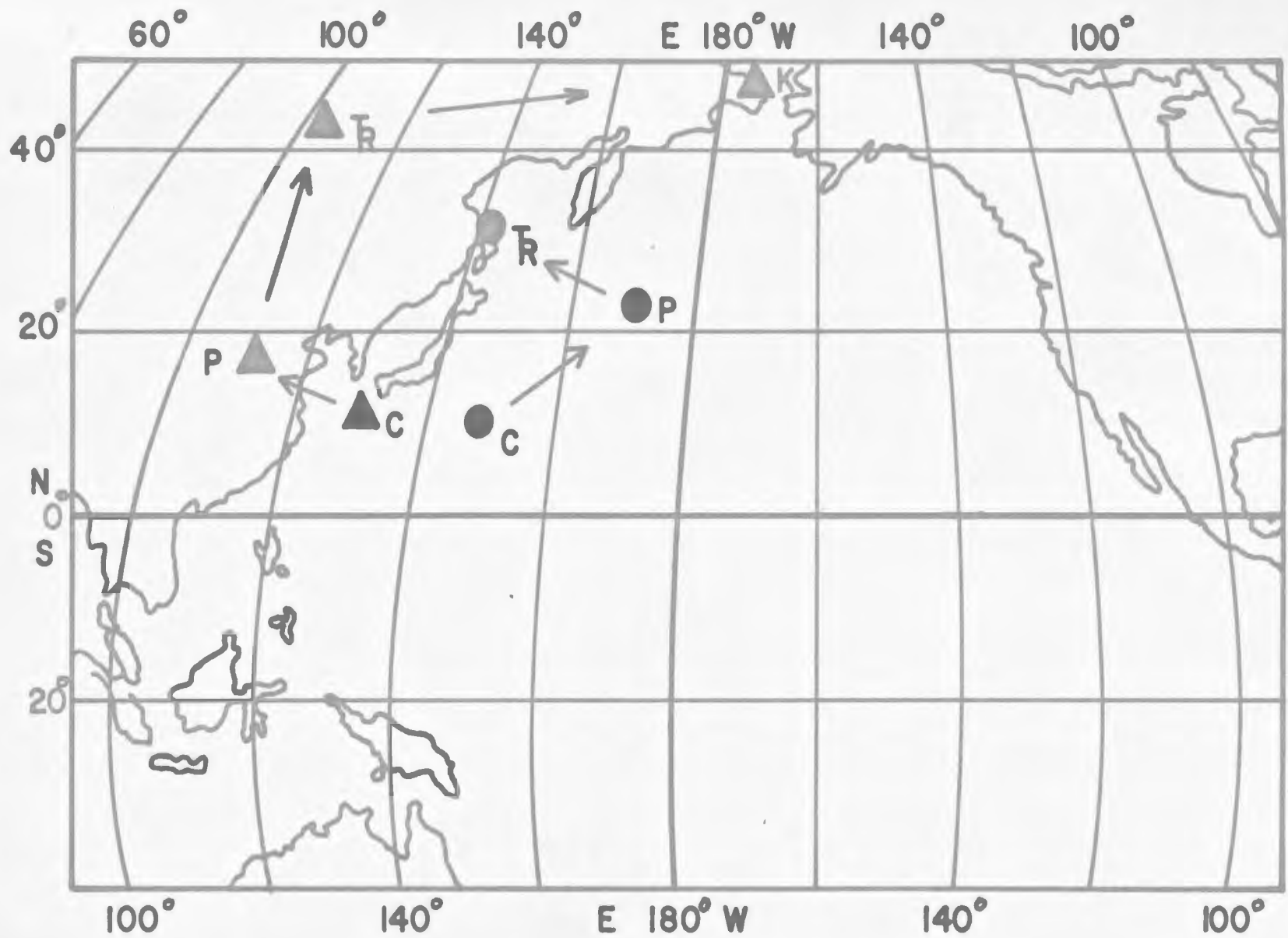
Directions of remanent magnetization obtained under (1) may be interpreted in terms of geographic coordinates under certain conditions. The most basic assumption is that the main geomagnetic field is, and has been in the geological past, dipolar and coaxial with the rotation axis of the earth when averaged over time spans of the order of the secular variation ( $10^3$  years). Recently, Hide (1967) has suggested that other deep seated mechanisms, with averaging time constants as large as  $10^5$ - $10^6$  years, may be important. Under favourable conditions, determination of the paleolocations of the pole is then capable of being used as evidence bearing on certain geophysical-geological hypotheses.

Continental drift, first seriously considered by Taylor (1910) and Wegener (1929), is defined as the horizontal displacement of parts of the Earth's crust relative to each other. Polar wandering may be defined as a shift of the Earth's crust as a whole relative to the poles, the spin axis remaining fixed in space. The possibility of an expanding Earth was studied by Egged (1956) who estimated that a mean increase in the circumference of 0.2-0.5 cm/year, would account for the amounts of heat flow energy, decrease in continental water level, and growth of the core, inferred from other evidence. Carey's (1958) and Heezen's (1960) estimates of mean expansion rate range from 0.5 to 4 cm/year, and are based on

world-wide tectonics, assumed growth of the ocean basins and divergence of the paleomagnetic polar wandering paths for different continents. Such large rates are ruled out by the result of certain paleomagnetic tests in which contemporaneous rocks at widely separated sites in a single land mass were compared. Cox and Doell (1961) and Ward (1963) concluded from such tests, with Permian and Devonian rocks, respectively, that expansion at Egyed's moderate rates could not be ruled out, but that larger rates are incompatible with the evidence.

Polar wandering, which would result in identical polar paths relative to all continents in the absence of relative crustal displacement, has not yet been found unambiguously in the evidence. Various authors, however, have interpreted the observed divergence of paleomagnetic polar paths for different land masses as being compatible with continental drift. An example is the postulated post-Paleozoic opening of the north Atlantic (Runcorn, 1965). Fig. 1.1 (Deutsch, 1969) based on the paleomagnetic literature until 1968, shows the inferred displacement of the north pole relative to North America and Europe between Carboniferous and Triassic periods. The westward displacement of the North American curve relative to the European one appears to be systematic, and the separation of the two Permian poles is compatible with a post-Permian opening of the North Atlantic (Wells and Verhoogen, 1967), about the pivot near the present north pole proposed by Bullard et al, (1965).

Some independent support for the conclusions from paleomagnetism favouring continental drift has come from paleoclimatology, e.g. the inferred Permo-Carboniferous glaciation of Gondwanaland (Holmes, 1965). Comparisons of the evidence from paleoclimatology and paleomagnetism



C. Carboniferous  
 P. Permian  
 T.R. Triassic  
 K. Cretaceous

▲ [Mean paleomagnetic] N. America  
 ● [North poles for] Europe

Fig. 1.1. Apparent polar wandering curves between N.America and Europe\*  
 (Adopted from Deutsch, 1969)

\* Excludes Iberian peninsula and Alps

(Blackett, 1956; 1961; Opdyke, 1962), show that these two lines of evidence in many cases are mutually compatible in supporting some relative movement of the continents.

Earlier episodes of continental drift have also been postulated. Thus, the existence of a "proto-Atlantic" during the early Paleozoic has been proposed by Wilson (1966), who suggests that this earlier ocean gradually closed during the Paleozoic, and reopened after the Paleozoic. While the paleomagnetism of late Paleozoic and younger rocks is relevant to the problem of the opening of the present Atlantic, a test of Wilson's hypotheses requires paleomagnetic data from middle Paleozoic and older rocks.

### 1.3. Process of Magnetization of rocks.

The acquisition of a remanent magnetization, in the direction of the ambient field by rocks cooling from high temperature was first reported by Melloni (1853). Königsberger (1930) introduced the concept of "thermoremanent magnetization" (TRM) in which an igneous rock may acquire a stable, and sometimes strong, magnetic moment parallel to a weak ambient field while cooling below the Curie points of its magnetic constituents.

On the other hand, "isothermal remanent magnetization" (IRM), is acquired at constant temperature in a steady magnetic field. McNish and Johnson (1938) proposed that a "remanent magnetization of sediments" or "detrital" or "depositional" remanent magnetization (DRM) is acquired when previously magnetized grains are deposited with a preferential alignment in the direction of the external field, e.g. while settling in

water. "Chemical remanent magnetization" (CRM), which can be acquired by the magnetic particles during their chemical change (e.g. reduction of  $\text{Fe}_2\text{O}_3$  to  $\text{Fe}_3\text{O}_4$ ) under the influence of a magnetic field, was first noticed by Maurain (1901). Rimbart (1956) has shown that the remanent magnetization of a rock can be modified isothermally by the action of a magnetic field for a sufficiently long period; this process is known as "viscous remanent magnetization" (VRM).

Remanence may be acquired by one of the above processes either at the time the rocks are formed ("primary" magnetization), or at a geologically significant time afterwards ("secondary" magnetization).

#### 1.4. Lower Paleozoic paleomagnetism.

Extensive, but far from exhaustive data are now available from paleomagnetic studies from all continents, representing much of the geological columns. Several authors, notably Cox and Doell (1960), and Irving (1964), have discussed the physical basis of rock magnetism in terms of its applicability to a description of the ancient geomagnetic field, and have summarized the published work leading to inferred pole positions for different geological periods and continents. However, Lower Paleozoic rocks have not yet been extensively studied, most of the existing results (Fig. 5.6) being based on preliminary studies made before methods of establishing magnetic stability had been sufficiently developed. If more data from suitable Lower Paleozoic lava exposures, and particularly, more paleomagnetic comparisons between adjacent sedimentary and volcanic formation of the same age were available, the evidence could be greatly strengthened. Unfortunately, most of the few

relatively reliable results for the Lower Paleozoic (e.g. Khranov et al, 1965; Rodionov, 1966; Roy et al, 1967) are based on sedimentary rocks.

The present investigation is concerned with igneous rocks, of which the Ordovician ignimbrites in Eire add a useful result to the literature from the Atlantic east coast. The single lavas from Labrador and Newfoundland proved to be only partially stable and in any case represent a time interval too short for paleomagnetic interpretation, but the knowledge gained from their study might be helpful in interpreting the results of future, more comprehensive work on Lower to Middle Paleozoic igneous and sedimentary rocks from the northwest coast of the Atlantic. One model to which Paleozoic data from that region would be applicable is the proposed anticlockwise rotation of Newfoundland (Wegener, 1928, p.79) to which further reference will be made in Chapter 6. A decisive paleomagnetic test of Wilson's (1966) paleogeography would require a substantial increase in the volume of evidence for the Lower to Middle Paleozoic interval, from both sides of the north Atlantic.

## CHAPTER 2

### GEOLOGY AND NATURAL REMANENT MAGNETISM OF THE

#### KILLARY HARBOUR IGNIMBRITES.

##### 2.1. Geological Setting.

The Lower Paleozoic stratigraphy of Central Murrisk, County Mayo, has been described by Dewey (1963). The ignimbrite exposures near Killary Harbour form part of the Mweelrea Group of the Partry Series which is underlain by the Glenummera Series of possible Llanvirn age (Table 2.1). The Partry Series underlies unconformably the Silurian Lower Owenduff Group, and hence the age of the ignimbrites is probably Middle to Upper Ordovician, possibly Caradocian. Six ignimbrite bands are interbedded with the grits of the Mweelrea Group, forming the Mweelrea syncline which can be traced in a roughly east-westerly direction for many miles with nearly zero plunge (Fig. 2.1). The six ignimbrite bands on the northern limb of the syncline have been correlated to the six bands on the southern limb by McKerrow and Campbell (1960), but Dewey (1963) regards this correlation as unjustified, because of a lack of diachronous behaviour. Bands 1 and 5 have been traced continuously over the total length of ignimbrite exposures while Band 2 thins eastward and disappears; this might be due to east-west tilting and erosion (Dewey, 1963).

##### 2.2. Tectonics and petrology of the ignimbrites:

Some characteristics of the ignimbrites are (Dewey, 1963): columnar and sheet jointing due to temperature and pressure effects; and decrease in grain size with increase in the content of disseminated magnetite. The samples collected are from both limbs of the Mweelrea

TABLE 2.1

Lower Paleozoic strata exposed in CentralMurrisk (after Dewey, 1963)

Period	Group or Formation	Thickness (ft.)	Series or Age
SILURIAN	Owenwee Group	2000	Croagh Patrick Series (Wenlock)
	Lough Nacorra Group	1500	
	Fiddaunarinnia Group	600	
	Oughty Group	360	
	Pollanoughty Group	450	
	////// UNCONFORMITY	//////	
ORDOVICIAN	Lower Owenduff Group	0-20	(Upper Llandovery)
	////// UNCONFORMITY	//////	
	Maumtrasna Group	8000	Partry Series
	Mweelrea Group	7000	(Caradocian ?)
		(4000)	Glenumma Series (Llanvirn ?)
	Derrylea Group	5000	Murrisk Series (Arenig)
Lug-gloss Formation	350		
Creggan Formation	1750		
Cuilmore Formation	650		
Lugacollivee Formation	5000		
Lugaloughan Formation	170		
Drummin Formation	250		

TABLE 2.1 (Continued)

Period	Group or Formation	Thickness (ft.)	Series or Age
Disconformity			
↓	Derrymore Group	1200	↑
	Letterbrock Group	800	Owenmore Series
			(Arenig) ↓

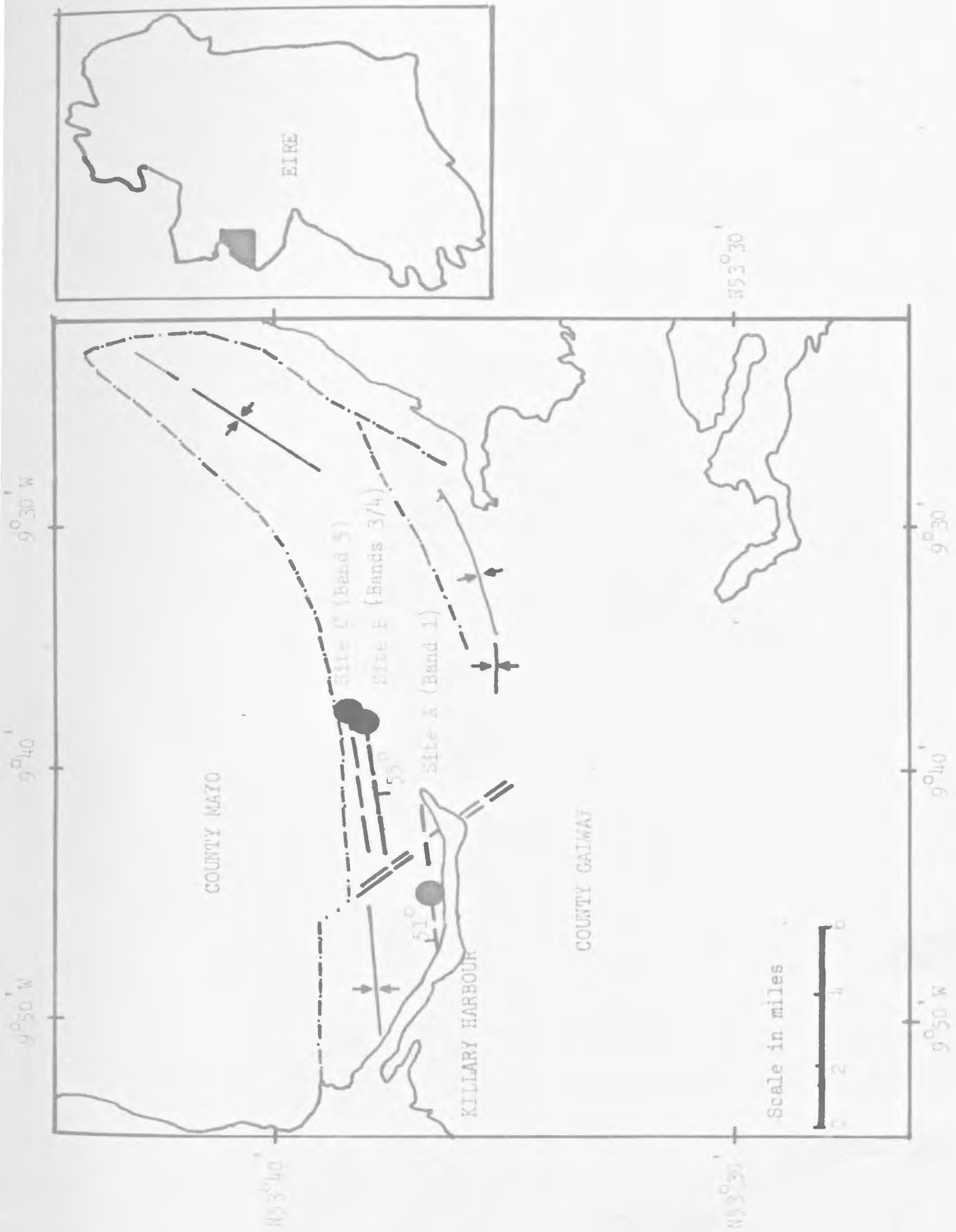


Fig 2.1 Location of ignimbrite sampling sites near Killary Harbour, Eire

syncline, the folding of which is considered by Dewey to be of pre-Llandovery age, and hence to predate the Silurian. He notes also that the beds have remained relatively undisturbed since they were folded into the syncline. Such a relatively simple tectonic history tends to simplify the paleomagnetic interpretation, and in the present case it permits the application of a fold test of magnetic stability (Graham, 1949).

Dr. N. D. Watkins of the Geology Department, Florida State University, has kindly examined polished sections from two of the ignimbrite samples. His study (Appendix 3) revealed that the original titanomagnetite is in the highest oxidation state (Index VI in the notation of Watkins and Haggerty, 1965; and Wilson and Watkins, 1967), as characterized by the presence of the high-temperature mineral Pseudobrookite. Considering the relatively undisturbed nature of the folds containing the ignimbrite bands, the oxidation might have plausibly occurred during a later stage of the same Ordovician igneous activity which produced the ignimbrites. In that case the Earth's field responsible for impressing a stable chemical remanent magnetization on the rock during oxidation would still be an "Ordovician" one.

### 2.3. Paleomagnetic sampling at Killary Harbour:

On petrological and tectonic grounds the ignimbrites thus promised to be useful for paleomagnetic study. Moreover, they represent a Lower Paleozoic igneous formation in Western Europe, an area from which few paleomagnetic results for that age have been reported, and apparently none at all relative to Ireland, from either igneous or sedimentary formations.

In the summer of 1965, 25 oriented hand samples of ignimbrite were collected by Professor E. R. Deutsch of Memorial University and Professor Marshall Kay of Columbia University, New York, at three sites near Killary Harbour (Deutsch, 1969). The lowest ignimbrite band, no. 1 (Fig. 2.1; Table 2.2), was sampled at Site A on the southern limb of the Wheelrearsyncline, while Sites B and C are on the northern limb, about 6 miles east of Site A. At Site B, Bands 3 and 4 are not necessarily distinct but possibly may be distinguishable by a thin zone of weathering (Dewey, 1963). Band 5 is exposed at Site C.

#### 2.4. Measurement of the natural remanent magnetization of the ignimbrites.

At the laboratory the 25 samples were cored and cut into a total of 80 cylindrical specimens of 2.2 cms diameter and about 1.8 cms mean height, giving just over 3 specimens per sample on the average. The natural remanent magnetization (NRM) of the rocks relative to the in-situ horizontal plane at the collection sites was measured in the laboratory with the astatic magnetometer of the Physics Department (Murty, 1966, Deutsch et al, 1967). This instrument has a reciprocal sensitivity of  $3.9 \times 10^{-7}$  oe/mm deflection at a scale distance of 1.8 m. The measurement of the direction and intensity of the NRM followed standard procedures described by several authors (Roy, 1967, Creer, 1967).

Table 3.2, column 4 shows that the intensity of the NRM (in  $\text{emu/cc} \times 10^{-6}$ ) is in the ranges 30 - 240 for samples from Sites A and B; and 10 - 70 for those from Site C. The NRM intensities of 21 additional specimens measured one year later (Table 5.2) were higher, with the ranges 50 - 740 at Sites A and B, and 20 - 130 at Site C (all in  $\text{emu/cc} \times 10^{-6}$ ).

TABLE 2.2

Sampling data at Killary Harbour, Eire.

Site	Location	Band	Sample Nos.	Strike*	Dip*	Limb of Syncline
A	53.6°N, 9.7°W	1	1-9	263°	50½°N	southern
B	53.6°N, 9.6°W	3-4	18-25	75°	55°S	northern
C	53.6°N, 9.6°W	5	10-17	75°	55°S	northern

\*Structural information at Site B and for the general area is due to Dewey (1963). Strike and Dip values at Sites A and C have been kindly supplied by Professor Marshall Kay of Columbia University, New York.

The vector mean directions for two specimens each from all 25 samples have been plotted in Fig. 3.2, and statistical data for the site mean directions are listed in Table 3.3. The vector mean directions, and statistical data for the 21 specimens measured later (Chapter 5) are shown in Fig. 5.2 and Table 5.3. The mean directions and Fisher statistics were obtained from an IBM 1620 computer program.

At Site A (mean declination,  $D = 138^\circ$ , mean inclination,  $I = -5^\circ$ ) the mean sample directions mostly make large angles with the 1965 Earth's field ( $D = 13^\circ\text{W}$ ,  $I = +68\frac{1}{2}^\circ$ ) and axial dipole field ( $D = 0^\circ$ ,  $I = +70^\circ$ ) relative to the sampling area. However, they show considerable scatter, with  $k = 2.2$ ,  $\alpha_{95} = 45.8^\circ$ , where  $k$  is the best estimate of the precision parameter and  $\alpha_{95}$  the radius of the 95% circle of the confidence (Fisher, 1953). For Site B, the sample directions are tightly clustered ( $k = 127$ ,  $\alpha_{95} = 4.9^\circ$ ), and the departure of the site mean direction from the present and axial dipole field directions is again significant, though less pronounced than at Site A. In terms of scattering of NRM directions, Site C is intermediate ( $k = 54.3$ ,  $\alpha_{95} = 7.6^\circ$ ) between Sites A and B, but the mean site direction is no longer significantly different from the present or axial dipole field directions.

After laboratory storage for about one year and remeasurement, some specimen directions had significantly changed, probably due to superposition of a VRM with short time constant. For N samples remeasured at each site the new mean directions and Fisher statistics were: (compare Table 3.3)

Site A:  $N = 3$ ,  $D = 154^\circ$ ,  $I = -4^\circ$ ,  $k = 5.1$ ,  $\alpha_{95} = 61.1^\circ$

Site B:  $N = 4$ ,  $D = 98^\circ$ ,  $I = +72^\circ$ ,  $k = 43.5$ ,  $\alpha_{95} = 14.1^\circ$

Site C:  $N = 4$ ,  $D = 39^\circ$ ,  $I = +75^\circ$ ,  $k = 59.0$ ,  $\alpha_{95} = 12.1^\circ$

## 2.5. Stability Criteria in the present study.

The large deviation of the mean direction at Site A from the present field and dipole field directions may be partly related to the small precision, since the presence of a "soft" VRM component in some of the samples tending to deflect the resultant direction towards the present field (notably samples KH 8, 9) can then be most effective in producing scatter of the sample directions. The mean directions at Site B also departs significantly from the present and dipole field directions, but, with relatively close alignment of individual directions. Hence the NRM results from the two sites indicate partial magnetic stability of the ignimbrites.

Alternative meaning of magnetic "stability" will be discussed in Section 3.1. In either case, the main purpose of stability testing in paleomagnetic applications is to isolate a primary component of magnetization from other components masking it; one assumes that the primary component was acquired during the formation of the rock or a geologically insignificant time afterwards by one of the processes described in Section 1.3. The direction of this primary magnetization may have remain unchanged, but the actual NRM direction tends to be the resultant of this primary component and one or more superposed secondary components that may be larger than the former and will probably differ in direction from it.

Since it was evident from the NRM study of the Killary Harbour ignimbrites that one cannot necessarily assume any one of the site mean directions of magnetization to be of primary origin (and hence

by implication to represent the original ambient field direction) it is important to carry out suitable laboratory or field techniques aimed at identifying the primary (presumed "stable") component through removal of secondary components. The laboratory and field techniques are summarized in Chapter 3.

CHAPTER 3ALTERNATING-FIELD DEMAGNETIZATIONOF THE ICNIMBRITES3.1. Definitions of stability.

The word "stable", as defined here, refers to a magnetization component acquired by the rock in the ambient Earth's field a geologically long time ago, and essentially unchanged in direction. Some authors prefer a narrower definition, equating "geologically long" with the total age of the rock, in which case any component added a significant time afterwards (by one of the processes described in Section 1.3) would be considered "unstable". However, such non-original components are frequently persistent in direction over long time intervals, i.e. "stable" in the broader sense. An example is the Devonian Old Red Sandstones of Britain, which are believed to have been remagnetized at the time of their deformation during the late Paleozoic, acquiring a very "hard" component that masks the original "Devonian" magnetization (Chamalaun, and Creer, 1964). "Hard" is related to "stable" as defined here, and refers to a spectral range of relatively large coercivities. Conversely, a "soft" (or "unstable") component is one of predominantly low coercivity and tends to decay with a low time constant. In turn the coercivity of a ferromagnetic constituent is a function of size and shape of the grains, their spontaneous magnetization, and the temperature range over which the magnetization was acquired.

Since in paleomagnetism the original (or "primary") magnetization direction is generally of greatest interest, the aim of most demagnetization procedures is to remove both "hard" and "soft" components that may have

been superimposed on a primary, stable magnetization. To recognize whether a particular stable component is of primary or secondary origin one must apply separate tests or criteria, usually of a geological nature.

Two empirical procedures for determining the stage at which a given demagnetization technique has achieved optimum effectiveness have been proposed:

- (1) As and Zijderveld (1958), and McElhinny and Gough (1963) use the criterion of rotation of the "vector magnetization". The direction corresponding to the step in the treatment at which the remanent magnetization vector ceases to change direction and continues to change only in magnitude is considered to be the "stable" direction, implying that the low-stability components have been removed.
- (2) Irving et al, (1961 a) compare the calculated dispersion in the magnetization directions of the specimens from a given site before and after every step in the treatment. The direction corresponding to that demagnetizing field or temperature for which the dispersion is minimum, is then considered to be the stable one.

The former method is more useful for the study of individual specimens, whereas the latter is preferable when vector groupings are being compared. In the present study, emphasis has been given to the second procedure (Irving et al, 1961 a).

### 3.2. Field and laboratory procedures for assessing stability.

Magnetic stability can be tested by field or laboratory tests, or a combination of both. Field tests have the advantage of being capable of relating a given magnetization to a specified geological

event, and hence of assigning time limits to its origin: this makes them potentially quite powerful. However, frequently and moreover they cannot separate secondary from primary components, for which purpose laboratory procedures are necessary.

### 3.2.1. Field tests.

Two classical field tests due to Graham (1949) are the 'conglomerate test' and the 'fold test'.

In the fold test, if the original ("pre-folding") direction of magnetization has not been significantly altered or masked after the rocks were folded, then a "correction" for geological tilt (i.e. referring the magnetization back to the original horizontal plane) should give better alignment between directions representing different parts of the structure, than in the absence of such a correction.

### 3.2.2. Laboratory tests.

Laboratory procedures include demagnetization by steady magnetic fields, and by heat treatment. The principle "magnetic" methods employ respectively steady and alternating fields. Steady-field methods were introduced by Johnson, Murphy and Torreson (1948) and have been favoured especially in Soviet laboratories (Petrova and Koroleva, 1959; Petrova, 1961; Lin'kova, 1961).

Thermal demagnetization procedures are based upon the addition law of partial thermoremanent magnetization (PTRM) (Nagata, 1961, p. 159), which is given by

$$\begin{array}{c}
 T_i = T_c \\
 \left. \begin{array}{l} \text{---} \\ \text{---} \end{array} \right\} J_{T_i}^{T_{i-1}} \\
 T_{i-1} = T_o
 \end{array}
 H_{ex}(T_o) = J_{T_c}^{T_o} H_{ex}(T_o) \dots (3.2.1)$$

where  $T_{i-1} < T_i < T_c$ , and  $i = 1 \dots n$  designates the number of temperature intervals,  $H_{ex}$  is the external field present during cooling between the temperature interval  $T_i$  and  $T_{i-1}$ . The PTRM produced by weak-field cooling through the range  $(T_2 - T_1)$  is independent of the magnetization acquired while the specimen cools through other temperature intervals. Hence all the temperature ranges have a "memory" given by the addition law, which can be removed by heating to the higher temperature of the appropriate interval, and cooling in zero field. Two procedures are in general use:

(i) In the stepwise method, the specimens are heated to a specified temperature  $T_1 < T_c$  (where  $T_c$  is the highest Curie point among the constituent minerals in the rock), and then cooled in field-free space. After remeasurement, they are reheated to a temperature  $T_2$ , where  $T_1 < T_2 < T_c$ , and the procedure is repeated until any undesirable components are considered to have been removed.

(ii) An alternative method is "continuous demagnetization", in which the direction and intensity of the remanence is measured at specified temperature intervals while the specimen is being heated or cooled in an oven placed under the magnetometer. This procedure yields a complete demagnetization curve, with smaller risk that a chemical change occurring prior to measurement will be undetected than in the stepwise method. Stepwise demagnetization is faster since several specimens can be treated at a time, but this advantage is partly offset by the need to extend effective field-nulling to a correspondingly larger specimen-occupied region than during continuous demagnetization of a single specimen.

Thermal demagnetization methods were introduced by Thellier (1938); have since been developed further (Wilson, 1962; Wilson and Everitt, 1963; Chamalaun, 1963, 1964; Chamalaun and Creer, 1964; Irving et al, 1961 b; and others); and are widely used. Their main advantage over "magnetic" treatments is that two or more "hard" components having different Curie points may be separated due to the addition properties of the PTRM's.

In alternating-field demagnetization, the specimen is subjected to progressively higher peak fields that are smoothly reduced to zero during each step in the treatment. In this way, increasingly "harder" magnetization components are removed, leaving intact those having the largest coercivities; additional criteria might indicate whether this residual is furthermore likely to represent the primary magnetization. In common practice, the specimen is "tumbled" simultaneously about two or more axes to ensure effective randomization of magnetization directions. A major advantage over thermal demagnetization (above) is that no chemical alteration of specimens during treatment is involved.

Alternating-field demagnetization was introduced by Thellier and Rimbart (1955) for paleomagnetic work and later successfully employed by Brynjolfsson (1957); As and Zijdeveld (1958); Creer (1959); Irving et al, (1961 a); Doell and Cox (1964); McElhinny (1966); and others.

### 3.3. Alternating-field demagnetization of the Killary Harbour ignimbrites

In the present study, the first stability treatment was by alternating field demagnetization, using the unit in the Physics Department (Pearce, 1967). In this device the specimen tumbles about three

axes simultaneously, an arrangement tending to reduce significant spurious and anhysteretic magnetization components compared with two-axes tumbling. For other details of this unit see Appendix 1.2.

To determine the optimum demagnetizing field for removing secondary components, it is often useful to carry out a detailed, initial demagnetization of a few representative specimens only; this removes the need for intermediate steps in any subsequent systematic treatment that may involve all samples. Such a "pilot" study was carried out with five ignimbrite specimens selected from the three sites near Killary Harbour, using the "vector rotation" criterion to determine the optimum field (Section 3.1). Results are shown in Table 3.1 and Fig. 3.1, and discussed below.

### 3.3.1. Pilot study.

#### Site A: Specimen KH 2bI.

The NRM direction which differed by a large angle from the present field, hardly changed during the eleven demagnetization steps up to 560 oe (peak); at the same time the intensity of magnetization progressively decreased (Table 3.1). This behaviour suggests that the direction at 560 oe represents a stable component possibly of primary origin. Beyond 560 oe the direction of the vector changes through larger angles, but the large intensity increase after the last step may be due to the acquisition of a spurious magnetization.

#### Specimen KH 8a.

Though this specimen is from the same band (no.1) as KH 2bI, the NRM direction is not far from those of the 1965 field in western

Ireland ( $D = 347^\circ$ ,  $I = +68\frac{1}{2}^\circ$ ) and the axial dipole field ( $0^\circ$ ,  $+70^\circ$ ).

As demagnetization progressed, a substantial, systematic change in the direction occurred in quite low fields, accompanied at first by a sharp intensity increase to 25 oe, followed by an even sharper drop that levelled off below 100 oe. This suggests that a relatively "soft" VRM component, which might have been acquired fairly recently (perhaps even in the laboratory) has been removed. Above 100 oe, further steps in the treatment brought the directions progressively closer to the "stable" direction characteristic of specimen KH 2bI, until the two directions became nearly parallel after 560 oe. This is expected in specimens from the same band, and the conclusion that the high-field direction in specimen KH 2bI probably represents a stable (possibly primary) magnetization is thereby strengthened.

Site B: Specimen KH 25aII

The NRM is significantly different from the present field (though by a relatively small angle), suggests at least partial stability. With increasing fields the intensity decreased smoothly without erratic behaviour. No systematic change in directions occurred assuming that the D and I values for 560 oe (Table 3.1) resulted from a measurement error or a spurious magnetization picked up in the laboratory.

Site C: Specimen KH 13a

The NRM direction is close to the 1965 field and axial dipole field, and the directions remain relatively undisturbed, except for the anomalous values after the 515 oe and 670-695 oe steps. These results indicate that the magnetization is stable but was not necessarily

TABLE 3.1

Pilot alternating-field demagnetization of ignimbritespecimens from Killary Harbour

$\tilde{H}$ , demagnetizing field (oersteds, peak); D, declination (degrees taken clockwise from north through 360°); I, inclination (degrees, + indicates north pole in the lower hemisphere); J, intensity of magnetization (emu/cc):

<u>Specimen KH 2bI</u>				<u>KH 8a</u>			
$\tilde{H}$	D	I	Jx10 <sup>-6</sup>	$\tilde{H}$	D	I	Jx10 <sup>-6</sup>
0	120	-15	60.6	0	171	81	115
25	114	-16	62.7	25	123	77	179
50	118	-16	61.3	50	123	45	64.3
100	120	-15	64.7	100	123	28	54.5
150	119	-15	58.6	150	134	9	56.2
230	120	-15	55.2	230	128	11	52.9
260	119	-14	50.6	260	129	3	46.0
310	118	-14	45.0	310	139	13	44.9
360	118	-15	40.2	360	132	-1	43.4
410	121	-12	31.8	410	131	-11	-
515	114	-12	23.2	515	145	-11	32.7
560	119	-13	13.9	560	107	-6	22.9
670	120	-4	15.9	675	110	2	18.4
795	102	7	86.3	795	135	-17	40.1

TABLE 3.1 (Continued)

<u>KH 25aII</u>				<u>KH 13a</u>			
$\tilde{H}$	D	I	$J \times 10^{-6}$	$\tilde{H}$	D	I	$J \times 10^{-6}$
0	81	67	155	0	327	77	39.5
25	77	59	154	25	342	64	31.4
50	85	60	136	50	358	69	23.3
100	95	54	129	100	337	56	14.2
150	87	56	120	150	333	64	9.9
230	91	55	107	230	316	64	8.9
260	86	53	103	260	332	57	12.9
310	91	54	91.6	310	327	83	8.1
360	85	58	80.2	360	306	66	8.5
410	74	45	71.5	410	325	56	5.0
515	89	58	60.4	515	228	30	13.7
540	177	45	40.3	560	312	65	9.4
670	86	67	43.2	670	50	-9	6.5
770	81	54	23.8	770	320	61	9.2

TABLE 3.1 (Continued)

---

KH 16b			
$\tilde{H}$	D	I	$J \times 10^{-6}$
0	50	71	28.6
25	36	65	25.9
50	42	73	22.4
100	42	64	21.7
150	27	66	21.0
230	33	70	20.0
260	41	63	20.4
310	36	64	19.6
360	18	71	19.4
410	37	65	18.5
515	38	70	18.9
560	14	73	19.8
670	45	60	19.4
795	21	72	17.7

---

Caption for Fig 3.1.

Fig 3.1. Pilot alternating field demagnetization of ignimbrite specimens from Killary Harbour

Directions are plotted on an equal area net, with numbers indicating demagnetizing fields

H, demagnetizing field (peak oersteds)

$J/J_n$ , normalized intensity of magnetization ( $J_n$  is J at NRM)

Site A, Band 1

- north pole in lower hemisphere
- north pole in upper hemisphere

Site B, Bands 3/4;

- ▲ north pole in lower hemisphere
- △ north pole in upper hemisphere

Site C, Band 5;

- X north pole in lower hemisphere
- ⊗ north pole in upper hemisphere
- ⊙ Axial dipole direction
- ⊕ Present field at site

Dotted circles designate area confining directions during indicated steps in the treatment

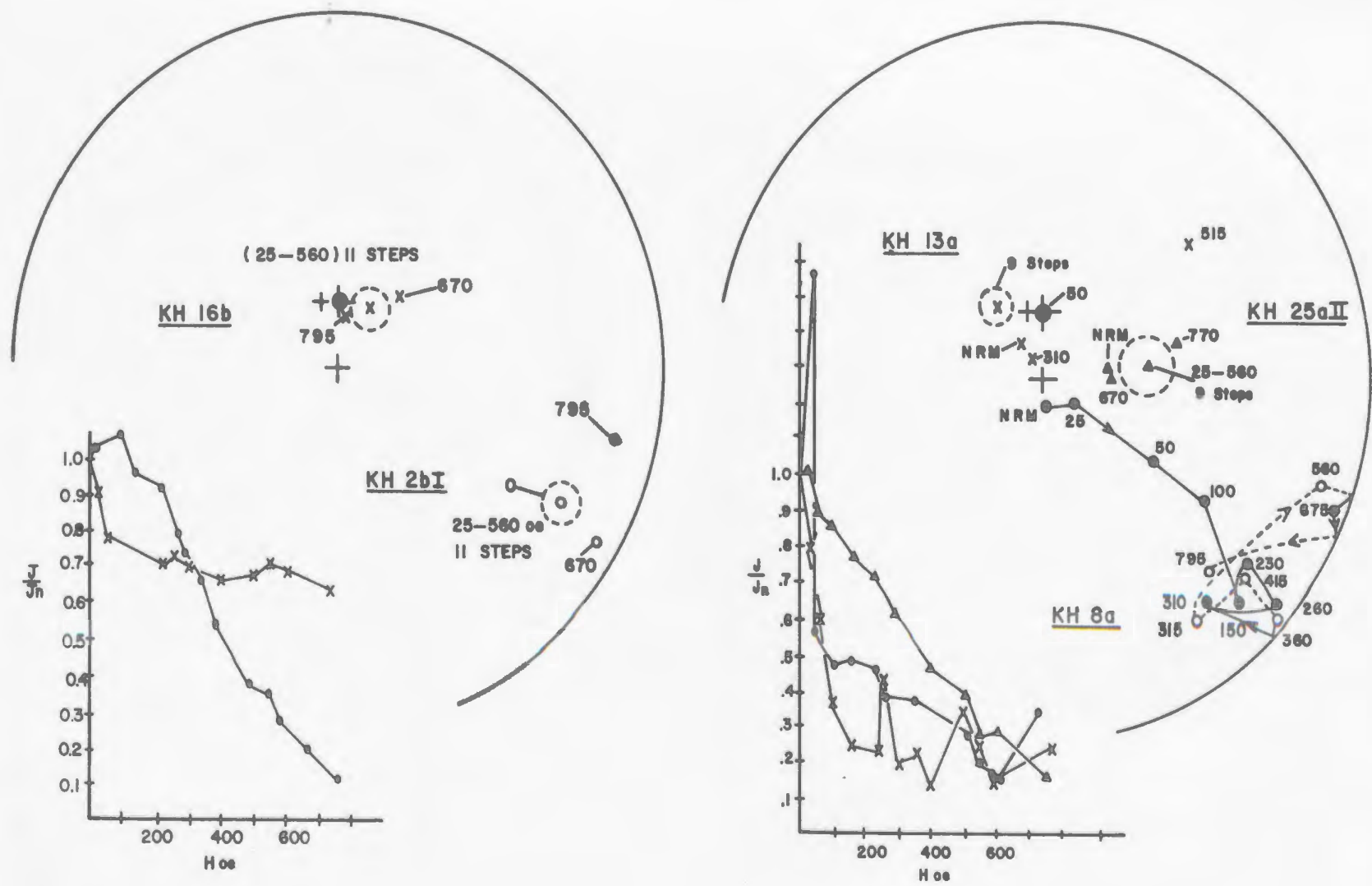


Fig 3.1. Pilot alternating-field demagnetization of ignimbrite specimens from Killary Harbour

acquired prior to folding, in view of its proximity to the dipole and 1965 field directions. Hence any separate test for demonstrating its primary origin will have to be especially rigorous. The intensity dropped quite sharply until 150 oe, which could be due to removal of a viscous component.

#### Specimen KH 16b

The NRM is again fairly close to the present field direction, and the treatment causes little change in direction and only a modest decrease in intensity, leaving 60% of the original intensity after the final step. These results indicate that the magnetization of KH 16b is harder than that of the other four pilot specimens. As in the previous case, the direction remains close to the axial dipole and present field directions, necessitating the same caution in assuming that the magnetization is primary.

#### 3.3.2. Systematic a.c. demagnetization.

The directions of magnetization of all five pilot specimens seem to have been stabilized after the 410 oe step. At 310 oe the viscous component has not been entirely removed from specimen KH 8c, whereas above 700 oe some specimens show erratic behaviour. Hence for a systematic treatment the following demagnetizing fields were chosen: (i) a low field, 310 oe; (ii) a high field, 770 oe; (iii) a field, 540 oe, having the mean value between (i) and (ii). The pilot study results suggest that demagnetization at 540 oe constitutes the optimum step compared to 310 oe, 770 oe, or the NRM itself, and this is further discussed below on the basis of the results of systematic demagnetization.

Two specimens from each of the 25 samples were demagnetized with results shown in Table 3.2 and Fig. 3.2. Table 3.3 lists the site average directions, with Fisher (1953) statistics, which were obtained from an IBM 1620 computer program values for  $k$ , the best estimate of the precision parameter, show that demagnetization greatly improves the grouping for Site A, with maximum precision at 540 oe, though the precision maxima for Sites B and C conform to the NRM. At both sites, the precision values change very little between 310 and 540 oe, and remain well above the  $k$  values for Site A. Demagnetization to 770 oe has scattered the magnetizations at all sites. No large changes of mean site directions occur throughout the treatment, indicating the presence of a prominent, stable component in the NRM. This tends to make it difficult to decide upon the optimum demagnetization step (Irving, 1964, P. 89). One possibility would be to adopt different steps corresponding to  $k$  maxima for different sites, i.e. 540 oe for Site A, and NRM for B and C. This would be undesirable, however, since the magnetic petrology and the history of the various ignimbrite bands is probably quite similar (see also Section 5.6.2.). Moreover, it is important to note that the Site A resultant directions tend to be far from the present field, causing  $k$  to increase upon the removal of a VRM directed close to the present field, whereas the converse effect in the case of Sites B and C (i.e. increased scatter after treatment) could again be due to the removal of such a VRM, since the mean directions at these sites are much closer to the present field. Hence the 540 oe step is likely to have led to somewhat more stable directions than found in the NRM, even at all three Sites. For this reason the mean

TABLE 3.2

Systematic a.c. demagnetization of theKillary Harbour ignimbrite

Symbols and units are as shown in 3.1

(\* indicates that no measurement was made)

Site A, Band 1, Samples KH1-9

Specimen	D	NRM		$\bar{H} = 310 \text{ oe}$			540 oe			770 oe		
		I	$J \times 10^{-6}$	D	I	$J \times 10^{-6}$	D	I	$J \times 10^{-6}$	D	I	$J \times 10^{-6}$
KH 1a	8	-4	139	133	+17	43.0	104	+25	26.2	98	+40	35.6
1b	2	+13	83.9	118	-16	12.8	134	+9	22.6	113	+40	22.1
2aI	134	-14	*	135	-8	*	136	+16	*	123	-9	15.6
2bI	120	-15	60.6	118	-14	44.9	119	-13	13.8	102	+7	86.2
3a	129	-31	66.2	147	-26	50.1	134	-22	20.2	109	-4	13.4
3b	114	-29	63.4	119	-24	44.8	112	-15	19.5	91	0	11.9
4a	145	-38	89.1	163	-39	32.4	168	-15	15.4	*	*	*
4b	145	-47	137	151	-59	41.7	148	-19	55.5	103	-2	13.4
5b	129	-25	40.9	128	-25	29.9	136	-15	16.4	103	+5	5.9
5d	129	-25	37.0	135	-26	28.6	126	-26	14.8	92	-17	5.1
6aI	150	+1	*	145	+43	*	168	+43	43.9	175	+45	112
6bII	180	-5	42.0	175	+39	26.0	141	+5	22.9	216	-44	30.1
7aI	179	-24	47.6	157	-27	37.2	170	-19	19.9	151	+9	12.5
7bI	173	-22	34.6	156	-37	19.1	175	-17	15.0	146	+10	14.1
8a	171	+81	116	139	+13	44.9	107	-6	22.9	135	-17	40.1
8b	120	+54	103	106	+15	*	108	+24	25.4	29	+8	31.5
9a	169	+43	55.7	137	-10	48.2	128	-3	22.8	275	-18	19.3
9b	151	+51	62.7	147	-30	38.2	178	-25	16.4	138	+32	43.4

TABLE 3.2 (Continued)

## Site B, Bands 3/4, Samples KH 18-25

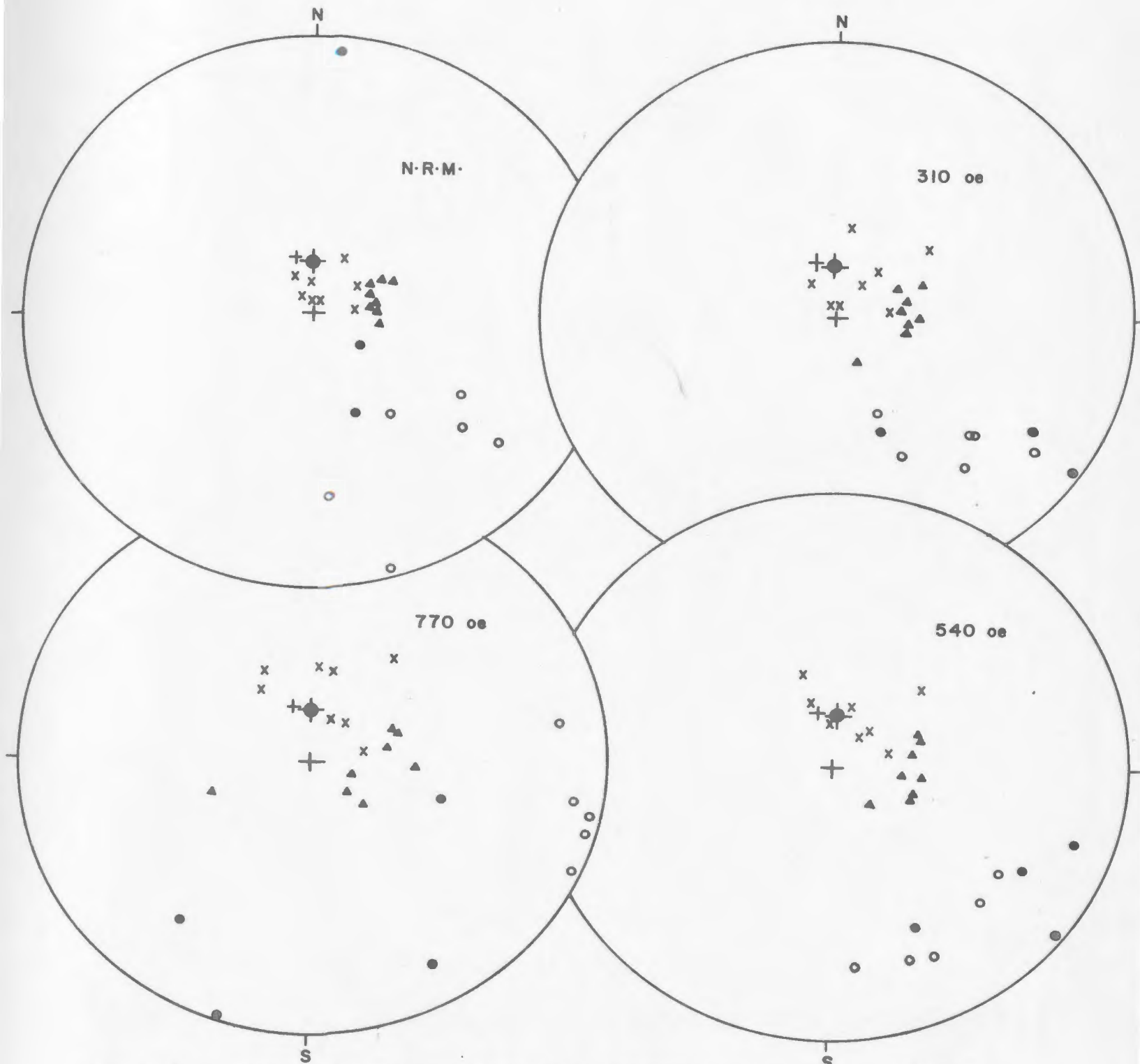
Specimen	D	NRM		$\tilde{H} = 310 \text{ oe}$			540 oe			770 oe		
		I	$J \times 10^{-6}$	D	I	$J \times 10^{-6}$	D	I	$J \times 10^{-6}$	D	I	$J \times 10^{-6}$
<u>Band 3:</u>												
KH 21aI	88	63	204	82	64	131	93	64	74.9	123	73	33.7
21bII	97	68	223	91	65	118	101	65	65.9	97	70	57.9
22aI	81	69	194	86	65	118	103	55	54.0	88	81	178
22b	91	63	201	106	61	122	115	57	80.1	142	58	40.9
23aI	99	65	209	99	64	121	113	64	75.5	138	56	39.7
23bII	109	64	238	109	58	143	105	49	73.4	116	69	52.1
24aII	44	63	172	129	71	102	130	65	39.4	253	46	26.9
24cI	85	67	216	174	64	121	146	74	65.7	243	58	53.9
<u>Band 4:</u>												
KH 18a	71	58	119	73	55	95.7	75	56	68.8	75	53	54.6
18b	67	58	122	63	55	103	68	57	70.0	67	58	63.9
19a	70	68	68.6	81	62	62.0	73	61	61.9	73	62	59.6
19b	73	69	46.8	78	63	39.8	84	58	39.5	81	58	40.6
20b	66	65	156	67	62	121	65	58	85.6	68	56	64.7
20cII	65	59	146	63	61	117	64	57	84.2	65	57	73.6
25aI	81	67	155	91	54	91.6	90	58	40.3	81	54	23.7
25bI	93	68	163	97	62	101	101	55	64.3	100	47	46.7

TABLE 3.2 (Continued)

(\* indicates that no measurement was made)

## Site C, Band 5, Samples 10 - 17

Specimen	NRM			$\tilde{H} = 310 \text{ oe}$			540 oe			770 oe		
	D	I	$J \times 10^{-6}$	D	I	$J \times 10^{-6}$	D	I	$J \times 10^{-6}$	D	I	$J \times 10^{-6}$
KH 10a	351	85	16.1	34	76	10.2	40	73	5.2	25	74	3.6
10bI	24	86	19.8	40	73	10.3	34	76	6.1	16	73	5.2
11b	27	63	13.1	45	47	8.8	42	37	7.4	37	41	5.3
11c	29	71	11.5	60	48	5.9	49	53	4.9	30	41	4.6
12aII	358	75	23.6	18	64	7.7	357	66	4.8	328	64	4.5
12b	356	81	24.8	4	45	4.2	334	38	8.8	340	34	3.6
13a	327	78	39.4	328	83	8.1	312	65	9.4	320	61	9.2
13b	337	68	37.7	322	67	11.3	0	56	9.4	328	51	9.5
14a	315	85	22.7	*	*	*	3	81	6.3	359	53	7.4
14c	324	81	19.0	3	82	7.5	349	64	5.5	6	51	6.4
15aII	91	74	51.3	77	68	42.7	73	66	38.4	82	67	39.3
15b	85	76	52.2	74	70	44.3	68	70	40.9	75	73	44.7
16b	51	71	31.9	36	64	19.6	14	73	19.8	21	72	17.6
16c	72	74	27.6	51	69	18.0	59	61	17.5	54	68	18.5
17a	37	84	31.6	26	82	9.9	357	64	6.6	25	32	4.6
17b	312	89	70.8	288	83	7.9	24	65	10.4	11	55	6.1



**Fig 3.2. Systematic alternating-field demagnetization of the Killary Harbour ignimbrites**

Equal area projection of mean directions of magnetization of 25 samples (2 specimens averaged per sample) for NRM and after demagnetization at 310, 540, and 770 oe (peak).

(All symbols as in Figure 3.1)

TABLE 3.3

Mean site magnetization of the Killary Harbour ignimbrites  
after stepwise demagnetization.

Site	Band	$\tilde{H}$ (oe, peak)	$\bar{D}$	$\bar{I}$	N	R	k	$\alpha_{95}$
A	1	0	138	-5	9	5.3964	2.2	45.8
B	3/4	0	79	+65	8	7.9449	127	4.9
C	5	0	23	+80	8	7.8711	54.3	7.6
A	1	310	136	-14	9	7.9189	7.4	20.4
B	3/4	310	89	+63	8	7.8309	41.4	8.7
C	5	310	32	+72	8	7.6698	21.2	12.3
A	1	540	137	-5	9	8.0698	8.6	18.2
B	3/4	540	93	+61	8	7.8431	44.6	8.4
C	5	540	18	+67	8	7.6667	21.0	12.3
A	1	770	123	+7	9	6.4194	3.1	35.2
B	3/4	770	97	+69	8	7.3000	10.0	18.4
C	5	770	9	+62	8	7.5484	15.5	14.5

TABLE 3.3 (Continued)

$\tilde{H}$	demagnetizing field
$\bar{D}$	mean declination at the site
$\bar{I}$	mean inclination at the site (+ denotes north pole in lower hemisphere)
N	number of samples averaged
k	best estimate of the precision parameter
$\alpha_{95}$	radius of 95% cone of confidence
R	magnitude of resultant of the N unit vectors

Directions are relative to the present horizontal plane.

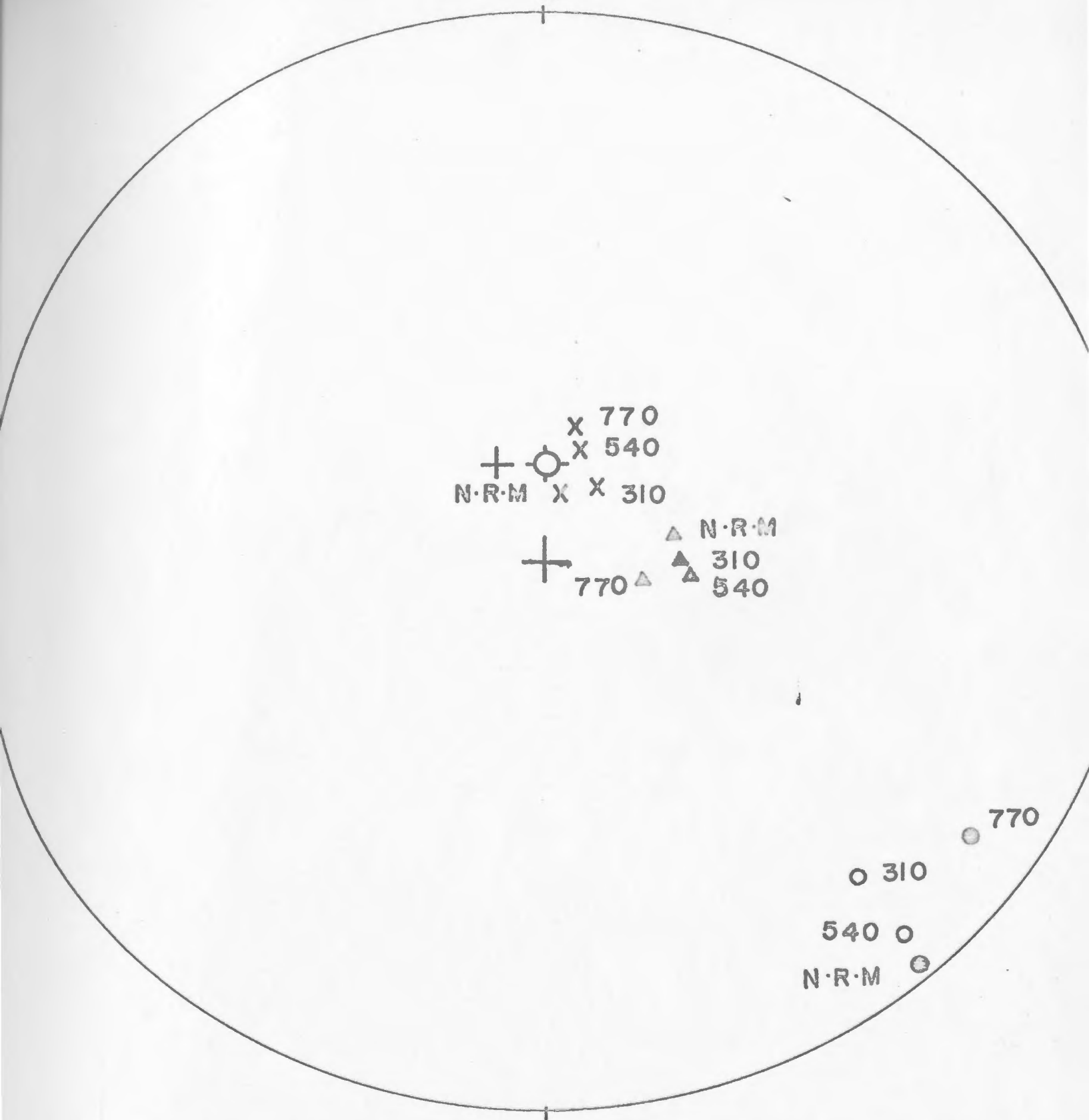


Fig 3.4. Mean directions of magnetization at the three Killary Harbour sites for NRM and after 3 steps of alternating field demagnetization, relative to the present horizontal plane  
 Numbers refer to the demagnetizing field (oe, peak)

(All symbols as in Fig 3.1)

directions and Fisher statistics corresponding to the 540 or step have been adopted as representative in all cases.

#### 3.4. Separation of Bands 3 and 4

On the southern limb of the Mweelrea syncline, ignimbrite Bands 3 and 4 are clearly distinct, whereas this is not the case on the northern limb, where Stanton (1960) suggests that Band 4 is absent. Dewey (1963), however, finds Stanton's 'Band 3' to be composite, a 3 to 4 inch weathering zone separating a 2-foot 'upper unit' (Band 4 ?) from the underlying Band 3 in a combined band thickness of 25 feet. He regards the time interval represented by the weathering to be 'considerable'; hence if Bands 3 and 4 are really distinct at Site B, their mean directions of magnetization may be significantly different as a result of secular variation.

To test this statistically, the 8 samples from Site B were divided into two groups of 4 samples each, Samples KH21-24 being from Dewey's 'lower unit' (Band 3), and KH 18-20 and 25 from the 'upper unit' (i.e. either Band 3 or 4). A variance-ratio test may then be used to determine whether the mean directions of the two populations are significantly different with a given probability.

##### 3.4.1. Test for non-randomness

An initial step was to test, for the single and combined bands, the hypothesis that the  $N$  given vectors are from an isotropic population. In Table 3.4,  $R$  is the magnitude of the resultant of the  $N$  unit vectors, and  $(R_0)_{.01}$  is the limiting value of the resultant vector for an isotropic population at 99% probability level (Stephens, 1964). The hypothesis of

TABLE 3.4

Statistical data on ignimbrite Bands 3 and 4 at Site B, Killary Harbour.

Band	Treatment	$\bar{D}$	$\bar{I}$	N	k	R	$(R_0)_{.01}$	$R/R_0$	$\bar{\delta}^2$
3	NRM	86.5	+66.0	4	131	3.9771	3.490	1.1396	0.0153
4	NRM	72.1	+64.0	4	163	3.9816	3.490	1.1408	0.0123
3+4	NRM	78.9	+65.2	8	127	7.9449	5.263	1.5096	0.0157
3	540	110.6	+61.9	4	72.1	3.9584	3.490	1.1343	0.0277
4	540	77.0	+57.5	4	120	3.9750	3.490	1.1389	0.0167
3+4	540	92.5	60.8	8	44.6	7.8431	5.263	1.4903	0.0448

$(R_0)_{.01}$  = limiting value of the resultant vector for an isotropic population at 99% probability level  
(Stephen, 1964).

$\bar{\delta}^2$  = estimate of population variance

(Other symbols as in Table 3.3)

an isotropic (i.e. random) population may then be rejected with the specified probability when  $R > R_0$ . The data in Table 3.4 show that this is so (i.e. the vector distributions are non-random) with greater than 99% probability in all cases, both for NRM and after 540 oe treatment.

### 3.4.2. F-test for similar variances

To apply the "F-test" for determining whether the two bands are significantly different (Section 3.4.3, below) one must assume that the dispersions  $\bar{\delta}_1^2$  and  $\bar{\delta}_2^2$ , for the presumed different bands are approximately equal (Larochelle, 1967). To test this assumption, one compares the dispersion ratio with tabulated values of the "F-ratio",  $F_{2(N_1 - 1), 2(N_2 - 1), \alpha}$ , where  $N_1$  and  $N_2$  are the number of samples per band and  $\alpha$  is the probability level. The variances are taken to be approximately equal when (for  $\bar{\delta}_1^2 \geq \bar{\delta}_2^2$ )

$$\frac{\bar{\delta}_1^2}{\bar{\delta}_2^2} \leq F_{2(N_1 - 1), 2(N_2 - 1), \alpha} \quad (3.4.1)$$

The results in Table 3.5 show that the assumption of approximately equal variances is justified at the 99% and 95% levels, both for NRM and after 540 oe treatment.

### 3.4.3. F-test for significantly different band-directions

"Between-band" and "within-band" variances are defined by (Watson, 1956, Larochelle, 1967):

$$\bar{\delta}_b^2 = \frac{2(\Sigma R_i - R)}{B-1} \quad \text{and} \quad \bar{\delta}_w^2 = \frac{2(N - \Sigma R_i)}{N-B} \quad (3.4.2)$$

TABLE 3.5

Separation of ignimbrite Bands 3 and 4 at Site B

Treatment	$\frac{\bar{\delta}_1^{-2}}{\bar{\delta}_2^{-2}}$	$F_{6,6,.01}$	$F_{6,6,.05}$	$\bar{\delta}_b^{-2}$	$\bar{\delta}_w^{-2}$	$\frac{\bar{\delta}_b^{-2}}{\bar{\delta}_w^{-2}}$	$F_{2,12,.01}$	$F_{2,12,.05}$
NRM	1.24	8.47	4.28	0.0258	0.0139	1.86	6.93	3.89
540 oe	1.66	8.47	4.28	0.1806	0.0222	8.13	6.93	3.89

$\bar{\delta}_1^{-2}, \bar{\delta}_2^{-2}$  = dispersion,  $\bar{\delta}^{-2}$ , for Bands 3 and 4, respectively (Table 3.4, last column)

$F_{6,6,.01}, F_{6,6,.05}$  = F-ratio,  $F_{2(N_1 - 1), 2(N_2 - 1), \alpha}$ , for  $N_1 = N_2 = 4$  samples at Bands 3 and 4, respectively, and at 99% and 95% probability levels.

$\bar{\delta}_b^{-2}, \bar{\delta}_w^{-2}$  = between-band and within-band dispersion.

$F_{2,12,.01}, F_{2,12,.05}$  = F-ratio,  $F_{2(B - 1), 2(N - B), \alpha}$ , for  $B = 2$  bands,  $N = N_1 + N_2 = 8$  samples, and at 99% and 95% probability levels.

where  $R_i$  and  $R$  are the magnitudes of the unit vector resultants for the  $i^{\text{th}}$  band and the  $N(=8)$  samples, respectively, and  $B$  is the number of Bands (2). Then if

$$\frac{\bar{\delta}_b^2}{\bar{\delta}_w^2} \leq F_{2(B-1), 2(N-B), \alpha} \quad (3.4.3)$$

it may be concluded that the mean directions of the  $B$  groups are not significantly different with probability  $\alpha$ .

Table 3.5 shows that this is indeed so (i.e. two separate bands cannot be distinguished) at either the 99% or 95% probability level in the case of NRM, whereas after demagnetization to 540 oe the two bands become distinct at both levels. Hence in further discussions of the results, Bands 3 and 4 will be taken to be separately exposed at Site B. It should be stressed, however, that this is only a tentative result, in the absence of similar comparisons at other sites where Band 4 may, or may not, be associated with Band 3.

### 3.5. Application of the fold test

The stability treatment described in Section 3.3.2 has confirmed stable directions. To draw paleomagnetic conclusions these must be referred to the ancient horizontal plane, which in turn will be assumed to correspond to the bedding planes of the ignimbrites. The correction was made by rotating the bedding about strike, using the geological data in Table 2.2. A simple rotation about strike was justified in this case, since the axis of the Mweelrea syncline was close to horizontal over the whole sampling region (Chapter 2). The correction was carried out for all samples separately, and for site mean and band mean directions, using an IBM 1620 computer program.

The results (Fig. 3.3, Table 3.6) show a grouping of positive (north pole downward) directions in the second quadrant, relative to the ancient horizontal. They also constitute a positive fold test (essentially a comparison between Site A on the southern limb, and Sites B and C on the northern limb of the syncline), since there is an obvious improvement in the grouping. This is reflected by an increase in the value of  $k$  from 2.7 to 11.7 before and after tilt correction. However, McElhinny's (1964) significance criterion is not strictly applicable in this case, since (a) the distribution before tilt correction is not a Fisherian one; (b) different bands are being compared at the two limbs of the syncline.

On the basis of qualitatively judging the fold test, however, it will be assumed that the magnetization was acquired prior to the folding, and hence is most probably of primary origin in the Ordovician.

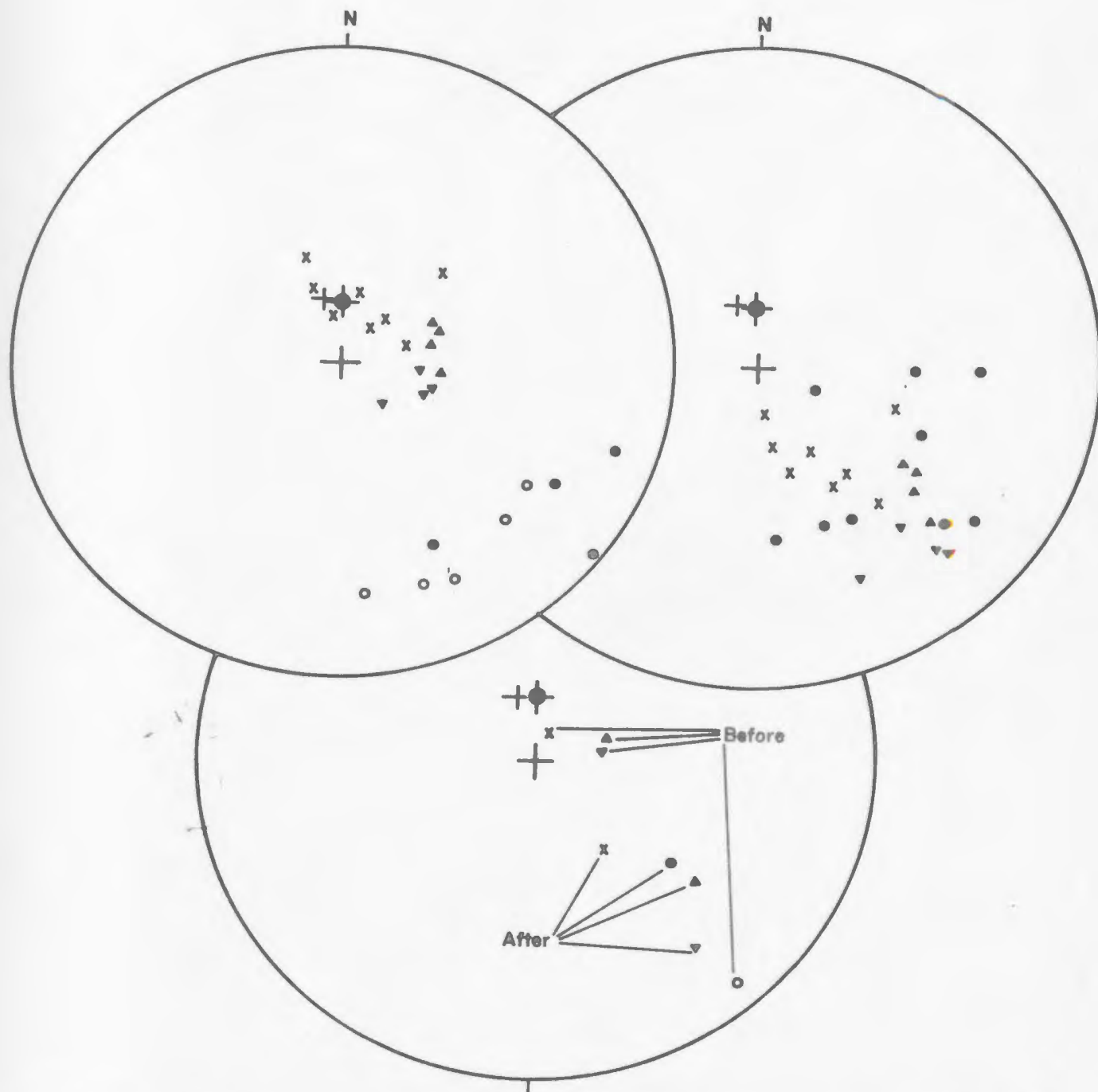


Fig 3.3. Tilt correction of the directions of magnetization for the Killary Harbour ignimbrites, after demagnetization to 540 oe

Equal area projections, showing (a) mean directions for all 25 samples, before and after tilt correction; (b) mean band directions, before and after tilt correction. For strike and dip data, refer Table 2.2.

- Band 1, north pole in upper hemisphere;
- Band 1, ▼ Band 3, ▲ Band 4, X Band 5 : north pole in lower hemisphere; axial dipole; present field at site.

TABLE 3.6

Mean site magnetization of the Killary Harbour ignimbrites after  
540 oe (peak) a.c. demagnetization and tilt correction.

Site	Band	$\bar{D}$	$\bar{I}$	N	R	k	$\alpha_5$
A	1	128°	+35°	9	8.074	8.6	18.6°
B	3	141°	+15°	4	3.959	72.1	10.9°
B	4	128°	+27°	4	3.975	120	8.4°
C	5	144°	+52°	8	7.667	21.0	12.4°
All samples		134.8°	+36.2°	25	22.949	11.7	8.9°
All bands		134.1°	+32.0°	4	3.870	23.0	19.6°

Symbols as in Table 3.3

## CHAPTER 4

### DESIGN AND CALIBRATION OF THE

### THERMAL DEMAGNETIZATION UNIT

This Chapter deals with the construction and results of performance tests of a unit for progressive thermal demagnetization. The latter technique was briefly described in Section 3.2.2, while reasons for its application to volcanic rocks in the present study, along with results, will be discussed in Chapter 5.

#### 4.1. Magnetic environment

The laboratory space available for the thermal demagnetization unit was in the basement of the Chemistry-Physics building, which contains loading areas, supply stores and a variety of fixed and moving ferromagnetic objects, along with a.c. and time-varying d.c. sources. All these are potential causes of field distortion in the working space for the oven, in which a close approach to perfect field nulling is essential, particularly at high temperatures. To reduce field gradients adequately, one might confine research time to "quiet" periods (nights, weekends, etc.), but most important initial step was to select a working space combining optimum uniformity of the permanent magnetic background (i.e. removed from steel girders, major plumbing, etc.) with relative remoteness from a.c. and d.c. sources and movable ferromagnetic objects. Without costly magnetic shielding such a space is usually difficult to find within a general research building, but a favourably situated laboratory (7.6 m x 6.3 m) for installing the demagnetization unit was finally located.

The next objective was to determine within this room the potential working-space having the smallest magnetic gradients over a volume equal to that to be occupied by specimens (about 0.12m x 0.12m x 0.12m). For this purpose a survey was carried out in the empty laboratory, using a Sharpe Instruments Ltd., model MF-100 fluxgate magnetometer, to obtain the vertical component of the anomaly field relative to an arbitrary zero setting. Readings were taken over a rectangular grid of 7 x 6 stations spaced 1.2 meters apart, at each of three elevations above the floor: 0.4, 0.9, and 1.7 meters; the intermediate value is close to the altitude of the central part of the demagnetizing furnace.

Isoanomaly values with 1000  $\gamma$  intervals ( $1\gamma = 10^5$  oe) are shown in Fig. 4.1 (a) - (c). The maximum observed field variation is large (+5000 $\gamma$  to -7000 $\gamma$ ), with positive, relatively uniform field values predominating in central parts of the room, while negative fields having larger gradients tend to be near the walls. The most favourable region was C2E2E4C4 where Fig. 4.1 (d) shows the mean horizontal and vertical gradients of the vertical field over appropriate sides of the prism R. This corresponds to a grid at the corners of the area C3D3D4C4 (1.5 m<sup>2</sup>) and at each of the three elevations where data had been obtained. The center of the oven was then specified to lie within this optimum region, where in the absence of additional field distortion the maximum horizontal and vertical gradients of the total residual field after field nulling are estimated to be in the ranges 1 - 5 $\gamma$ /cm, and 0.1 - 3 $\gamma$ /cm, respectively. The field monitoring system (Fig. 4.5) allows one also to control short-term variations in the

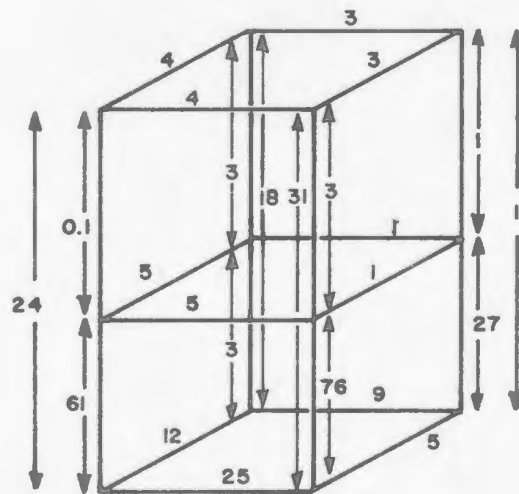
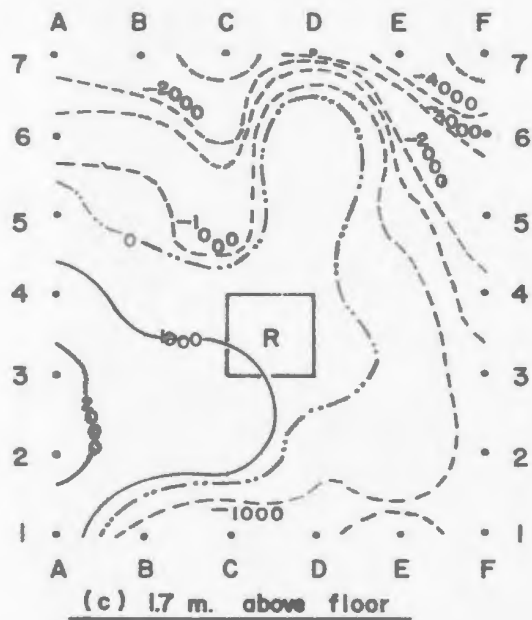
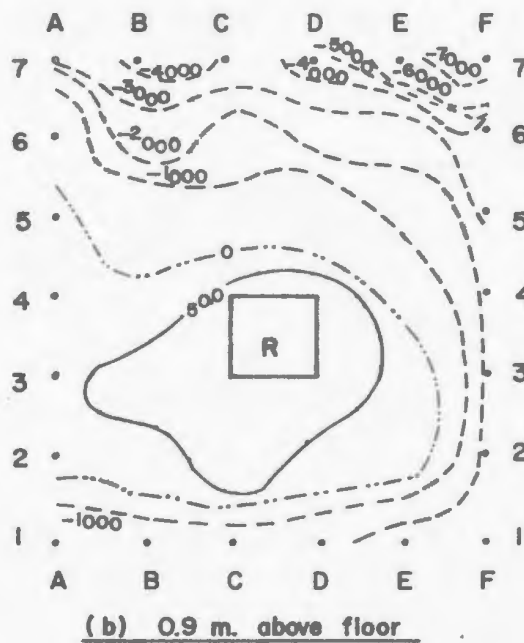
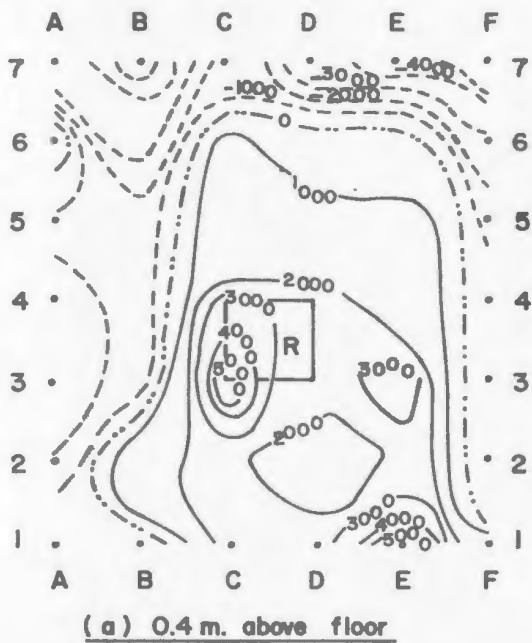


Fig 4.1 Fluxgate magnetometer survey at three levels of the laboratory accomodating the thermal demagnetizing unit.

R= region finally selected.

Contour figures in,  $\gamma$  ( $10^{-5}oe$ ).

Horizontal spacing between grid points = 1.2 m.

laboratory field (due to geomagnetic field variations, stray fields from sources within the building, etc.), provided they originate far enough from the demagnetization unit so that no additional significant gradients are introduced.

#### 4.2. Design of the thermal demagnetization unit.

The unit (Figs. 4.2, 4.3) closely follows a design by Irving et al, (1961 b). The principal changes were in the reduction of the size of the oven (diameter of the cylindrical heating section reduced from 20.3 cm to 13.0 cm in the present unit), use of circular helmholtz coils (diameter 90 - 110 cm) instead of square "Parry" coils (sides 160 - 180 cm), and addition of a fluxgate monitoring assembly as an aid in controlling the field nulling.

Construction of the main parts of the oven and auxiliary components was carried out by the Technical Services Department, of Memorial University, with the aid of the design drawings kindly made available by Dr. E. Irving of the Dominion Observatory, Ottawa. The smaller size of the oven reduces the available space for accommodating specimens, but also shortens the time required to attain a specified temperature with a given heating current. On the other hand, the reduced oven size may aggravate certain difficulties due to the greater proximity of the heating element to the center of the oven: (1) any inductive effects of the element (a commercial, relatively non-inductive design also used in the Irving oven); (2) stray fields due to the ferromagnetism of the nichrome heating wire at temperatures up to its Curie point ( $298^{\circ}\text{C}$ ); (3) large thermal

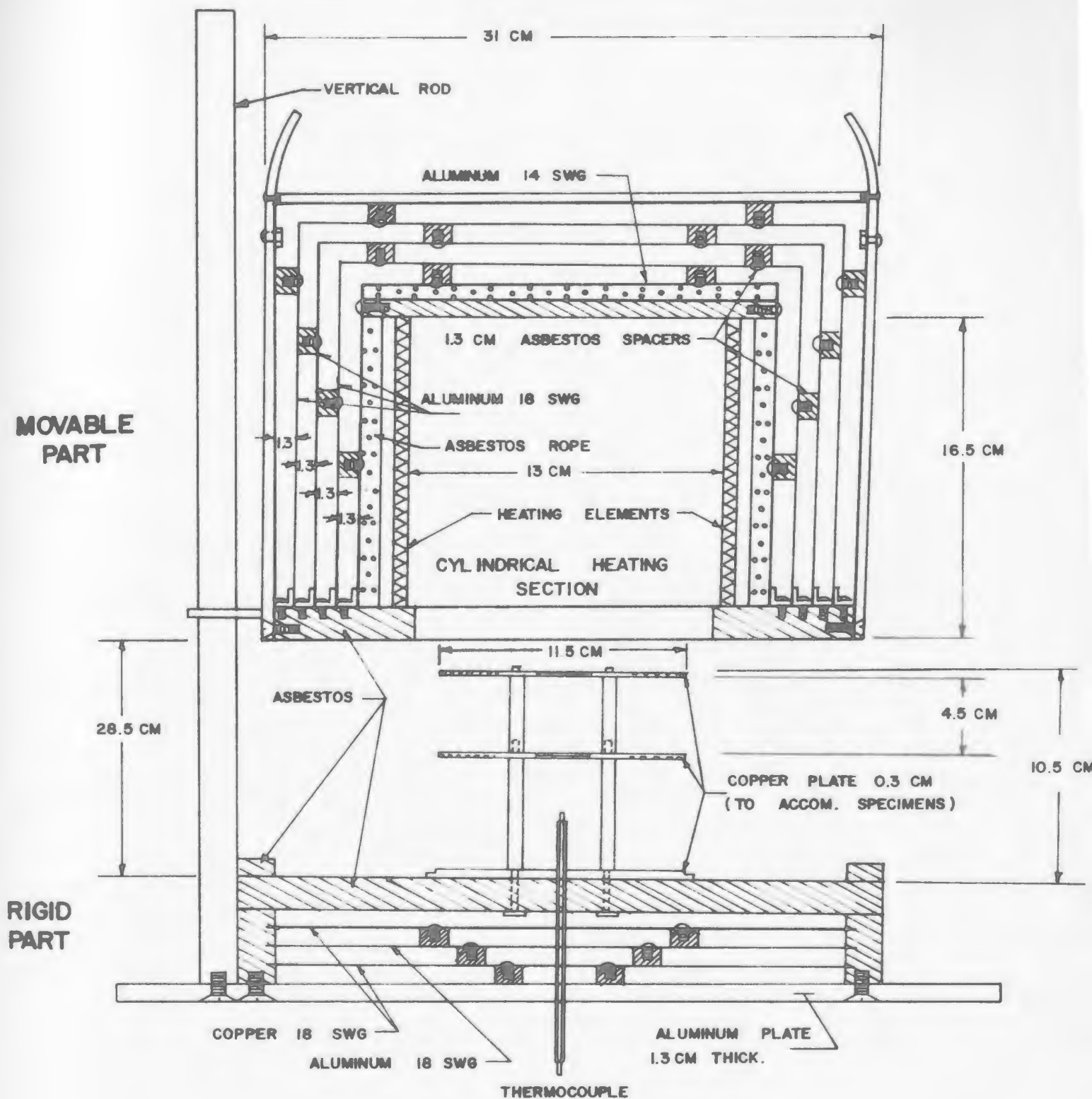


**Fig. 4.2 Cross-section of non-magnetic oven**

Original design by Irving et al (1961b). Dimensions shown are for adapted design at Memorial University. The figure shows only one of the four vertical rods along which the movable part is rested.

gradients in the vicinity of the heating wire.

#### 4.3. Description of the unit.

##### 4.3.1. The oven

With an internal working space of  $3250 \text{ cm}^3$  (but in practice only the smaller region occupied by the specimen stand) the oven can accommodate eighteen cylindrical specimens (2.2 cm diameter, 1.8 cm height) with an average separation of 1.6 cm between rock surfaces on the two compartments of the copper stand (Fig. 4.2). Two inlets near the center of the base are (i) for insertion of a nitrogen supply through a copper tube encircling the specimen stand; (ii) to accommodate the thermocouple. During heating an inverted copper pot (not shown) of 12.5 cm diameter and 14.5 cm height, and hence occupying much of the working space is placed over the specimen stand to achieve more uniform temperature distribution inside, its function is not only as a radiating surface, but as an enclosure from which the escape of the warmed air or nitrogen can be sufficiently slowed down to render thermal gradients due to this cause insignificant. The nichrome wire is wound inside the heating jacket in such a way that the alternating current from the 220 volts main supply will produce no significant net inducing field within the specimen region. The jacket is surrounded by asbestos rope and an aluminium sheet to improve thermal insulation. Rapid cooling of the specimens is brought about by lifting the jacket with a counter-weighted hoist and pulley system (Fig. 4.3).

##### 4.3.2. The field nulling and control assemblies.

Three orthogonal pairs of helmholtz coils wound with 18 SWG

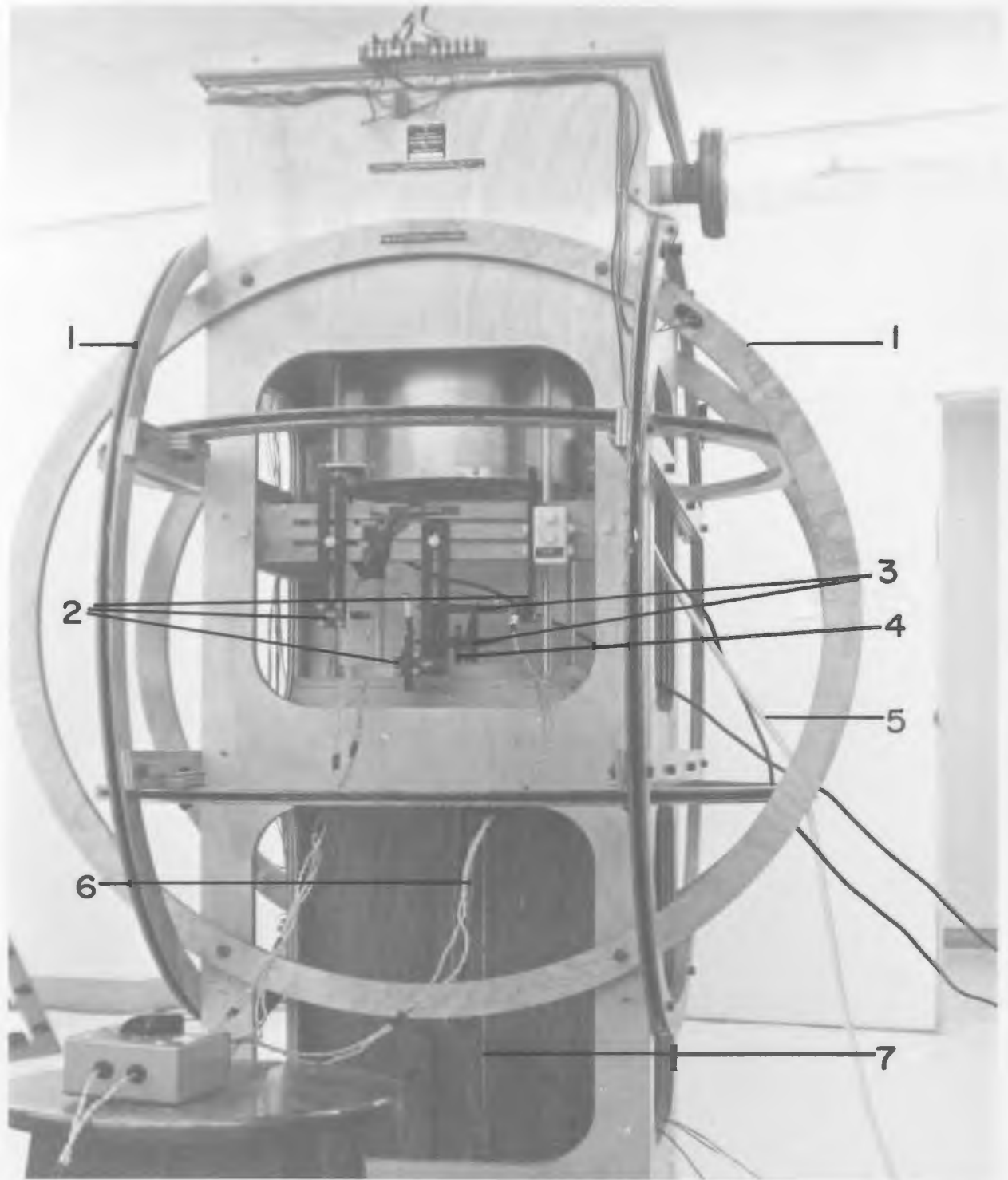


Fig 4.3. The demagnetizing unit

- |                    |                      |
|--------------------|----------------------|
| 1. Helmholtz coils | 2. Fluxgate assembly |
| 3. Specimen stand  | 4. Thermocouple      |
| 5. Nitrogen inlet  | 6. Thermostat probe  |
| 7. Counterweight   |                      |

enamelled copper wire were mounted around the oven to cancel the local field in the (i) vertical, (ii) north-south, and (iii) east-west directions. For convenience in nulling the horizontal field, the axes of coil pairs (ii) and (iii) were chosen to make small angles of a few degrees with the magnetic north-south and east-west directions, respectively. The helmholtz coil constants are similar to those of the astatic magnetometer (Appendix 1). The input is provided by two d.c. power supplies (Power Designs Inc.) and regulated by a resistor control unit built at Memorial University (Fig. 4.4). To measure and adjust the currents required for nulling the local field, three orthogonally oriented fluxgate detectors were mounted outside the oven. (Fig. 4.5 - Section 4.4).

#### 4.3.3. Measurement of temperature.

A platinum-platinum/10% rhodium thermocouple calibrated at the National Research Council, Ottawa is inserted through the base of the specimen stand to measure the oven temperature at a point close to the center of the helmholtz coils. A separate sensor operated a thermostat (Hallikainen Inst. Co.) included in the heating circuit; this permitted temperature control to  $\pm 10^{\circ}\text{C}$  at  $100 - 200^{\circ}\text{C}$ , and  $\pm 5^{\circ}\text{C}$  above  $200^{\circ}\text{C}$ . A Leeds and Northrup Inc. potentiometer was used with the thermocouple, and a calibration converting uncorrected  $^{\circ}\text{F}$  scale readings into centigrade values corresponding to the N.R.C. calibration is described in Appendix 2, along with the measurements of the thermal gradients in the working space. The latter calibration (Table A 2.3, Fig. A 2.3) allows one to convert the corrected temperature readings into actual temperatures

at the specimen location with combined calibration and measurement errors estimated to be  $\pm 28 - 14^{\circ}\text{C}$  in the ranges 250 - 300 $^{\circ}\text{C}$ , and  $\pm 6 - 4^{\circ}\text{C}$  in the range 350 - 750 $^{\circ}\text{C}$ . This assumes that after the 20 minute period allowed to ensure the thermal equilibrium at the operating temperature, no significant thermal gradients remain within the specimen volume itself.

Raising the heating jacket permits rapid cooling of the oven through contact with cool air, but this method cannot be used when the atmosphere is nitrogen. In either case induction effects from the heating current are absent, as the current is shut off.

#### 4.4. The fluxgate monitoring system.

Up to three identical fluxgate elements (Table 4.1), were used for measuring residual magnetic fields inside the oven.

The output of any fluxgate element was connected to an oscilloscope through an amplifier, while the input for exciting the primary winding at 400 Hz was obtained from a signal generator (Fig. 4.4). In the absence of an external magnetic field, the output contains harmonics due to the unavoidable instrumental noise. In the presence of an external field an unsymmetrical wave form results from superposition of these harmonics on the fundamental. Restoration of a zero field may be confirmed through a symmetry test, i.e. one assumes that the fundamental mode is zero, when, in the composite harmonics pattern on the oscilloscope, corresponding amplitudes above and below the field axis are equal. The error in judging this symmetry by direct observation was estimated to correspond to  $< 5 \gamma$  on the most sensitive scale.

TABLE 4.1Particulars of the fluxgate elements(Data supplied by the manufacturerSmiths Ltd., England).

Model no.	LDC A20
Overall length	3.0 in.
Excitation at 400 H <sub>z</sub>	
Voltage	0.25 volts
Current	15.0 ma
Output	890 mv/oersted
Noise	1.4 mv

FIG 4.4(a) Auxiliary equipment used in field nulling and field monitoring

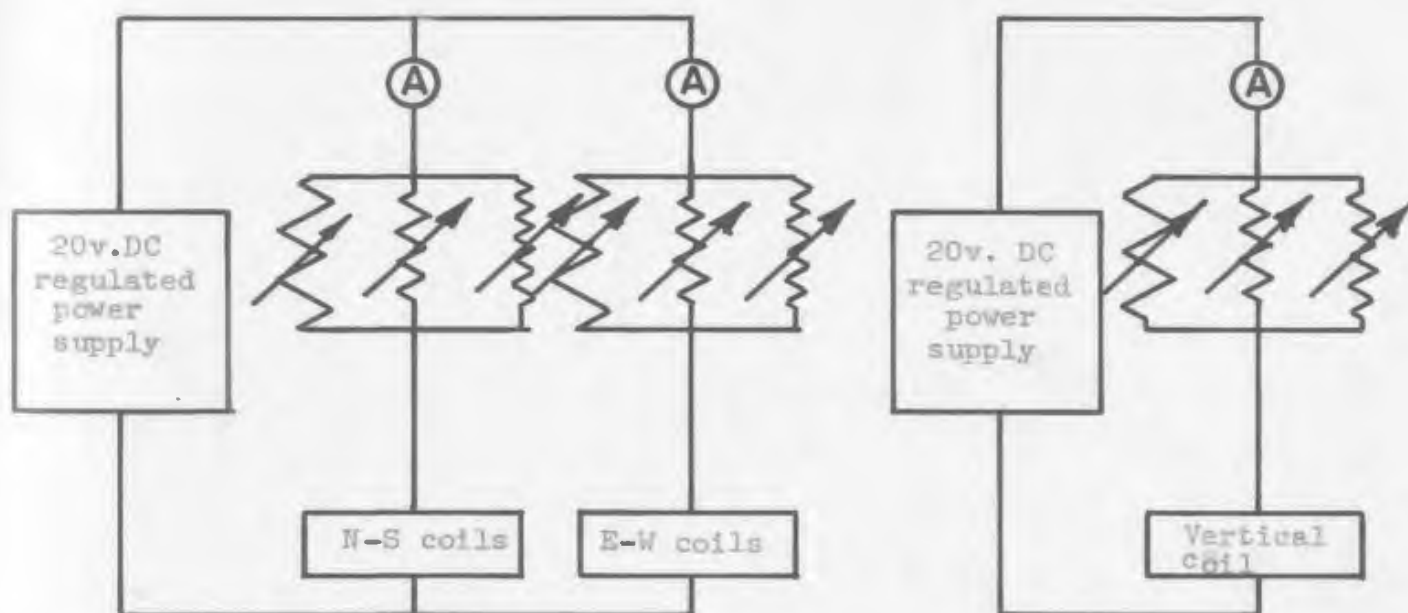
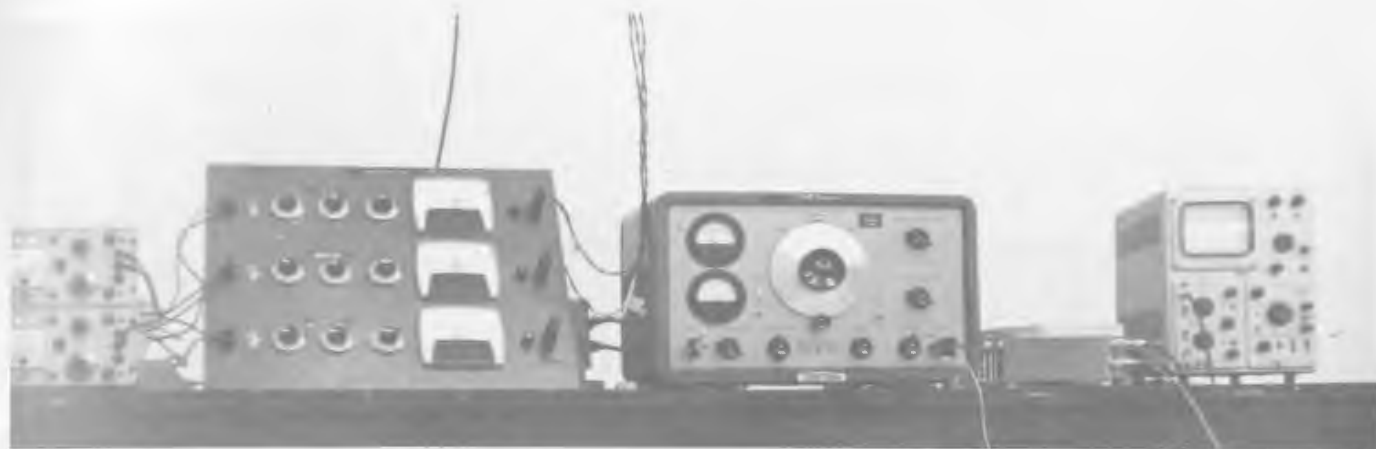


Fig 4.4(b) Helmholtz coil circuits

#### 4.4.1. Nulling of helmholtz coil fields.

The three fluxgate elements were mounted orthogonally on a wooden stand close to the oven center, with their axes along the three respective helmholtz coil axes. The current was switched on for one coil pair at a time, and was adjusted through a fine control (Fig. 4.4 (b)) until the corresponding fluxgate element indicated that the appropriate field component has been nullified. The error in this measurement is largely confined to the symmetry - judging error discussed above, say  $5 \gamma$ .

The other two coil pairs were then adjusted individually for field-free space in the same manner. However, because of small departures from perfect orthogonality, the separate nulling of the three coil pairs did not produce zero field at the center. Starting with the current settings determined by individual field nulling the previous procedure was therefore repeated with the compensating current flowing in two of the coil pairs at a time, and finally in all three pairs.

#### 4.4.2. Calibration of the fluxgate elements.

The measurement of small fields other than for the purpose of nulling required a calibration in terms of the fluxgate output amplitude. A known, small external field was produced along the axis of a centrally placed fluxgate element, by changing the compensating current in the corresponding helmholtz coil pair. The resulting change from the symmetrical condition in the amplified output voltage was then observed. For comparison the current was then reduced to a value below the field-

nulling value by an amount equal to the previous excess current, and corresponding voltages on opposite sides of the balance condition were compared and averaged. The measurements were repeated for the other two components, and from the known dimensions and number of turns of the coils, the fields corresponding to given voltage changes were found (Table 4.2).

#### 4.5. Fluxgate survey of the oven area.

The fluxgate elements were now set up in field-free space at the oven center. Since the specimens during demagnetization are generally placed off-center, by a few cm, it was necessary to survey the entire region concerned. A continuous-recording survey was made by moving each of the three fluxgate elements alternately in a horizontal direction, successively in the east-west and north-south planes, and at different levels (3 cm above to 3 cm below a horizontal plane through the oven center). This gave coverage both inside and outside the working space, after the oven head had been raised 28.5 cm above the "closed" position. Recordings of the fluxgate output (not reproducible for inclusion here) showed that the maximum change from the central field was within 10  $\gamma$  up to 8 cm from the oven center in the case of all three components, but at greater distances anomalous field variations of the order of 100  $\gamma$  were observed, the largest effect being in the vertical component. From the localized nature of these anomalies (a 50  $\gamma$  - 100  $\gamma$  change occurring over a few cm distance) their likely source was suspected to be in the oven itself.

The anomalous field was at first thought to be due to some ferromagnetic material present in the base of the oven. Since the

TABLE 4.2

Calibration of the fluxgate elements (for horizontal field components)

Fluxgate components	current for field nulling (ma)	change in current (ma)	Mean* voltage (volts)	Helmholtz coils		corresponding* field (gamma/volt)
				No. of turns single coil	Radius (cm)	
North-South	201	± 1.00	2.0	50	50.2	44.5
East-West	36	± 5.00	2.5	15	55.1	49.9

\*This refers to the amplified output voltage observed on the oscilloscope (accuracy  $\pm 0.05$  volt); average values, corresponding to the mean positive and negative current changes in column 3, are quoted.

oven can be raised only to a limited height (28.5 cm), it was necessary to check this as well as the possibility that the nichrome wire in the heating element might introduce a magnetic gradient into the space occupied by the specimens. Accordingly, the field variation at the oven center (vertical component) was checked while the oven was lowered from its highest position to the closed position.

The corresponding field anomaly values ranged from + 50  $\gamma$  to - 80  $\gamma$ , passing through a "zero" value. Direct examination of nichrome wire confirmed that this was considerably ferromagnetic and accounted for the bulk of the anomalous variation observed.

Raising the oven at the start of the cooling stage was therefore found inadequate in removing equipment-induced fields. To correct this fault, it was decided to preface each actual demagnetization run by an "empty" run (without specimens), in which the oven in the closed position is heated to a temperature of 750°C at its center, so that the wire temperature would be well above the Curie points not only of the nichrome (298°C), but of any other ferromagnetic components in the oven (e.g. iron present at some wire terminals). The oven was then allowed to cool in "zero" field, so that all ferromagnetic materials present should be nearly demagnetized (complete demagnetization being difficult to achieve in view of the small finite fields existing off-center when the field is perfectly nulled at the center).

The fluxgate survey of the working space was repeated with the oven raised, after several such "empty" runs had been performed. The anomalous field variation was now found to be absent in the case of all three components, leaving only the "normal"  $\pm 10\gamma$  variations observed

previously. Hence the "empty-run" demagnetization procedure has been successful in reducing stray magnetic fields typically of 100  $\gamma$  by an order of magnitude. Expressed as the mean gradient (vertical or horizontal) of the field over the working-space (up to 7.5 cm diagonally from the oven center), this field variation was estimated to be 1 - 2  $\gamma$ /cm.

Assuming that the empty run has been performed, it is then possible to estimate the maximum field acting on a specimen during demagnetization, taking 2  $\gamma$ /cm as the mean gradient inside the wiring section the greatest departure from a zero field at the center would be about 30  $\gamma$ . Adding the 5  $\gamma$  uncertainty (Section 4.4) in measuring the fluxgate output one obtains 35  $\gamma$ . However, a changing laboratory field requiring adjustment of the field-nulling currents impose a time-lag until adjustments can be effectively made. The error due to this is difficult to estimate, but a change of 100 - 200  $\gamma$  in, say, then minutes is perhaps of the right order, and if the restoration of nulling takes one minute, then a 10 - 20  $\gamma$  imbalance might build up. Roughly, therefore the actual field in parts of the surveyed region may be as much as 50  $\gamma$ .

On the other hand the specimens occupy a more confined space, with a maximum radial distance of 4.5 cm from the oven center. Hence the maximum error due to the field gradient need not exceed 15  $\gamma$  or so, so that the maximum estimated uncertainty in the field acting on a specimen during demagnetization is very roughly 30 - 40  $\gamma$ . The corresponding maximum field variation existing at a given time between any two points in the region to be occupied by specimens is 15  $\gamma$ . Therefore the largest

net fields and field differences estimated to exist in the working space of the oven are  $< 0.1\%$  of the present Earth's field. While further reduction of the field nulling error would be desirable<sup>1</sup>, it was concluded that the presence of fields of the above magnitude probably has only an unimportant effect on the results of the demagnetizations described in Chapters 5 and 6. (See also Irving et al, 1961 b; Chamalaun and Creer, 1964; Jones and McElhinny, 1967; Vincenz, 1968). However, this assumption was subjected to a direct test, with results described in Sections 4.8 - 4.9 .

#### 4.6. Field monitoring outside the oven.

The field variation could not be monitored at the oven center itself, because the fluxgate elements would then be heated. They were therefore mounted outside the oven, though still within the region enclosed by a particular pair of helmholtz coils (Fig. 4.3, 4.5). This required that for each component an external position be found at which the compensating field due to the helmholtz coils would be equal to the corresponding field component at the coil center. Accordingly two

---

<sup>1</sup>After completion of the work described in this thesis, the present helmholtz coils were replaced by Parry coils of about twice the linear dimensions of the former, thus reducing the gradients in the working space. Moreover, ferromagnetic components in the oven (particularly the nichrome wire) were replaced with essentially non-magnetic ones; this eliminated the awkward "empty run" procedure to reduce stray fields.

fluxgate elements were mounted vertically, the first at the oven center and the second in various outside positions, until one was found at which both elements registered the same field for different compensating currents in the helmholtz coils, including the "nulling" current. The outside element was then permanently attached to the helmholtz coil frame in the final calibrating position, and the procedure repeated, with the two elements placed first north-southwards and finally east-westwards. The two horizontal fluxgate elements were then mounted in their appropriate external positions near the vertical element (Fig. 4.5). The estimated error in comparing the centrally mounted and external elements for a given component when the fields were judged to be equal, was  $\pm 10 \gamma$ . A corresponding figure must then be added to the maximum zero field error estimated in Section 4.5 raising the total uncertainty from  $40 \gamma$  to  $50 \gamma$ . However, a large error could be produced if a magnetic disturbance originating in the neighbourhood of the demagnetizing unit should distort the magnetic flux differentially at the oven center and at the external locality where the field is being monitored. This means that large sources of stray fields close to the laboratory must be especially avoided.

#### 4.7. Procedure for demagnetization.

The following sequence was adopted for stepwise thermal demagnetization:

1. The remanent magnetization directions and intensities of the specimens are measured with the astatic magnetometer.
2. 20 - 25 minutes before starting the experiment, the d.c. power supplies for field compensation, and electronic units for field monitoring, are switched on to ensure stabilizing.

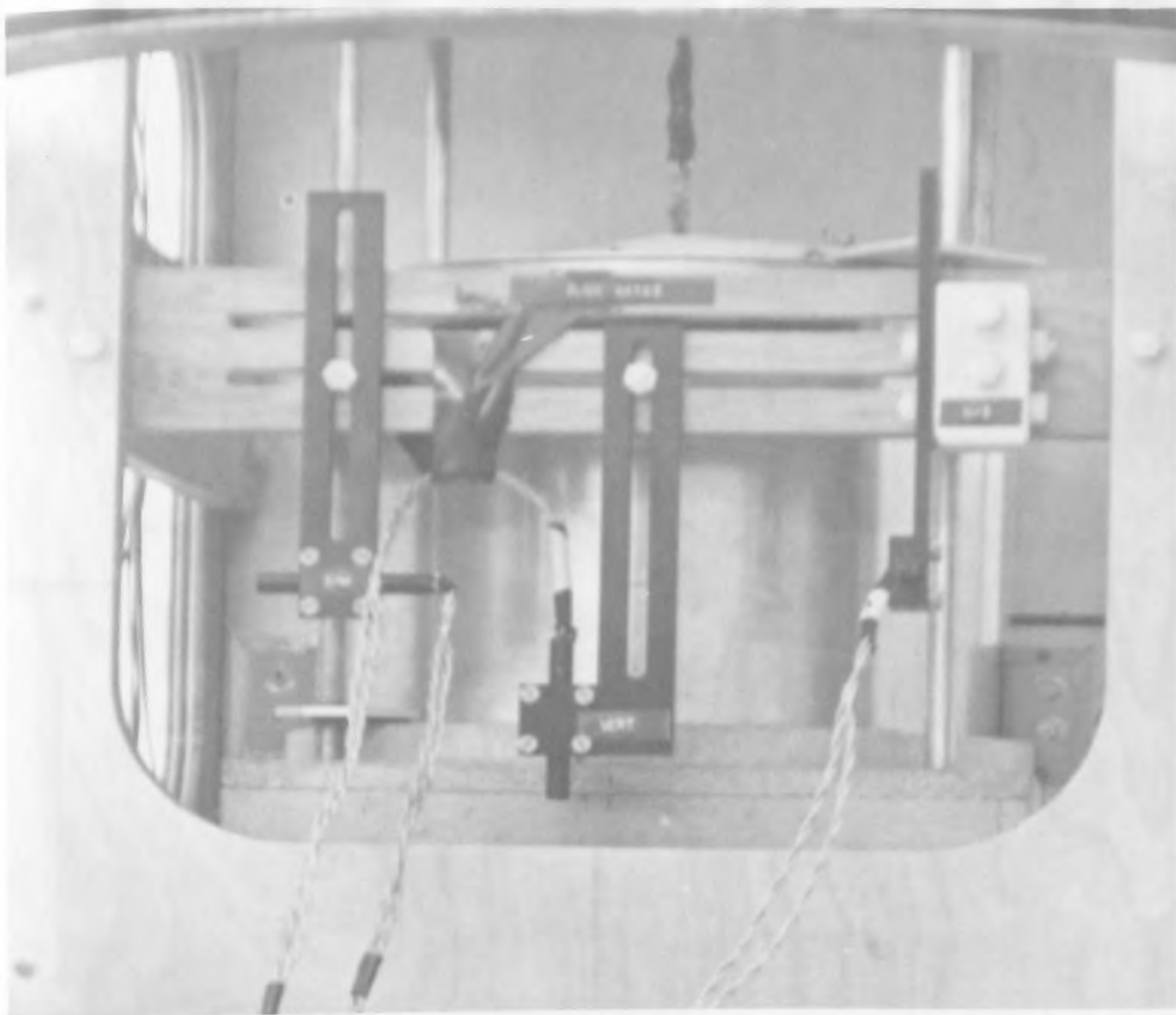


Fig 4.5. Fluxgate assembly for field monitoring

The three elements are attached outside the oven (Fig 4.3)

3. The "empty run" to 750<sup>o</sup>C is performed.
4. The specimens are arranged on the two copper shelves in "random" positions (see Section 4.8), with 1.6 cm minimum separation between their surfaces.
5. The specimens are covered with the inverted copper pot to reduce temperature gradients.
6. The oven is closed, and the thermostat adjusted to the desired maximum temperature.
7. The currents in the coils are monitored with the fluxgate system, and adjusted separately for nulling each field component.
8. If the demagnetization is to be carried out in inert atmosphere, nitrogen is allowed slowly to enter the specimen region through the nitrogen inlet at the oven base. The rate of inflow of nitrogen is adjusted to compensate for its gradual escape across the rim of the inverted copper pot.
9. The heating current is switched on, and when the set temperature has been approximately reached, it is measured and maintained constant for at least 20 - 25 minutes, during which time the field is monitored again. This is an important step, particularly at temperatures close to the highest Curie point of the ferromagnetic constituents of the rock, since even small stray fields may then introduce significant TRM's that could dominate its remanence spectrum. Departures from zero reading in any component must be corrected by hand-adjusting the current in the appropriate pair of helmholtz coils. Also during this period, the temperature is remeasured.

10. The heating current is switched off and the oven raised to the highest position (unless nitrogen is used, in which case it remains closed). The three field components are carefully monitored throughout the cooling period, and any necessary adjustments in the helmholtz coil currents are made.

11. When the specimens have cooled down to the laboratory temperature they are quickly transferred into a magnetic-shielding can (Appendix 5), inside which the magnetic field is several orders of magnitude less than the surrounding laboratory field. This greatly reduces the risk that the specimens may acquire a significant VRM in the laboratory.

12. The remanent directions and intensities of magnetization are re-measured.

#### 4.8. First test of the oven

Before proceeding with the actual demagnetization programme, it was necessary to evaluate the performance of the oven, and to establish that it was randomizing the field directions without introducing field components in a preferred direction. The following procedure was adopted:

Ten specimens (nos. 1-9 and 16 in Table 4.3) from the Killary Harbour ignimbrites (Chapters 2, 3), and six (nos. 10-15) from the Henley Harbour basalts (Chapter 6), were selected for the test. Previous measurements on these rocks (Chapter 3; and Murty, 1966) had shown them to satisfy at least minimum stability criteria. The ignimbrite specimens used for the present test had been previously demagnetized

in alternating fields to 770 oe (peak), while the basalt specimens had received no stability treatment. All except one of the NRM directions (Fig. 4.6; Table 4.3) had steep inclinations, while declinations ranged over all four quadrants.

Following an "empty run" (Sections 4.5, 4.7), the specimens were arranged on the specimen stand in the oven with the directions of their remanent magnetization vectors as shown in Fig. 4.7.1. This resulted from the inversion of half of the specimens (thus changing the inclination of their vectors from positive in Fig. 4.6 to negative), and their repositioning, so that four horizontal vector components each pointed towards magnetic north, east, south, and west with respect to the laboratory. In this manner the vector sum of the 16 unit remanence vectors was substantially reduced, though not to zero. Half the specimens (nos. 1-8) were arranged on the upper compartment of the specimen stand, and the other half (nos. 9-16) on the lower compartment; in all cases the center of the specimen was 5.0 cm away from the vertical axis through the oven center.

The specimens were now heated to 730°C and cooled in zero field, as described in Section 4.7. The directions of magnetization after this treatment are plotted in Fig. 4.7.2 relative to the oven coordinates, and in Fig. 4.7.3 relative to the sampling sites. In the former case, the directions after treatment show a tendency towards shallower inclinations in the upper hemisphere, suggesting the presence of some small, uncancelled field component during cooling. However, the scattering is considerable; compare also the low precision ( $k=1.60$  in Table 4.4). The fact that the scatter is even greater

TABLE 4.3

First test of the oven: Directions of magnetization  
after repeated demagnetization

(compare Figs. 4.6; 4.7.1-4.12.3)

Specimen nos. 1-9, 16: Killary Harbour ignimbrites:  
 Specimen nos: 10-15: Henley Harbour basalts.

H = field, excluding error, in  $\gamma$  ( $1\gamma = 10^{-5}$  oe), applied during cooling from temperature T in the direction shown.  
 D = declination (deg.), I = inclination (deg., positive downwards); relative to laboratory or sampling site coordinates.

Specimen positioning in the oven, prior to treatment:

N, E, S, W = arbitrary orientation of declination of the remanence vector relative to the laboratory;

u = specimen upright, i = inverted; both u and i are relative to the oven positioning in the previous demagnetization step (thus, while repositioning leaves the magnitude of the inclination unchanged, its sense is reversed after inverting the specimen).

Specimen in the rolling position ( $T = 750^{\circ}\text{C}$ ,  $H = 19,000\gamma$  north, only): the previous vertical plane containing the magnetization vector now lies horizontally (i.e.  $I = 0$  relative to laboratory), with declinations arbitrarily oriented as shown.

For total laboratory field (final treatment),  $H = 49,000\gamma$ , acting approximately towards laboratory north, and inclined  $67.5^{\circ}$  downwards.

TABLE 4.3

First test of the oven: Directions of magnetization after repeated demagnetization

Specimen No.	NRM		after T = 730°C, H = 0				after T = 800°C, H = 0				after T = 760°C, H = 100γ North						
	Rel.Site		Rel.Lab.		Rel.Site		Rel.Lab.		Rel.Site		Rel.Lab.		Rel.Site				
	D	I	Position	D	I	D	I	Position	D	I	D	I	Position	D	I		
1	36	+59	N u	147	+15	183	+15	N u	317	+30	140	+30	N u	48	+19	188	+19
2	101	+74	S i	14	-72	267	+72	S u	190	+5	278	+5	S i	350	-62	107	+62
3	53	+61	E u	204	-35	167	-35	E i	280	+82	358	+82	E u	64	+14	332	+14
4	43	+53	W i	226	-46	87	+46	W u	171	-15	349	-15	W u	185	-35	74	+35
5	99	+80	S u	183	-32	102	-32	S i	87	+43	10	+43	S u	325	-27	155	-27
6	268	+72	N i	147	-32	121	+32	N u	137	-29	258	-29	N u	279	-32	339	+32
7	63	+68	W u	173	+65	326	+65	W u	135	+52	191	+52	W u	216	+33	137	+33
8	34	+74	E i	147	-53	337	+53	E u	170	+5	58	+5	E i	115	-72	33	+72
9	160	+88	N i	294	-25	226	+25	N u	263	-2	130	-2	N u	12	-32	117	+32
10	237	+70	S u	105	-12	162	-12	S i	167	+43	149	+43	S u	187	+33	157	+33
11	331	+65	E i	128	-41	293	+41	E u	114	-16	318	-16	E u	122	-8	287	+8
12	326	+72	W u	288	-30	344	-30	W i	246	+69	320	+69	W u	230	-15	280	-15
13	66	+47	S i	24	-44	222	+44	S u	83	-37	125	-37	S u	71	-3	234	+3

TABLE 4.3 (Continued)

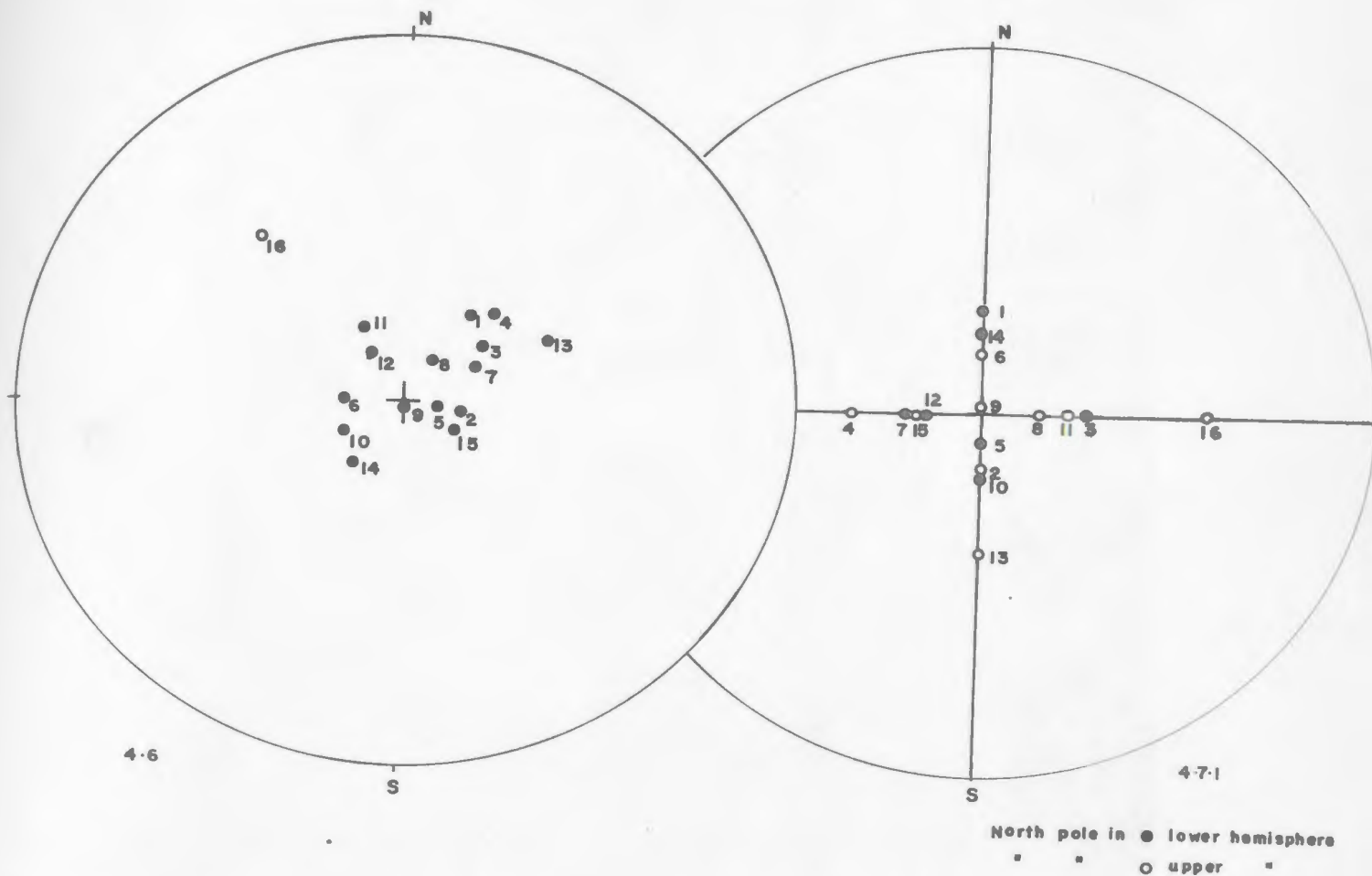
Specimen No.	NRM Rel.Site		after R = 730°C, H = 0				after T = 800°C, H = 0				after T = 760°C, H = 100γNorth						
	D	I	Position	Rel.Lab. D	Rel.Lab. I	Rel.Site D	Rel.Site I	Position	Rel.Lab. D	Rel.Lab. I	Rel.Site D	Rel.Site I	Position	Rel.Lab. D	Rel.Lab. I	Rel.Site D	Rel.Site I
14	216	+66	N u	65	-37	281	-37	N i	355	+37	276	+37	N u	299	+14	215	+14
15	121	+72	W i	260	-55	131	+55	W u	132	-23	353	-23	W u	211	-34	53	+34
16	320	-31	E u	76	+12	306	+12	E i	94	-43	302	+43	E u	150	-41	2	-41

TABLE 4.3 (Continued)

Specimen No.	after 760°C, .100γNorth		after T=750°C, H=500γSouth				after T=750°C, H=19000γNorth				after T=750°C, Total Lab.field						
	Rel. Site		Rel.Lab.		Rel.Site		Rel.Lab.		Rel.Site		Rel.Lab.		Rel.Site				
	D	I	Position	D	I	D	I	Position	D	I	D	I	D	I			
1	188	+19	S u	171	+5	179	+5	N	184	+5	175	+4	N u	359	+67	174	+67
2	107	+62	N i	192	-15	276	+15	S	161	-20	158	+18	S i	2	+68	336	-68
3	332	+14	E u	119	+2	1	+2	E	359	-1	337	+88	E u	297	+71	185	+71
4	74	+35	W i	194	-12	150	+12	W	3	-5	151	-84	W u	79	+71	342	-71
5	155	-27	S u	145	+5	190	-5	S	11	-33	33	+9	N u	322	+72	355	+72
6	339	+32	N u	136	+2	116	+2	N	179	+27	152	-1	S u	110	+70	222	-70
7	137	+33	W i	327	-31	80	+31	E	166	-1	85	-76	E i	176	+68	172	+68
8	33	+72	E u	124	+9	67	+9	W	85	+1	89	-5	W u	65	+66	294	-66
9	117	+32	N u	124	-13	241	-13	S	47	-60	68	+21	N u	67	+81	135	+81
10	157	+33	S i	165	-33	171	+33	N	174	-1	181	-6	S u	43	+63	317	+63
11	287	+8	E u	168	-4	5	-4	E	167	+1	95	-77	E i	186	+69	191	+69
12	280	-15	W u	194	+1	355	-1	W	173	-3	110	+82	W i	276	+63	104	-63
13	234	+3	S u	167	-8	221	-8	S	111	-88	90	+1	N u	75	+67	165	+67

TABLE 4.3 (Continued)

Specimen No.	after 760°C, .100γNorth		after T=750°C, H=500γSouth				after T=750°C, H=19000γNorth				after T=750°C, Total Lab.field						
	Rel. Site		Rel.Lab.		Rel.Site		Rel.Lab.		Rel.Site		Rel.Lab.		Rel.Site				
	D	I	Position	D	I	D	I	Position	D	I	D	K	D	I			
14	215	+14	N i	196	-8	19	+8	N	183	-79	259	+1	S i	224	+60	215	-60
15	53	+34	W u	169	-1	312	-1	E	4	-19	11	+70	E u	238	+69	159	+69
16	2	-41	E u	225	-29	227	+29	W	7	-1	94	-83	W u	6	+74	358	-74



Figs 4.6., 4.7.1. Testing of the oven: NRM directions before heating to 730°C and cooling in zero field

Fig 4.6. NRM directions relative to the sampling sites

Equal area projection, with the circumference corresponding to the horizontal plane at the sampling site

Fig 4.7.1. NRM directions relocated relative to the laboratory

Specimens have been rotated about the vertical to place the NRM declinations into N, E, S, or W directions; eight of the specimens have been placed upside down

North pole: ● in lower hemisphere: ○ in upper hemisphere

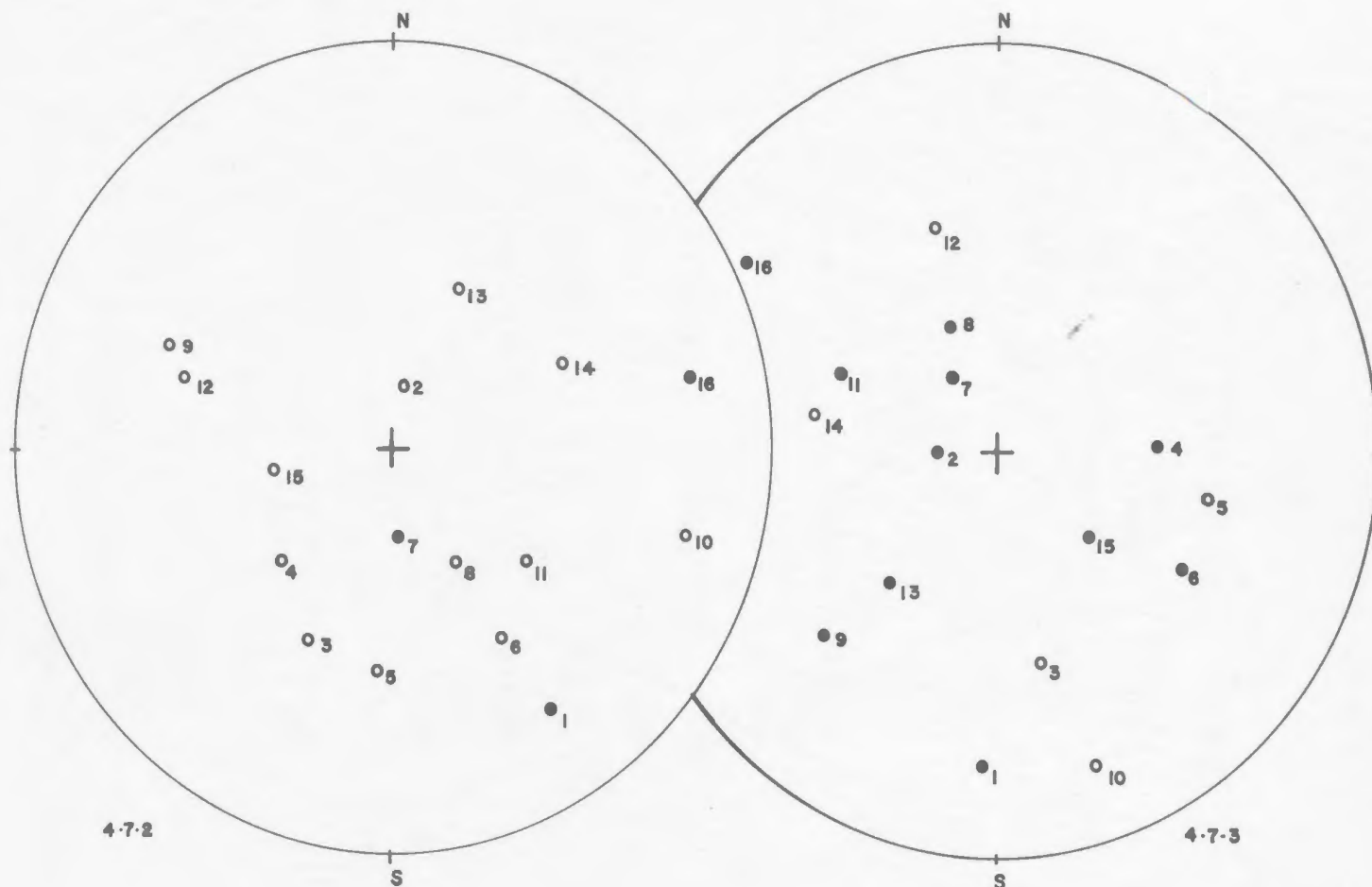
Numbers refer to specimens:

Killary Harbour ignimbrite: Nos. 1-9 16

Henley Harbour basalt: Nos. 10-15.

Figs 4.7.2.- 4.7.3. Testing of the oven: Directions of remanent magnetization (i) relative to the laboratory (4.7.2); and (ii) relative to the sampling sites (4.7.3), after heating to 730°C and cooling in zero field

The specimens are positioned as in Fig 4.7.1. The directions of the magnetization vector relative to orientation marks on the specimen are identical to those in Fig 4.7.2.



Numbers and symbols as in Fig 4.6.

relative to sampling sites ( $k = 1.38$ ) results from the inversion of half the specimens, and illustrated the advantage of randomizing specimen orientations in the oven prior to treatment to average out directional errors due to stray fields. However, the magnetization vectors for some of the specimens (nos. 4, 7, 8, 11, 15) have not moved far after treatment, suggesting that the Curie point was not reached in these cases.

The specimens were rearranged on the specimen stand (Fig. 4.8.1; Table 4.3, columns 10, 11), and the treatment repeated in zero field, but with the temperature being raised to  $800^{\circ}\text{C}$ ; it was hoped that this would result in complete demagnetization. The directions again became well-scattered (Fig. 4.8.2;  $k = 1.50$  in Table 4.4) with little evidence for a "memory" on the part of individual specimens (except possibly no. 16). Most declinations are in the range from east to south, suggesting again the presence of a small field while the specimens cooled. As in the previous treatment, the vector grouping became more nearly random when referred to the sampling sites (Fig. 4.8.3, Table 4.4,  $k = 1.30$ ).

To estimate the lower limit of any spurious field component in the oven that would significantly change the direction of magnetization of these specimens, the following procedure was adopted (Figs. 4.9.1-4.12.3): The 16 specimens were arranged in the oven with approximately random arrangement of declinations, but with all except two inclinations downward (Fig. 4.9.1). (i) Field nulling in the north-south pair of helmholtz coils was then adjusted to be undercompensated by  $100\gamma$ . i.e. a  $100\gamma$  field directed northward was present. With the two other components nulled,

TABLE 4.4

First test of the oven: Mean directions of magnetization and  
directional scatter of the test specimens

T	H	N	<u>Relative to sampling site</u>			<u>Relative to laboratory</u>		
			D	I	k	D	I	k
Lab.	0	15	47	+80	12.7			
730°C	0	16	212	+61	1.38	149	-56	1.60
800°C	0	16	323	+62	1.30	146	+26	1.50
760°C	100γ(N)	16	181	+76	1.34	174	-75	1.23
750°C	500γ(S)	16	210	+68	1.07	166	-10	3.79
750°C	19,000γ(N)	16	114	+29	1.21	122	-48	1.34
750°C	49,000γ Total lab. field	16	208	+53	1.10	19	+87	12.9

H = field, excluding error, applied during cooling from temperature T in the direction shown  
 (1γ = 10<sup>-5</sup> oe)

N = number of specimens averaged

D = declination (deg.), I = inclination (deg., positive downward)

k = best estimate of the precision parameter

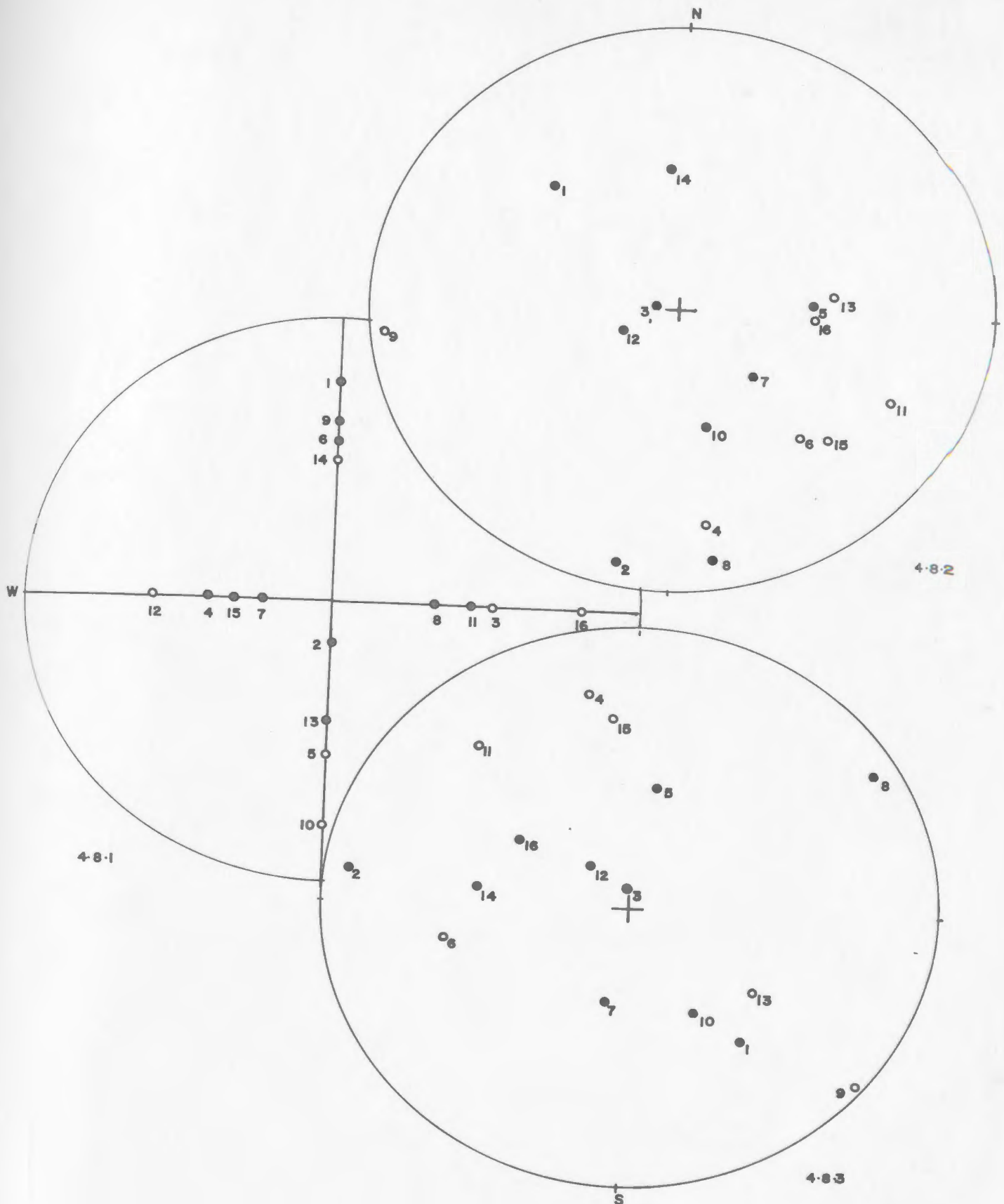
Caption to Figs. 4.8.1-4.8.3, 4.9.1-4.9.3

Figs. 4.8.1-4.8.3. Testing of the oven: Before and after heating to 800°C and cooling in zero field

- Fig. 4.8.1 Directions of remanent magnetization (Fig. 4.7.3) relocated relative to the laboratory, prior to heat treatment
- Specimens have been rotated about the vertical and, in one case placed upside down (compare Fig. 4.7.1)
- Fig. 4.8.2 Directions of remanent magnetization relative to the laboratory after heating to 800°C and cooling in zero field
- The specimens are positioned as in Fig. 4.8.1
- Fig. 4.8.3 Directions of remanent magnetization relative to the sampling sites, after heating to 800°C and cooling in zero field
- The directions of magnetization relative to orientation marks on the specimens are identical to those in Fig. 4.8.2

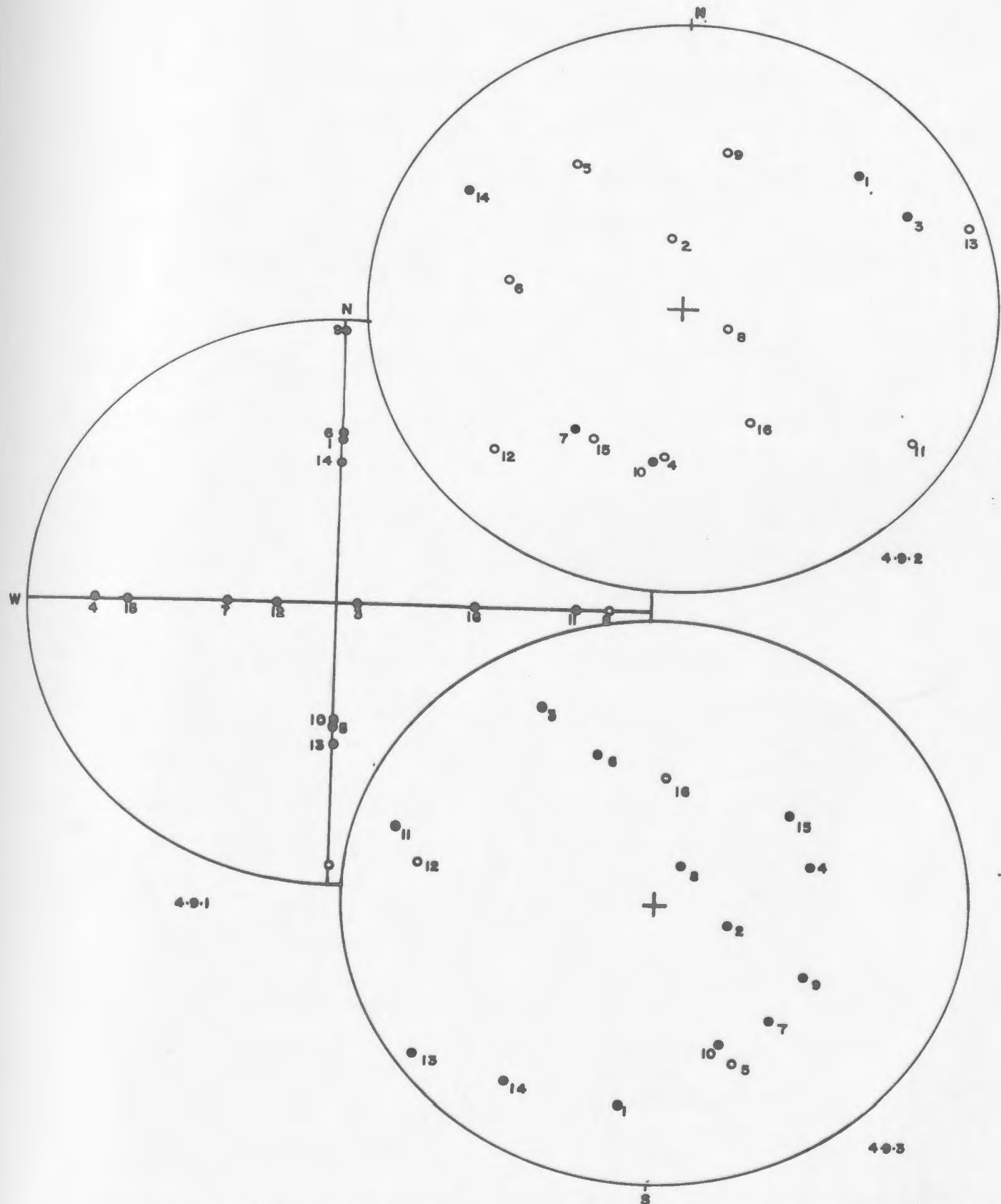
Figs. 4.9.1-4.9.3. Testing of the oven: Before and after heating to 760°C and cooling in 100γ horizontal field, acting northward

- Fig. 4.9.1 Directions of remanent magnetization (Fig. 4.8.3) relocated relative to the laboratory, prior to heat treatment
- Specimens have been rotated about the vertical and, in some cases, placed upside down (compare Fig. 4.7.1)
- Fig. 4.9.2 Directions of remanent magnetization relative to the laboratory after heating to 760°C and cooling in 100 horizontal field, acting northward
- Fig. 4.9.3 The specimens are positioned as in Fig. 4.9.1
- Fig. 4.9.3 Directions of remanent magnetization relative to the sampling sites, after heating to 760°C and cooling in 100γ horizontal field, acting northward
- The directions of the magnetization relative to the orientation marks on the specimens are identical to those in Fig. 4.9.2



Figs 4.8.1.-4.8.3. Testing of the oven: Before and after heating to 800°C and cooling in zero field

(refer caption)



Figs 4.9.1.-4.9.3. Testing of the oven: Before and after heating to 760°C and cooling in 100γ horizontal field, acting northward  
(refer caption)

the specimens were demagnetized to  $760^{\circ}\text{C}$ . The procedure was repeated three times, with demagnetization to  $750^{\circ}\text{C}$  in each case, and with the following fields applied during cooling: (ii) 500  $\gamma$  southwards; (iii) 19,000  $\gamma$  northwards (about equivalent to the horizontal component of the Earth's field); (iv) 49,000  $\gamma$ , declination  $\sim 0^{\circ}$ , inclination  $+67.5^{\circ}$ ; which is the total laboratory ( $\sim$  Earth's) field, obtained by switching off the field-nulling currents.

Prior to step (iii) (19,000  $\gamma$ ) only, the specimens were placed sideways, in "rolling" positions, to allow the remanence vectors to be placed into N, E, S, or W, directions horizontally (Fig. 4.11.1). Results of steps (i) - (iv) are shown in Figs. 4.9.2, 3; 4.10.2, 3; 4.11.2, 3; 4.12.2, 3; and Tables 4.3 and 4.4. With the 500  $\gamma$  southward field acting, there is a clear tendency towards lower inclinations relative to the laboratory, aligned towards south after treatment. The 19,000  $\gamma$  field, acting northward during cooling, aligned the directions mostly along the north-south meridian relative to the laboratory (Fig. 4.11.2). This spread of directions cannot easily be reconciled with the presence of a uniform inducing field of 19,000  $\gamma$ , when a 500  $\gamma$  field (i.e. only  $2\frac{1}{2}\%$  as large) resulted in the generally better alignment shown in Fig. 4.10.2.

Table 4.4 shows the directional scatter relative to the laboratory, with  $k$  remaining  $< 2$  (except for  $H = 500$   $\gamma$  south), even after the  $H = 19,000$   $\gamma$  step. Only after the final step (full laboratory field) does the grouping become tight ( $k = 12.9$ ), with steep downward inclinations as one would expect. The corresponding precision relative to sampling sites is again low ( $k = 1.10$ ), because

Figs. 4.10.1-4.10.3. Testing of the oven: Before and after heating to 750°C and cooling in 500γ horizontal field, acting southward.

Fig. 4.10.1 Directions of remanent magnetization (Fig. 4.9.3) relocated relative to the laboratory (prior to heating to 750°C and cooling in 500γ horizontal field, acting southward)

Specimens have been rotated about the vertical and, in some cases, placed upside down (compare Fig. 4.7.1)

Fig. 4.10.2 Directions of remanent magnetization relative to the laboratory, after heating to 750°C and cooling in 500γ horizontal field, acting southward

The specimens are positioned as in Fig. 4.10.1

Fig. 4.10.3 Directions of remanent magnetization relative to the sampling site, after heating to 750°C and cooling in 500γ horizontal field acting southward

The directions of the magnetization relative to the orientation marks on the specimen are identical to those in Fig. 4.10.2

Figs. 4.11.1-4.11.3. Testing of the oven: Before and after heating to 750°C and cooling in total horizontal field, acting northward.

Fig. 4.11.1 Directions of remanent magnetization (Fig. 4.10.3) relocated relative to the laboratory (prior to heating to 750°C and cooling in total horizontal field)

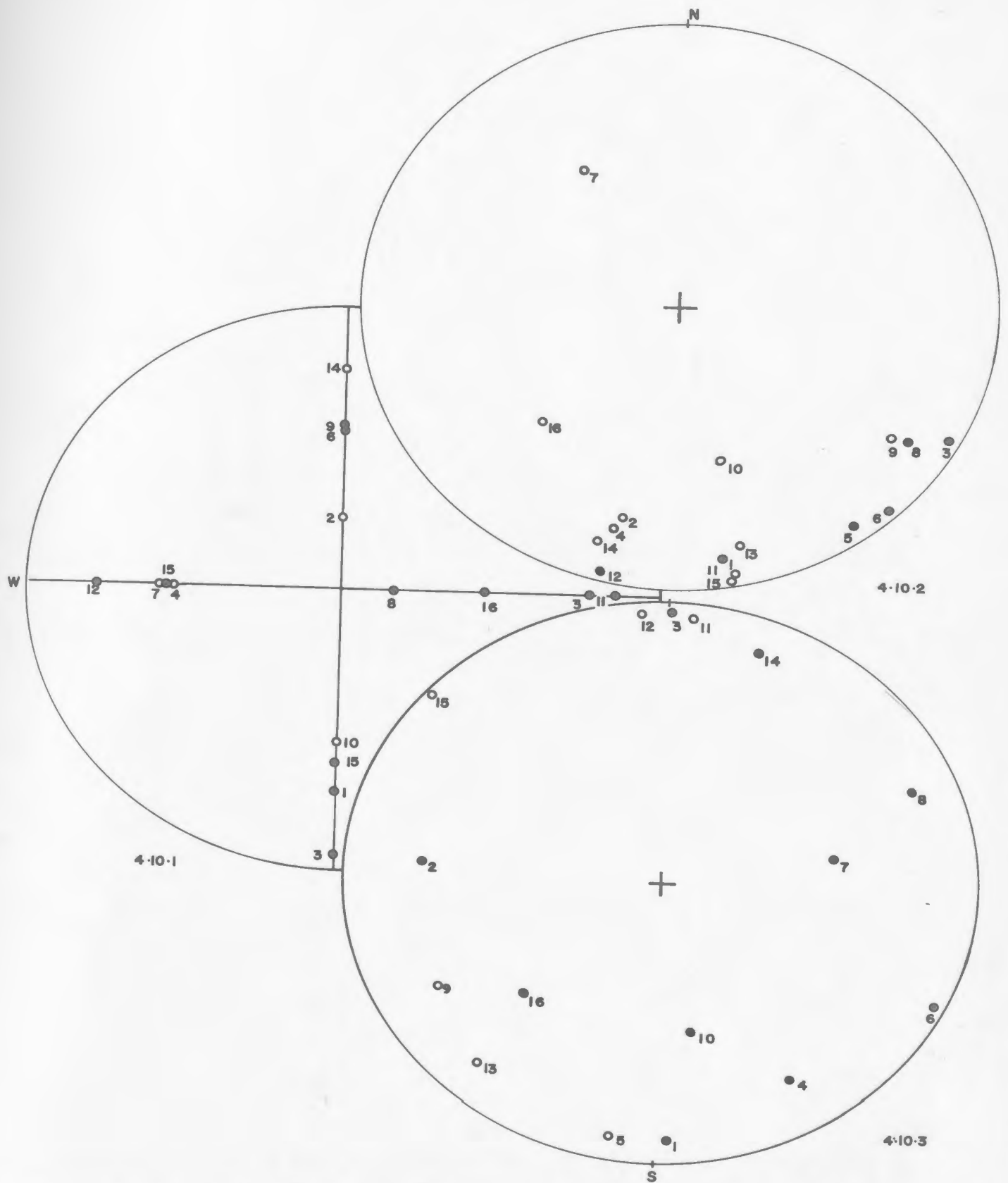
Specimens are placed sideways, with previously vertical plane containing the magnetization vector now lying horizontally and the vector pointing N.E.S. or W., as shown; i.e. all vectors have zero inclination relative to the laboratory.

Fig. 4.11.2 Directions of remanent magnetization relative to the laboratory, after heating to 750°C and cooling in total horizontal field (19,000γ), acting northward

The specimens are positioned as in Fig. 4.11.1

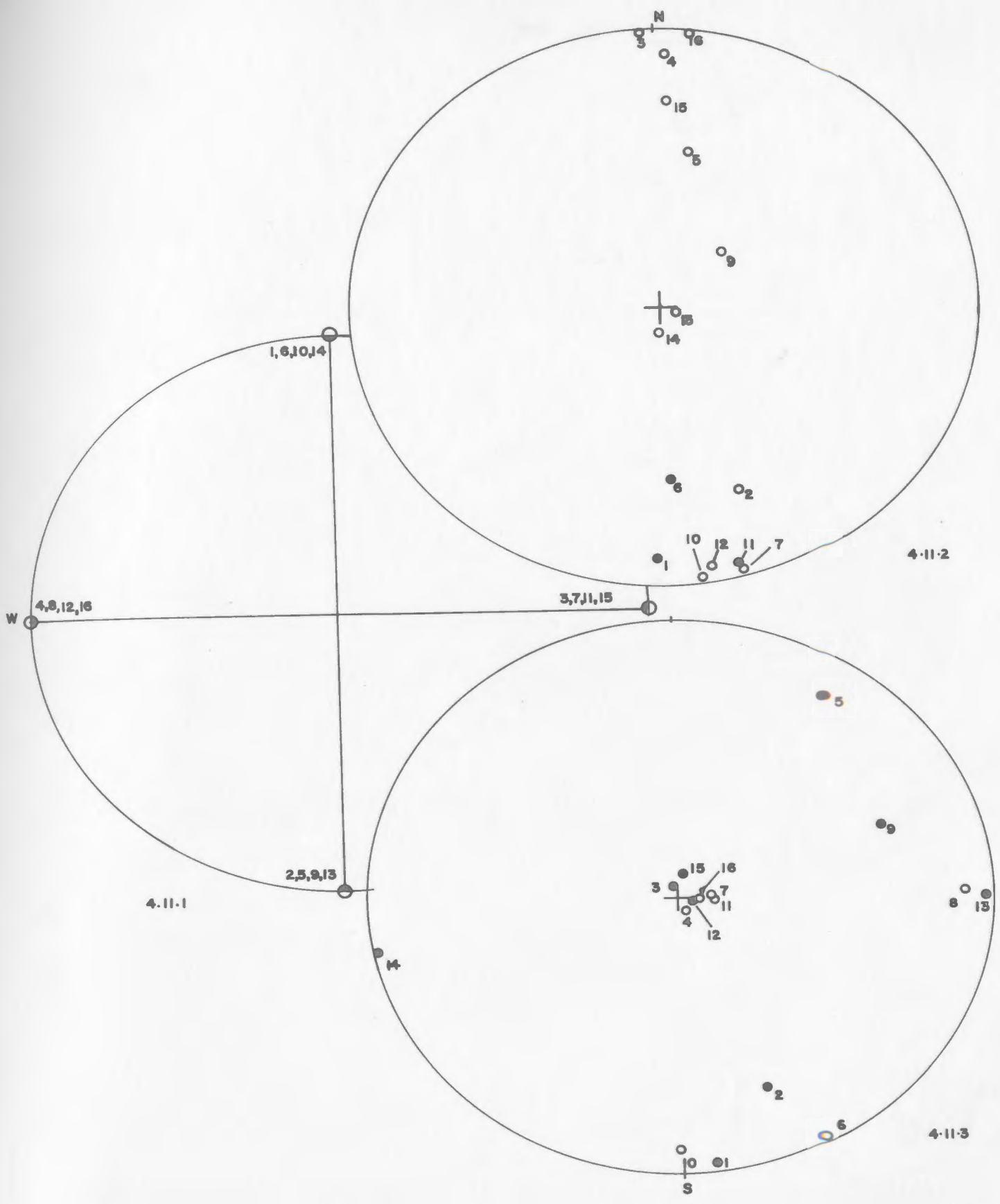
Fig. 4.11.3 Directions of remanent magnetization relative to the sampling site, after heating to 750°C and cooling in total horizontal field, (19,000γ) acting northward

The directions of the magnetization relative to the orientation marks on the specimen are identical to those in Fig. 4.11.2



Figs 4.10.1.-4.10.3. Testing of the oven: Before and after heating to 750°C and cooling in 500γ horizontal field, acting southward

(refer caption)



Figs 4.11.1.-4.11.3. Testing of the oven: Before and after heating to 750°C and cooling in total horizontal field, acting northward  
(refer caption)

Figs. 4.12.1-4.12.3. Testing of the oven: Before and after heating to 750°C and cooling in total laboratory field

Fig. 4.12.1 Directions of remanent magnetization (Fig. 4.11.3) relocated relative to the laboratory (prior to heating to 750°C and cooling in total laboratory field)

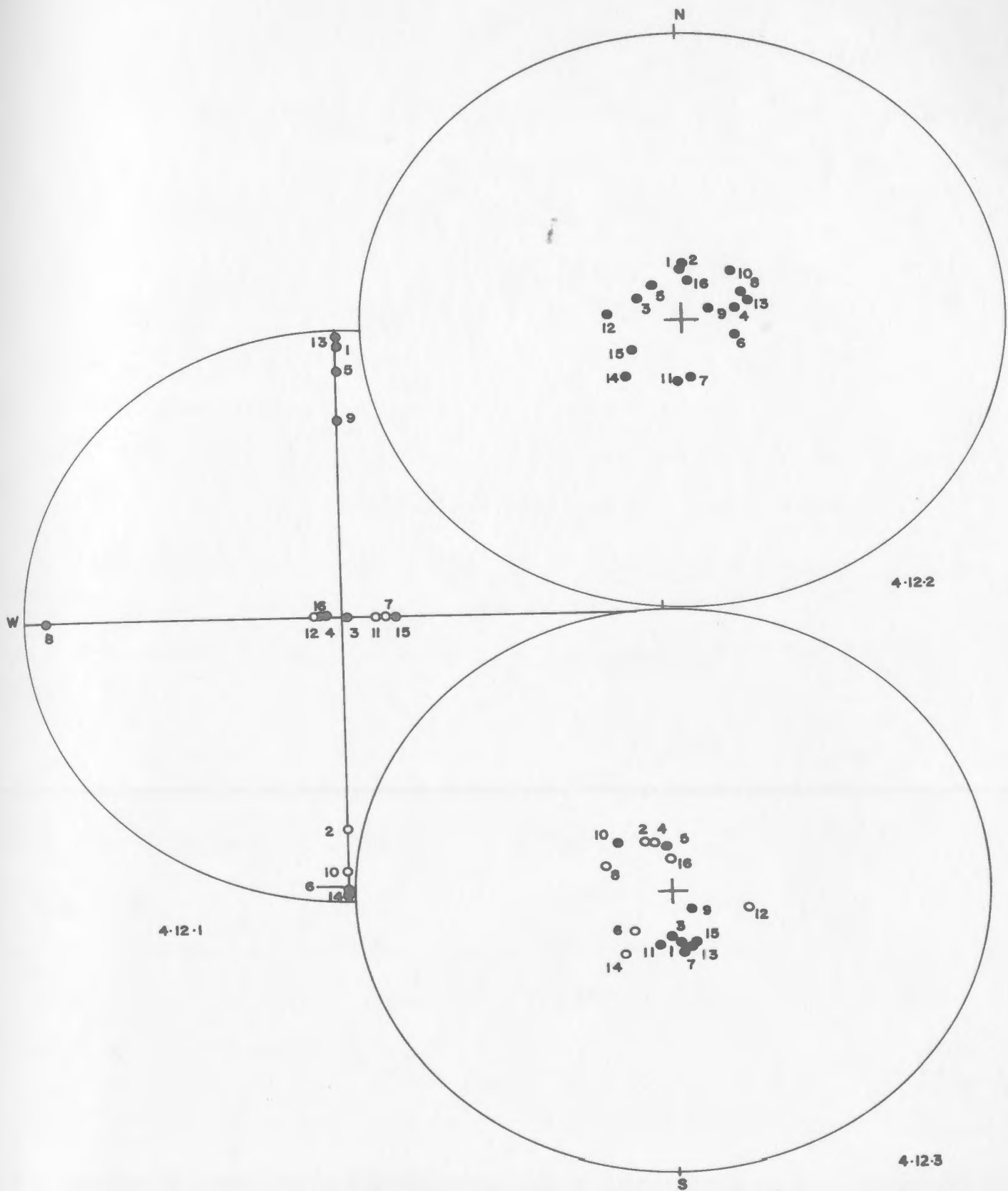
Specimens have been rotated about the vertical and, in some cases, placed upside down (compare Fig. 4.7.1)

Fig. 4.12.2 Directions of remanent magnetization relative to the laboratory, after heating to 750°C and cooling in total laboratory field (49,000γ)

The specimens are positioned as in Fig. 4.12.1

Fig. 4.12.3 Directions of remanent magnetization relative to the sampling site, after heating to 750°C and cooling in total laboratory field (49,000γ)

The directions of the magnetization relative to the orientation marks on the specimen are identical to those in Fig. 4.12.2



Figs 4.12.1.-4.12.3. Testing of the oven: Before and after heating to 750 C and cooling in total laboratory field  
(refer caption)

some of the specimens had been inverted as before.

The following conclusions were drawn from these oven tests:

(1) As the departures from complete randomization ( $k \sim 1$  for large  $N$ ) were similar in the magnitude after the second and third demagnetizations ( $T = 800^{\circ}\text{C}$ ,  $H = 0$ ;  $T = 760^{\circ}\text{C}$ ,  $H = 100 \gamma$ ) it is possible that fields up to about  $100 \gamma$  were in fact present also in the former case, though the field was then completely "nulled". This would be an "error" field corresponding to more than twice the field nulling error estimated in Section 4.5.

(2) Whilst the tendency towards systematic vector alignment was quite small after the treatments in  $H = 0$  or  $100 \gamma$  under (1), it became pronounced in fields of  $500 \gamma$  or more. To avoid causing significant errors in the remanence direction of any one specimen after treatment, the presence of fields exceeding  $100 \gamma$  during cooling should be avoided. In the case of specimens having prominent "soft" components, the maximum error fields to be tolerated may be less than  $100 \gamma$ .

(3) The effect of errors under (2) on the mean direction of  $N$  vectors subjected to simultaneous demagnetization can be largely (though not entirely) eliminated by suitable random positioning of remanence directions prior to treatment, provided  $N$  is sufficiently large.

#### 4.9. Second test of the oven.

Ten specimens (nos. 17 - 26) from the Henley Harbour basalts (Chapter 6) which had received no previous stability treatment, were selected for the test. The NRM directions (Table 4.5, Fig. 4.13) had

TABLE 4.5

## Second test of the oven

Specimen No.	Direction of magnetization						Intensity of magnetization			
	NRM		T=515°C, H=400γN		T=800°C, H=0		(emu/cc x 10 <sup>-4</sup> )			(Ratio)
	D	I	D	I	D	I	J <sub>n</sub>	J <sub>1</sub>	J <sub>2</sub>	J <sub>2</sub> /J <sub>1</sub>
17	334	+46	36	+1	321	-87	13.8	61.4	1.37	0.022
18	326	+82	39	+13	214	+43	14.4	22.9	2.40	0.105
19	359	+82	41	+12	11	+16	32.9	110	16.5	0.150
20	315	+68	326	+4	304	+55	32.3	104	4.32	0.042
21	99	+66	286	+14	188	-12	16.0	36.4	5.77	0.159
22	119	+77	305	+1	13	+7	16.6	78.6	5.41	0.070
23	20	+57	13	-1	56	-1	15.9	121	13.0	0.107
24	359	+62	49	+3	98	+31	17.7	85.4	6.83	0.080
25	68	+78	230	+7	247	+36	16.9	95.2	12.3	0.129
26	89	+66	335	+2	173	+32	11.8	60.6	0.48	0.008
Mean	19	+76	353	+8	95	+81	18.7	77.6	6.83	0.088
k	14.5		2.22		1.17					

The specimens are from basalt at Henley Harbour, Labrador (Chapter 6).

D = declination (deg.), I = inclination (deg., positive downward); D and I are quoted relative to the sampling site. H = applied field during cooling from temperature T. J<sub>n</sub>, J<sub>1</sub>, J<sub>2</sub> = intensity of magnetization of NRM, and after first and second demagnetization; k = best estimate of precision

a steep inclination, while declinations ranged over three quadrants.

After the "empty run" (Sections 4.5, 4.7) the specimens were arranged on the specimen stand in the oven, five each on the upper (17 - 21) and lower (22 - 26) compartment, with their remanent directions pointing to laboratory north. The specimens were now heated to  $515^{\circ}\text{C}$  and cooled in an uncompensated field directed northward. The directions after treatment (Figs. 4.14, Table 4.5), show a tendency towards shallow inclinations in the lower hemisphere (except specimen 23) with a precision of  $k = 2.22$  relative to the sampling sites. The declinations show a relatively wide distribution in the first and fourth quadrants (except no. 25), though the mean direction ( $D = 353^{\circ}$ ,  $I = +8^{\circ}$ ) is close to that of the applied field. The scatter may be at least partly due to the presence of PTRM components that were not randomized by the treatment, since the demagnetizing temperature ( $515^{\circ}\text{C}$ ) was below the highest Curie points associated with these specimens.

Once again the specimens were arranged with their declination pointing north, heated to  $800^{\circ}\text{C}$  and cooled in zero field. After this treatment, the scatter of directions relative to the sampling sites (Fig. 4.15) had increased ( $k = 1.17$ ) with a full range of positive and negative inclinations, and with declinations in all four quadrants.

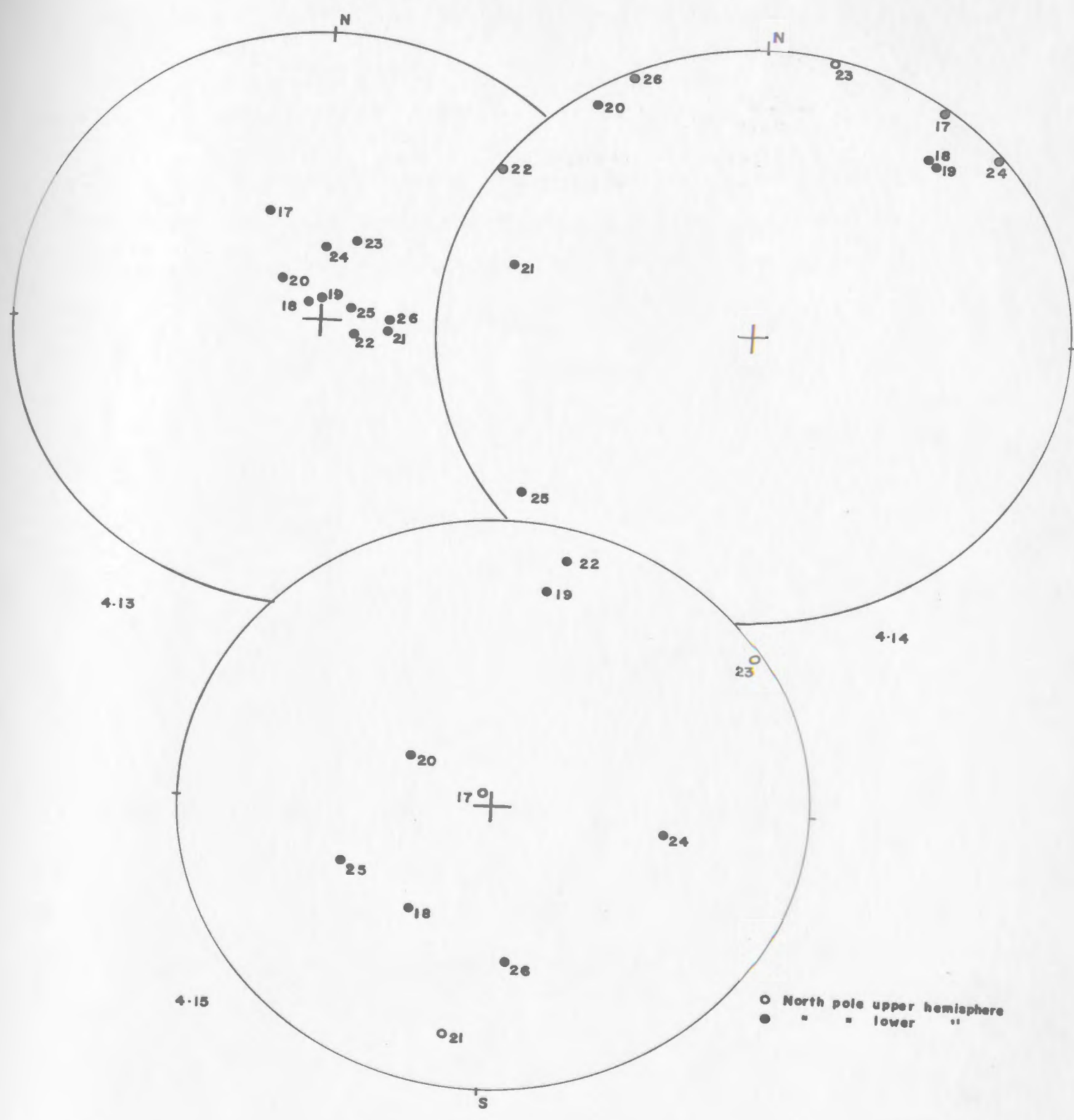
Directions and intensities of magnetization of the specimens after the two heat treatments are tabulated in Table 4.5. Intensities ( $J_1$ ) after the first treatment ( $T = 515^{\circ}\text{C}$ ,  $H = 400 \gamma$ ,  $N$ ) ranged from  $20 - 125 \times 10^{-4}$  emu/cc. After the second demagnetization ( $T = 800^{\circ}\text{C}$ ,  $H = 0$ ) the intensities were reduced to  $0.5 - 16.5 \times 10^{-4}$  emu/cc,

Caption for Figs 4.13.,4.14.,4.15. Second test of the oven

- Fig 4.13. NRM directions relative to the sampling sites  
Equal area projection, with the circumference corresponding to the horizontal plane at the sampling site
- Fig 4.14. Directions of remanent magnetization relative to the sampling sites, after heating to  $515^{\circ}\text{C}$  and cooling in  $400\gamma$  horizontal field, acting northward
- Fig 4.15. Directions of remanent magnetization relative to the sampling sites, after heating to  $800^{\circ}\text{C}$  and cooling in zero field

North pole : ● in lower hemisphere: ○ in upper hemisphere:

Numbers refer to specimens from Henley Harbour



Figs 4.13., 4.14., 4.15. Second test of the oven:

equivalent to an average demagnetization of the specimens by 90% since the first step.

The result of the treatment with  $H = 400 \gamma N$  (Fig. 4.14, Table 4.5) is not dissimilar to that obtained in a comparable field ( $H = 500 \gamma S$ ) during the first oven tests (Figs. 4.10.2, 4.10.3; Table 4.4); in both cases the resulting inclinations are systematically low, while there is a wide range of declinations. Comparison of the 500  $\gamma$  results with those of other steps of the first oven tests (Section 4.8) had led to the conclusion that fields up to 100  $\gamma$  may have been present in some cases when the field was "nulled"; however, in the case of the specimens actually used, such fields seemed to be insufficient to prevent almost complete randomization of directions when the specimens were cooled from above their Curie points.

These conclusions seem to be confirmed by the results of the second oven test. If one assumes that the intensity  $J_1$  is mainly due to the magnetization acquired in the 400  $\gamma$  field when the specimens cooled from 515°C, the mean value of  $J_2/J_1$  ( $\sim 0.1$ ) suggests that a field roughly one order of magnitude smaller than 400  $\gamma$  (say, 50 - 100  $\gamma$ ) was present during the second step ( $T = 800^\circ\text{C}$ ,  $H = "0"$ ). However, the latter step succeeded in randomizing the directions almost completely, despite the fact that absolute values of  $J_2$  remained relatively high (several times  $10^{-4}$  emu/cc).

From the results of the two oven tests, it was concluded that the unit was capable of performing satisfactory thermal demagnetization of rock specimens without introducing significant errors, provided a careful procedure was followed. The treatment of very weakly magnetized

or largely unstable specimens would require a further improvement in the apparatus.

## CHAPTER 5

### THERMAL DEMAGNETIZATION OF THE

#### KILLARY HARBOUR IGNIMBRITES

##### 5.1. Introduction

Results of alternating-field demagnetization of the ignimbrites from Killary Harbour, Eire (Chapter 3) showed that a stable component was responsible for most of the NRM in nearly all specimens. However, a.c. demagnetizations is not necessarily capable of removing stable secondary components (Wilson, 1961; Irving et al, 1965). With a sufficiently wide distribution of blocking temperatures, thermal demagnetization could then succeed when a.c. treatment has failed. More generally, thermal demagnetization is useful in providing an additional stability criterion by its unique ability of distinguishing different components through differences in blocking temperature.

Thermal analysis may be useful in separating the "thermally discrete" components of the remanent magnetization, in which the blocking temperatures are confined to a narrow temperature interval in the neighbourhood of 100°C below the Curie temperature, from the "thermally distributed" components, in which the blocking temperatures may range from room temperature to, say 500°C (Roy et al, 1967). Hence in volcanic rocks having, one or more components of partial thermoremanent (PTRM) origin in addition to a (presumed primary) TRM component, thermal demagnetization is likely to provide a useful supplementary, if not superior technique to alternating or a.c. demagnetization, particularly if the blocking temperatures of the

different components are well differentiated.

## 5.2. Polished section study.

Dr. N. D. Watkins of Florida State University has kindly examined a polished section each from two ignimbrite samples (KH2, KH 21; Sites A and B respectively). Details are given in Appendix 3. These sections revealed the prominent presence of hematite, in the form of relic structure or as intergrowths with the original titanomagnetite, and even pseudobrookite, which is characteristic of an advanced oxidation state. Accordingly, Dr. Watkins classified these specimens under "Oxidation Index VI" (Wilson et al, 1968), corresponding to the highest degree of oxidation. The oxidation might have accompanied some tectonic and volcanic activity occurring a geologically long time after the ignimbrites were formed, or alternatively in the late stages of the original volcanic activity (Watkins and Haggerty, 1965). The latter interpretation is favoured here, since the simple folding of the Mweelrea syncline indicates that the formations were not greatly affected by post-Ordovician tectonic movements (Chapter 2).

All thermal demagnetizations were carried out in air, since in the case of highly oxidized rocks an oxygen-bearing atmosphere probably has little effect in changing the remanent magnetization (Vincenz, 1968). On the other hand, heating in a reducing atmosphere such as nitrogen might have resulted in chemical changes likely to destroy any primary magnetization component, thus making the specimen useless.

### 5.3. Preliminary study of the ignimbrites.

Six ignimbrite specimens representing the three Killary Harbour sites were chosen for a pilot progressive demagnetization. They were arranged in the oven with randomly oriented NRM directions, three specimens each being placed on the upper and lower compartment; the separation between specimens was 4-5 cms. The demagnetization procedure was as described in Section 4.7. The aim of the pilot study was to determine some optimum demagnetization temperature. The same procedure as in the a.c. demagnetization (Section 3.1.) was adopted, i.e. the temperature above which further treatment produced no systematic changes in the remanence direction of the pilot specimens was tentatively regarded as the optimum one. Results are shown in Table 5.1. and Figures 5.1.1. - 5.1.6.

#### Site A, Specimen KH 7aII.

The NRM direction of this specimen (Fig. 5.1.1.) differed by a large angle from the present and dipole fields, but was typical of NRM directions found in other specimens from Site A (Fig. 3.1.). This, combined with the fact that the direction changed very little after demagnetization, is indicative of at least partial stability. The relatively large intensity increase observed after the first demagnetization step ( $150^{\circ}\text{C}$ ) may be due to removal of an unstable component directed nearly antiparallel to the principal component responsible for the NRM. The  $(J/J_n) - T$  graph suggests that the latter component has a blocking temperature above  $400^{\circ}\text{C}$ , where there is a sharp fall of intensity, accompanied by a change to both smaller inclination and

TABLE 5.1

Pilot thermal demagnetization of ignimbrite  
specimens from Killary Harbour

T (°C)	Site A Band 1						Site C Band 5		
	KH 7aII			KH 8a			KH 15aI		
	D	I	Jx10 <sup>-5</sup>	D	I	Jx10 <sup>-5</sup>	D	I	Jx10 <sup>-5</sup>
NRM	166	-23	5.0	96	-63	22.5	81	+75	12.7
150	161	-27	7.7	no measurement			87	+68	12.6
275	159	-23	6.9	50	+12	13.2	74	+67	11.4
300	163	-25	6.7	45	+2	13.4	82	+68	11.5
400	162	-20	6.4	35	+32	22.0	78	+65	11.3
500	131	0	2.9	38	+34	10.0	76	+64	10.4
550	103	-18	3.0	13	-5	25.7	80	+63	9.3
600	46	+21	5.1	13	-1	26.3	358	+60	3.0
650	82	-24	19.9	300	-53	27.2	350	+68	1.5
670	93	+19	8.6	38	+47	12.4	39	+59	0.9

D = declination (degrees, taken clockwise from north through 360°)

I = inclination (degrees, + indicates north pole in lower hemisphere)

J = intensity of magnetization in emu/cc

Values of D, I, and J quoted are after demagnetization in zero field, and in air, to the temperatures (T°C) indicated.

TABLE 5.1 (Continued)

T (°C)	Site B Band 3			Site B Band 4					
	KH 22a			KH 20			KH 25aI		
	D	I	Jx10 <sup>-5</sup>	D	I	Jx10 <sup>-5</sup>	D	I	Jx10 <sup>-5</sup>
NRM	90	+65	57.9	65	48	27.1	109	67	54.4
150	94	+66	56.8	62	49	31.6	103	64	48.4
275	95	+66	53.1	64	58	38.1	110	61	46.6
300	102	+62	47.0	62	56	35.8	98	57	44.4
400	98	+62	53.5	59	58	37.0	100	56	39.1
500	95	+65	29.2	63	55	23.5	101	56	39.7
550	203	+66	4.7	51	45	10.2	88	62	8.9
600	205	-31	3.2	76	74	5.6	350	67	8.9
650	115	-46	20.8	50	-47	8.7	297	58	38.0
670	149	-78	2.9	113	-23	5.4	18	62	21.2

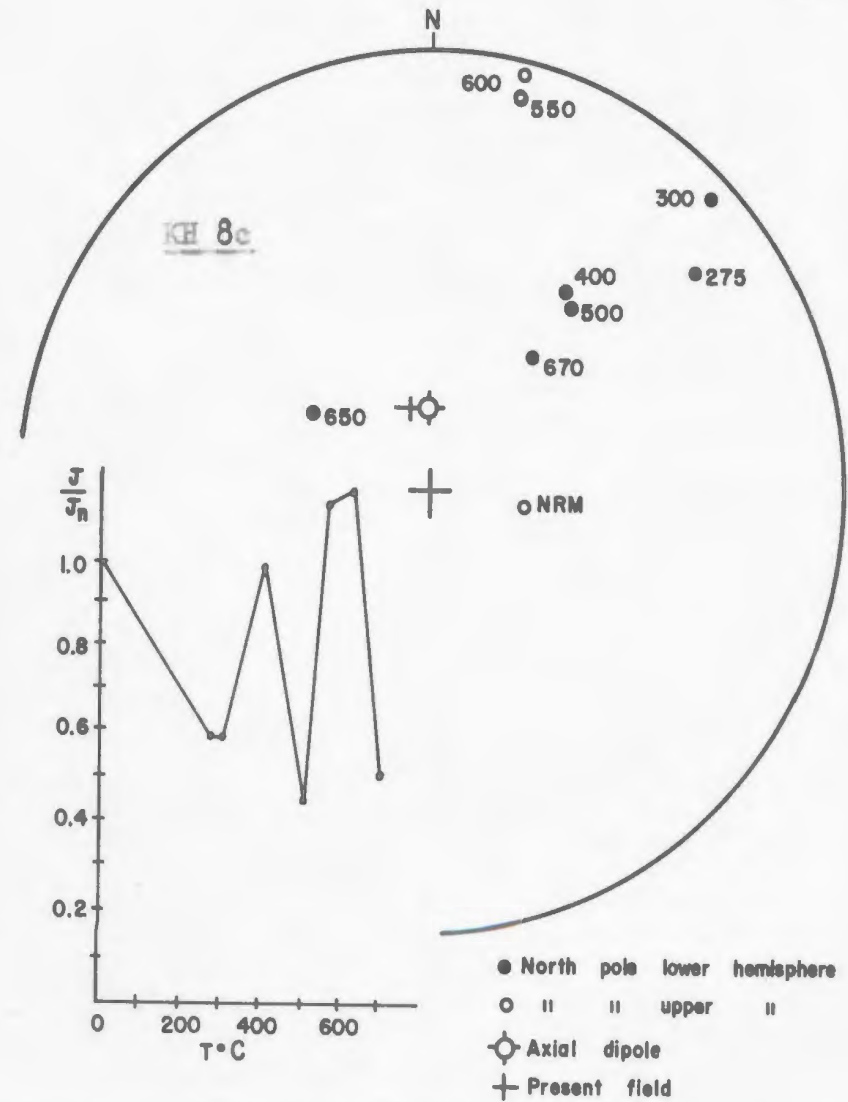
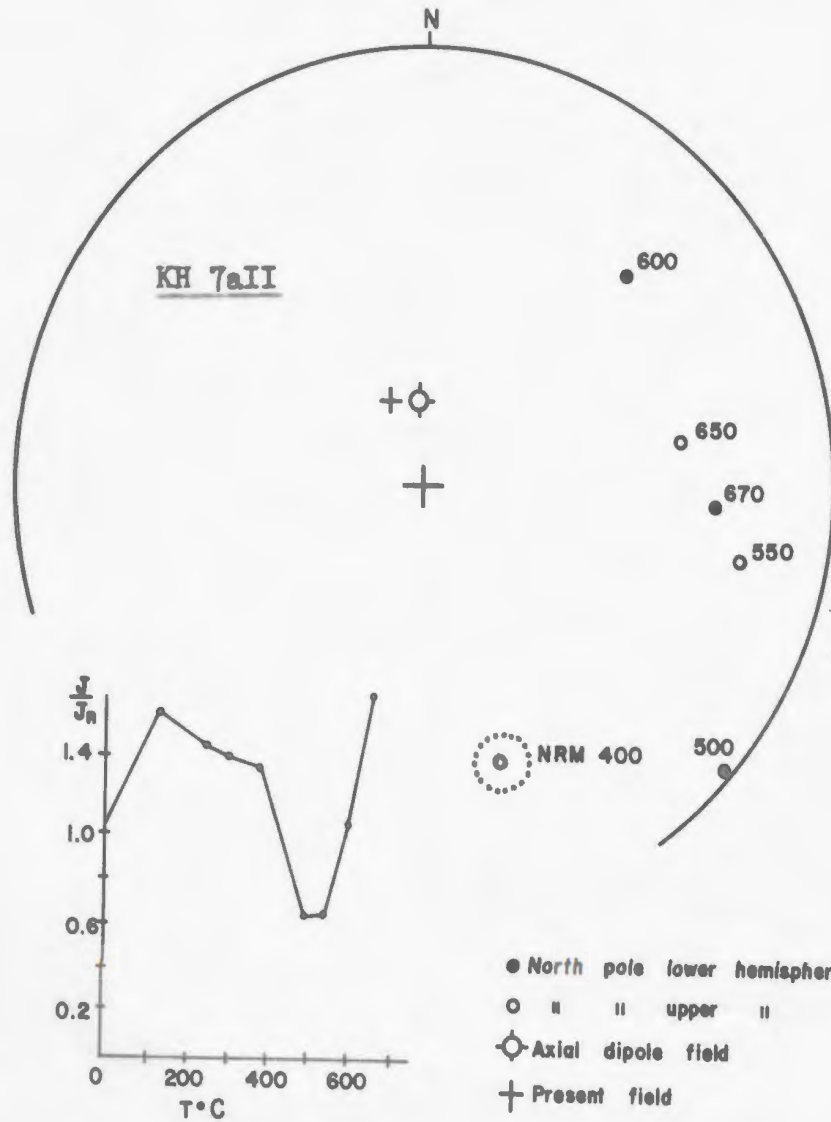
smaller declination at 500°C. A similar directional change occurred in the a.c. demagnetization of pilot specimen KH 2a (also Site A) between the 560 and 795 oe steps (Fig. 3.1) but was not observed in the specimens from other sites; hence it may indicate in the rocks at Site A the presence of a small, stable component with blocking temperature above 500°C. Between 550°C and 670°C, the declinations became eastward to northeastward, with erratic alterations of polarity. This was accompanied by a sharp increase in intensity above 550°C. Opdyke (1964) observed a similar anomalous intensity rise during demagnetization of partially stable red sediments above 550°C, and suggests that the cause may be a chemical change during heat treatment of unknown nature, though unlikely to be due to magnetite formation, as the specimens were heated in air (as in the present study).

#### KH 8C.

This specimen responded erratically to heat treatment with respect to both direction and intensity of magnetization (Fig. 5.1.2). The NRM changed into shallow positive inclination at 275°C and 300°C, accompanied by a fall in intensity. The directions corresponding to these and all but one of the remaining steps in the heat treatment lie in the first quadrant and diverge widely from the presumed "stable" directions in the second quadrant found in the previous case (specimen KH 7aII) at steps up to 500°C, and which in turn are similar to the directions of most Site A samples after a.c. demagnetization to 540 oe (Fig. 3.2, Table 3.2). The thermal results for KH 8C suggest the dominant presence of an unstable component. This may be compared to

Figs 5.1.1.-5.1.2. Pilot demagnetization of specimens KH 7aII, KH 8c, Site A, Band 1

Equal area plot of directions of magnetization after cooling from the temperature shown (in °C)



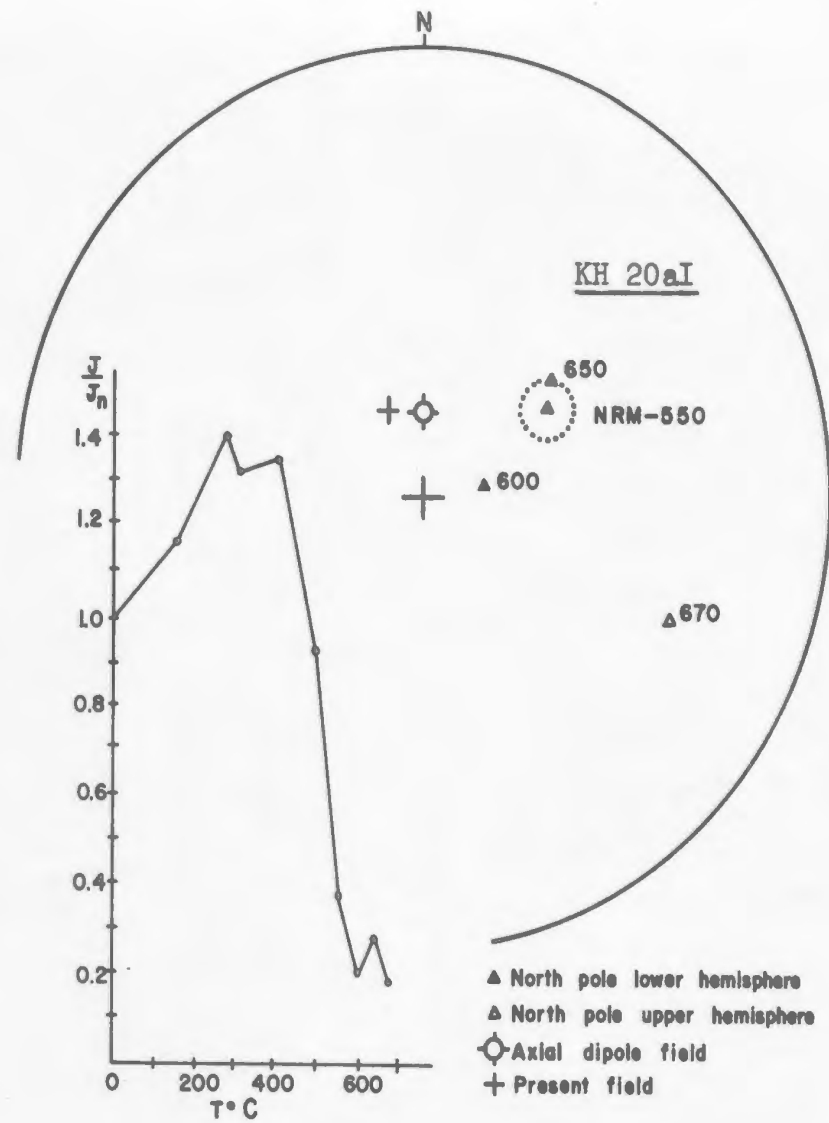
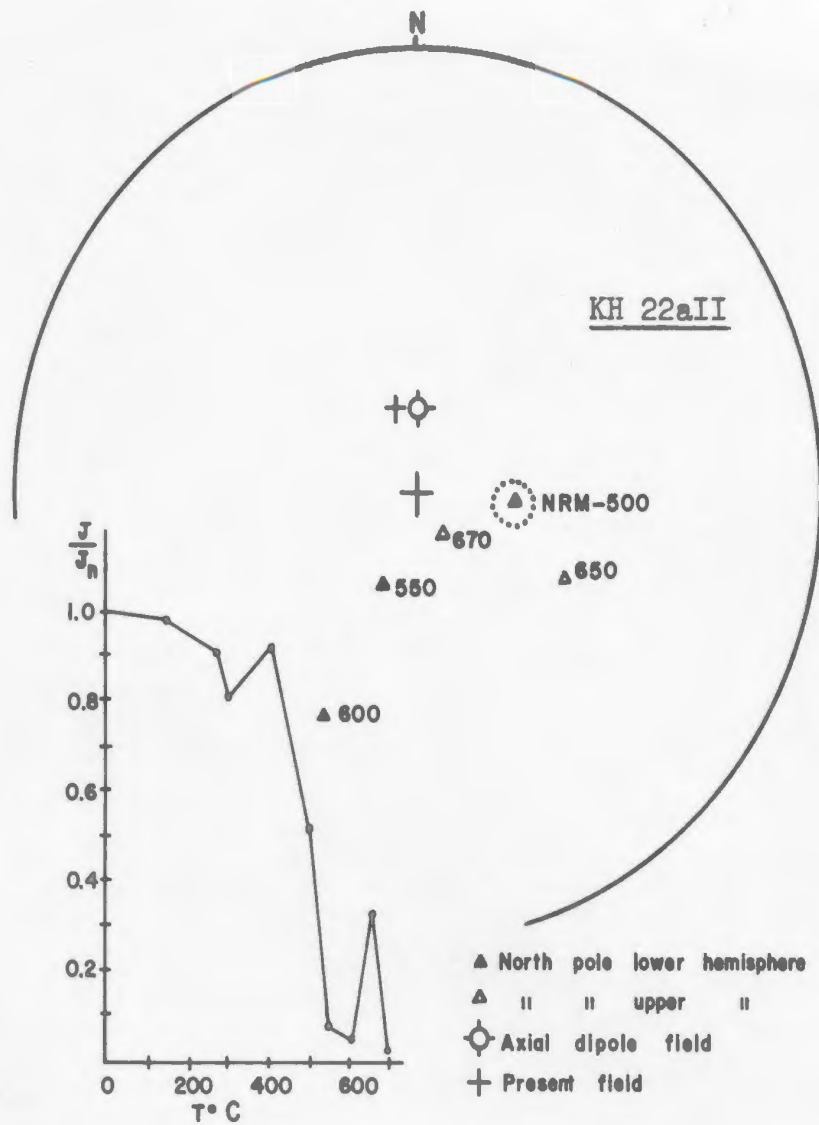
Within the dotted line, directions were nearly constant over the range of steps shown.  
Inset: Normalized intensity of magnetization,  $J/J_n$ , corresponding to the same steps in treatment

the a.c. demagnetization of pilot specimen KH 8a (from the same sample), where fields of the order of 100 oe were sufficient to remove a prominent (unstable) NRM component directed close to the present Earth's field, leaving a component in the second quadrant with direction close to the "stable" directions of specimen KH 7aII and KH 2a (Fig. 3.1).

It may therefore be concluded that, whereas specimens KH 8a and KH 8C both exhibited dominant unstable NRM components, thermal demagnetization of the latter, unlike a.c. treatment of the former, was unsuccessful in isolating a stable component.

#### Site B, Specimens KH 20a, 22a, 25aI.

The three specimens, having similar NRM directions, also responded in a fairly similar manner to heat treatment (Figs. 5.1.3. - 5.1.5). As was pointed out in connection with the a.c. treatment (Chapter 3) the results of stability studies are especially important in the case of specimens such as these, where the NRM directions lie fairly close to the present field and axial dipole directions. Except for an increase in intensity up to 275°C in the case of specimen KH 20a, the three (J/J<sub>n</sub>) -T curves are similar, exhibiting minima in the ranges 300 - 400°C and 550 - 600°C. The former minimum (also found in the case of Specimens KH 8C and, less prominently, KH 7aII and 15a) probably results from the removal of a relatively small secondary component. The high-temperature minimum in each case follows a sharp drop in intensity suggesting that the principal blocking temperature range is 400 - 600°C, but that a small component with Curie point above 600°C has not been removed at 600°C. Since the directions above 550°C seem to change erratically in the case of all three specimens, whereas



Figs 5.1.3.-5.1.4. Pilot demagnetization of specimens KH 22aII Site B, Band 3, KH 20aI, Site B, Band 4

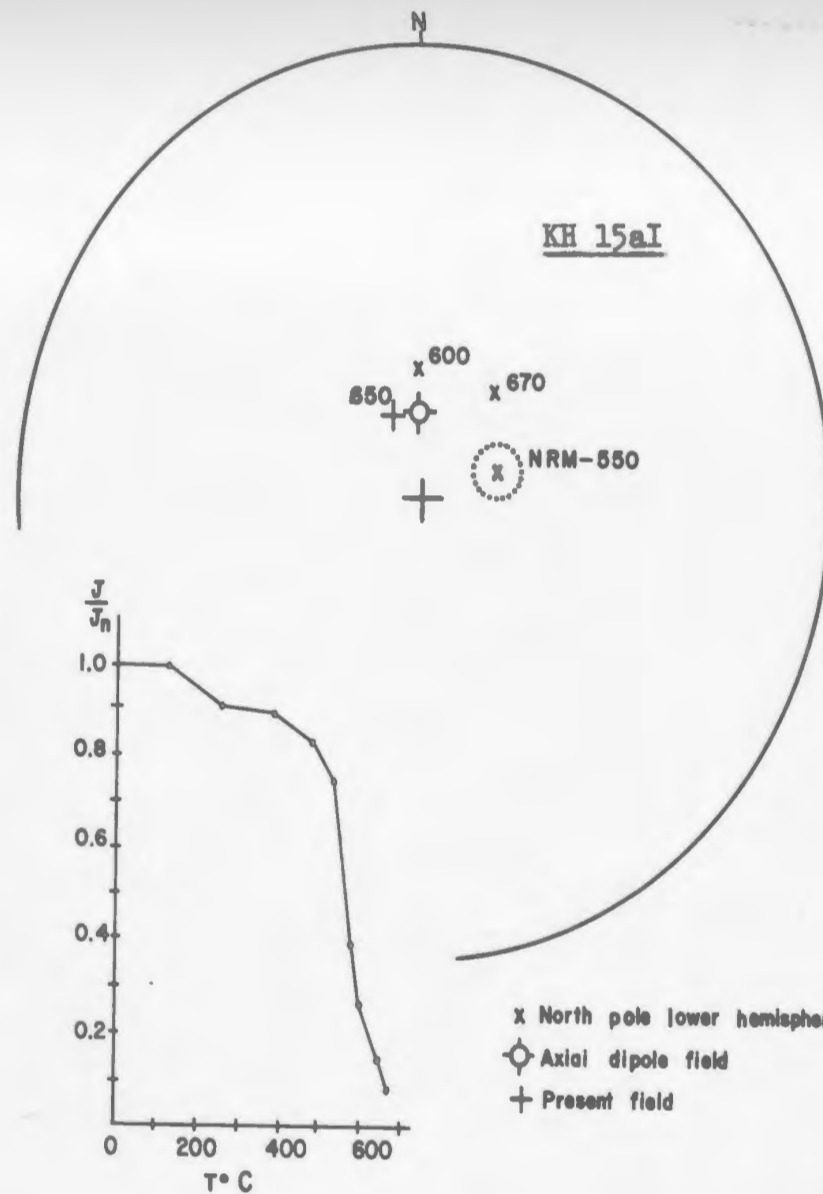
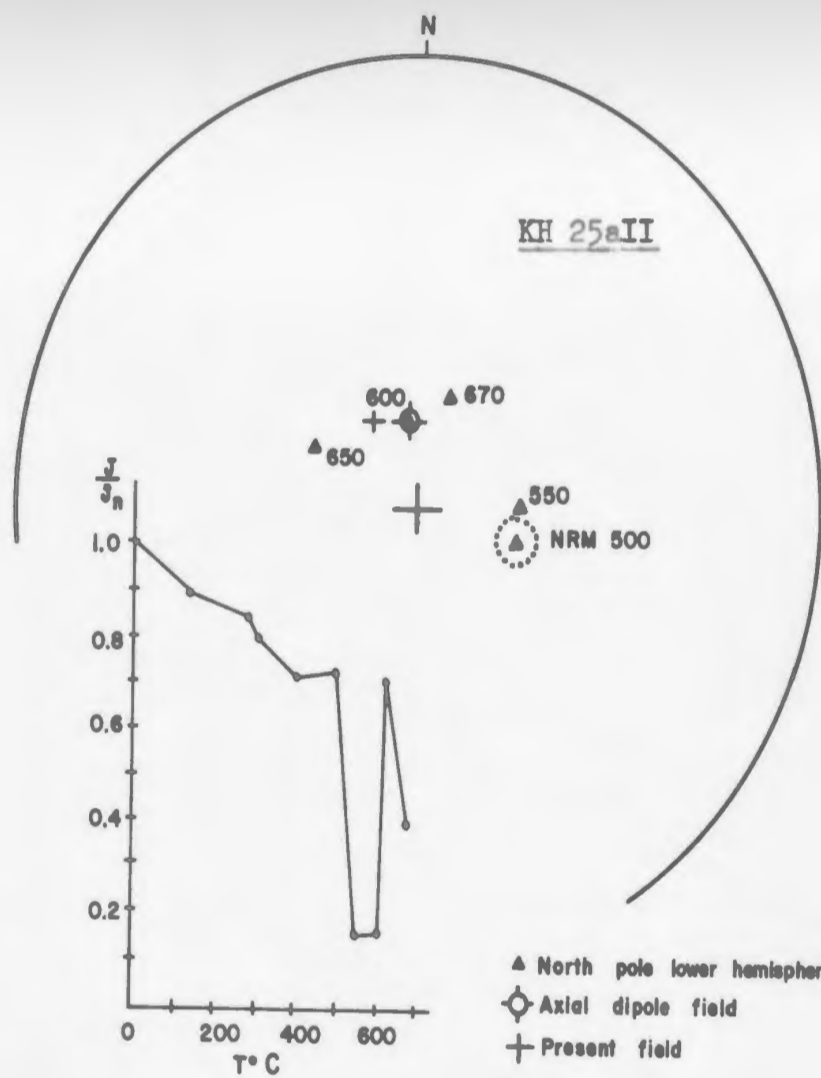
Notation as in figs 5.1.1-5.1.2.

they remain well-grouped up to that temperature, it is probably safe to conclude that the directions for the NRM and steps up to 550°C correspond mainly to a stable component. This conclusion is reinforced by the results of a.c. demagnetization of specimens from Site B (e.g. pilot Specimen KH 25aII, Fig. 3.1). For these, the directions after demagnetization to 540 oe or higher were mostly stable and similar to the directions of the present specimens (KH 20a, 22a, 25aI) up to 550°C.

Site C, Specimen KH 15a.

The directions before and after demagnetization to 550°C (Fig. 5.1.6) appear to be stable up to 550°C, and similar to Site B directions. At 600° to 670°C the direction has changed towards that of the present field. The  $(J/J_n) - T$  curve, except for the small suggested minimum at 300°C, shows the simple trend typical of single-component ferromagnetics with a dominant "thermally discrete" component (Irving and Opdyke, 1965) in the fairly narrow blocking temperature range of 500°C - 600°C, though a smaller component is apparently still present above 600°C. Both the observed directional stability up to 550°C and the trend of the  $(J/J_n) - T$  curve would be consistent with the behaviour of a high-coercivity component. This may correspond also to the "hard" component revealed in specimen KH 16b from the same Site (C), which retained over 60% of its NRM after a.c. demagnetization to 795 oe (Fig. 3.1).

In summary, specimen KH 8C, gave no evidence of stability, whereas the five other pilot specimens had well-grouped directions over the range NRM - 400°C. In Specimens 22aII, 20a, 25aI, and 15a, the



Figs 5.1.5.-5.1.6. Pilot demagnetization of specimens KH 25aII, Site B, Band 4, KH 15aI, Site C, Band 5

Notation as in Figs 5.1.1.-5.1.2.

grouping continued to be close up to the 500°C or 550°C steps, whereas in the case of KH 7aII the 500°C direction is removed from the close vector grouping over the NRM - 400°C range. Comparison with the results of a.c. demagnetization (Chapter 3) suggests however that the 500°C result may be as representative of a "stable" direction for Site A as are the ones up to 400°C. The  $(J/J_n) - T$  curves of the five "stable" specimens indicate the presence of "thermally distributed" components in the range NRM - 400°C or higher, and a more or less prominent "thermally discrete" component with blocking temperatures between 400°C and 600°C. The removal of a small component suggested by the trend of the curves between 300°C and 400°C was not accompanied by a signified directional change.

The directions of the five "stable" specimens were fairly close to those from representative samples at corresponding sites after a.c. demagnetization to 540 oe (Table 3.1, Fig. 3.1). To confirm and extend the pilot results, thermal treatment of additional samples from the three sites was desirable. From the pilot study it appeared that the best results would be achieved by demagnetization to temperatures in the 400 - 500°C region. Results of this further study are discussed below.

#### 5.4. Extended thermal demagnetization.

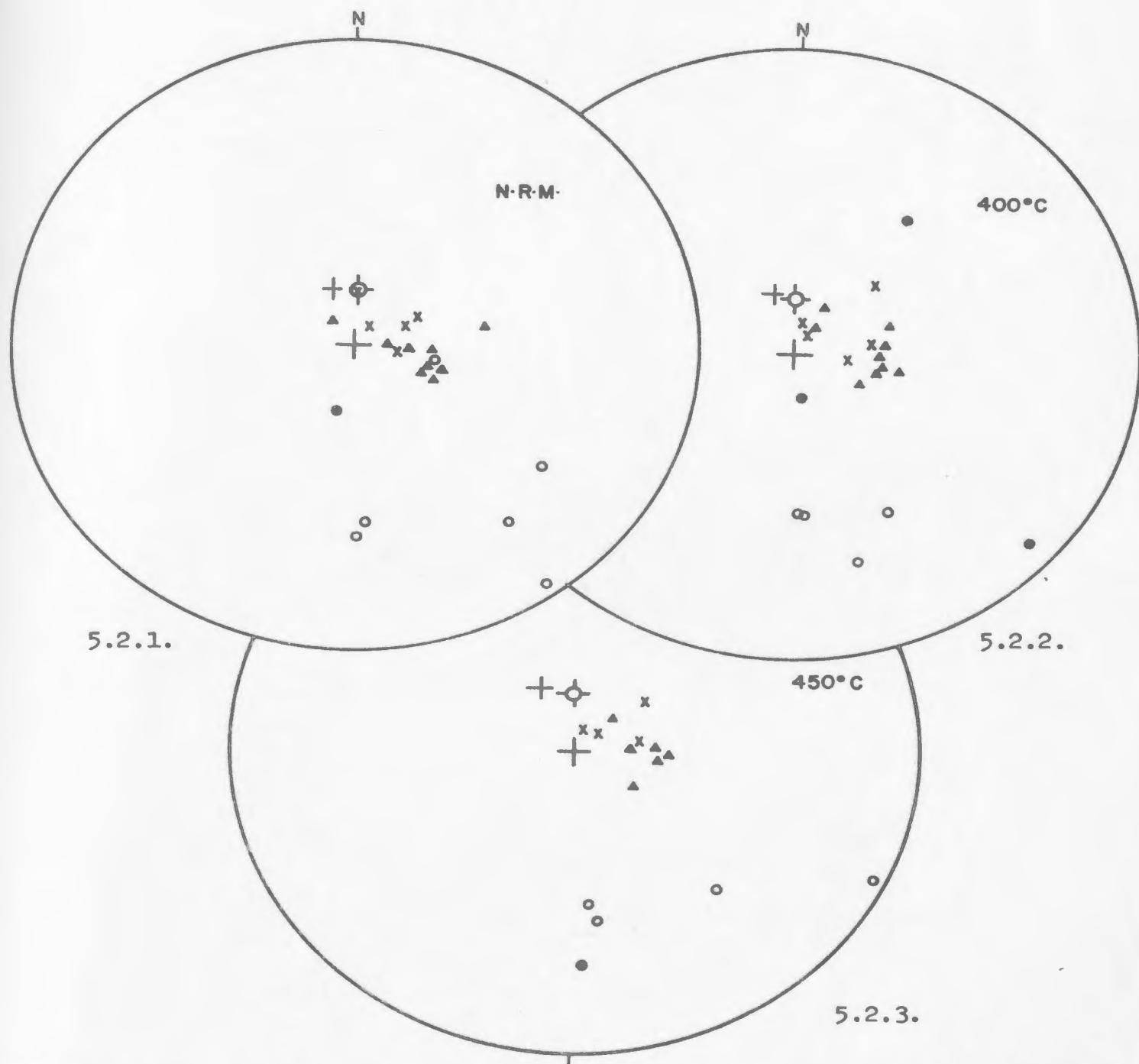
A total of 15 specimens (5, 6 and 4 from Sites A, B and C, respectively) were thermally demagnetized at 400°, 450°, 500° and 670°C. Since the pilot study was not carried out at 450°C, results shown for that temperature (Fig. 5.2.3) are based on the 15 specimens of the

TABLE 5.2

Extended demagnetization of ignimbrite specimens from Killary Harbour.

(Symbols as in Table 5.1)

Site Band	Specimen (KH)	NRM			400°C			450°C			500°C			670°C			
		D	I	Jx10 <sup>-5</sup>	D	I	Jx10 <sup>-5</sup>	D	I	Jx10 <sup>-5</sup>	D	I	Jx10 <sup>-5</sup>	D	I	Jx10 <sup>-5</sup>	
↑ A ↓	↑ 1 ↓	5aI	138	-17	16.1	139	-30	13.1	134	-27	13.9	161	-28	2.1	332	+29	2.6
		7dI	176	-25	12.2	175	-34	12.9	173	-37	11.7	164	-17	0.7	239	-52	5.2
		7eI	171	-29	11.1	173	-33	10.8	172	-33	10.5	177	-9	1.8	336	+29	5.4
		9c	187	+65	38.9	167	+73	6.6	176	+20	13.4	207	+23	9.8	262	+55	34.6
		9d	140	-2	15.1	129	+4	22.1	114	-1	20.1	97	+55	8.3	106	+79	12.4
↑ B ↓	↑ 3 ↓	23aI	103	+59	57.7	102	+62	48.6	95	+61	51.2	99	+58	45.6	346	-37	25.1
		23bI	114	+63	50.7	117	+67	44.0	120	+67	44.8	110	+61	39.6	260	-41	12.5
		24bII	90	+73	74.6	30	+69	43.8	43	+72	40.1	57	+72	38.6	5	-41	1.0
		24cII	319	+78	67.2	36	+78	67.8	85	+63	39.0	87	+64	40.3	50	-76	14.7
↑ B ↓	↑ 4 ↓	21aII	88	+79	53.3	81	+64	46.3	81	+71	42.6	66	+58	44.6	too weak to measure.		
		25aIII	105	+66	52.6	92	+61	42.7	95	+61	37.1	82	+56	40.5	77	-42	19.4
		10bII	29	+82	4.5	31	+80	3.6	35	+78	3.5	14	+87	1.1	352	-26	0.7
↑ C ↓	↑ 5 ↓	11a	58	+68	2.2	44	+54	1.1	48	+60	1.2	42	+69	0.7	69	+87	0.9
		14b	359	+72	4.1	16	+79	2.2	12	+81	2.8	346	+83	1.2	312	+72	2.0
		16a	61	+71	7.7	93	+72	5.3	77	+69	5.4	66	+68	5.2	too weak to measure.		



Figs 5.2.1. - 5.2.3. Extended progressive thermal demagnetization of the Killary Harbour ignimbrites

Equal area projections, showing 5.2.1. NRM directions of 21 specimens; 5.2.2. directions after demagnetization to 400°C (21 specimens); and 5.2.3. directions after demagnetization to 450°C (15 specimens, excluding 6 pilot study specimens).

(All symbols as in Figure 3.1)

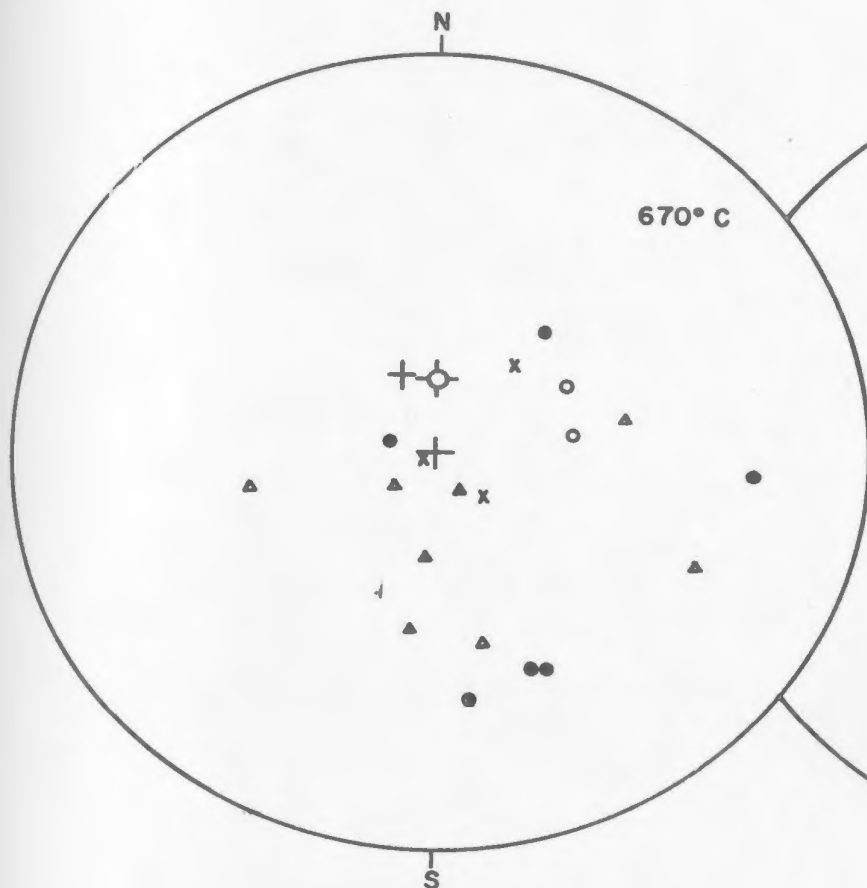


Fig 5.2.5.

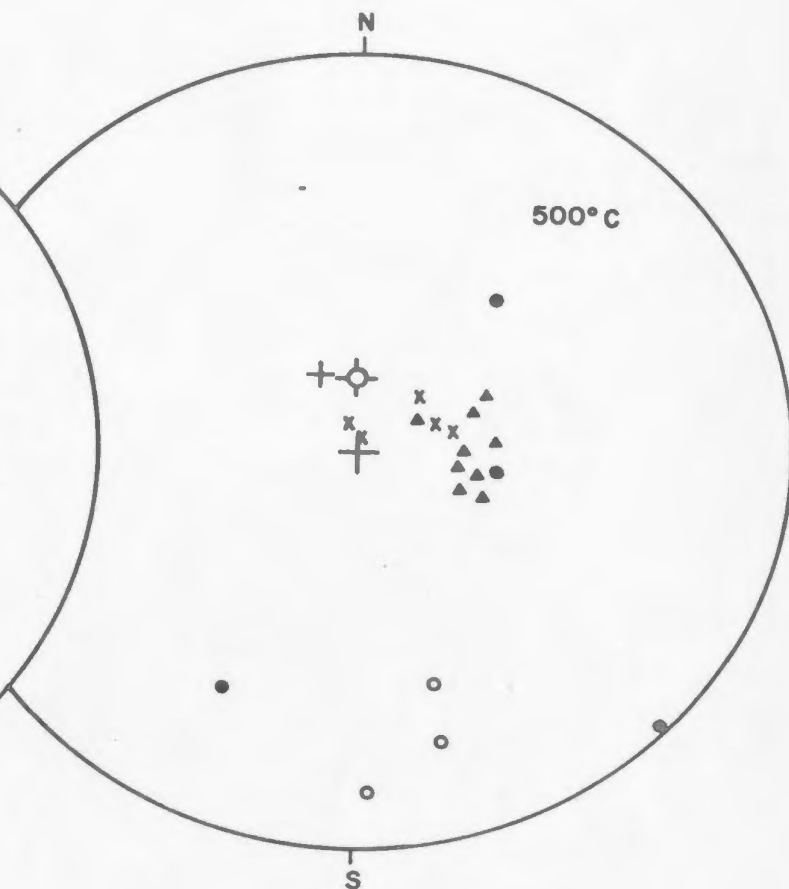


Fig 5.2.4.

Figs 5.2.4.- 5.2.5. Extended progressive thermal demagnetization of the Killary Harbour ignimbrites

Equal area projections, showing 5.2.4. directions after demagnetization to 500°C (21 specimens); and 5.2.5. directions after demagnetization to 670°C (19 specimens, excluding two weakly magnetized specimens), relative to the present horizontal plane.

⊗ Band 5, North pole in upper hemisphere

(All symbols as in Fig 3.1)

extended study, whereas they include data from the six pilot specimens in the case of NRM and other steps in the treatment (Figs. 5.2.1, 5.2.2, 5.2.4, 5.2.5). Directions and intensities of magnetization for the 15 specimens are tabulated in Table 5.2. Table 5.3 shows the site mean directions and statistical parameters for NRM and the various demagnetization steps.

The NRM directions for Site A (Fig. 5.2.1) make large angles with the present and axial dipole fields, but are quite scattered ( $k = 5.1$ , Table 5.3). The Site B and C directions are well-grouped ( $k = 43.5, 59.0$ , respectively), but are much more closely aligned with the axial dipole and present field directions, particularly in the case of Site C. The NRM intensities of Site A, B and C specimens (Table 5.2) are in the ranges ( $\text{emu/cc} \times 10^{-5}$ ), 10 - 40, 50 - 75, and 2 - 8 respectively; this is similar to the NRM intensity values for the specimens used later in a.c. demagnetization (Table 3.2).

Thermal cleaning at 400 and 450°C (Figs. 5.2.2, 5.2.3, 5.3; Tables 5.2, 5.3) caused little change in the mean site directions compared with NRM; however, relative to all sites the scatter had increased (i.e.  $k$  decreased) after the 400°C step; it decreased again after 450°C. For Sites A and B, the precision was largest after 450°C ( $k = 7.1$  and 99.2), whereas relative to Site C the maximum precision was at NRM ( $k = 59.0$ ), compared with  $k = 45.1$  and 47.2 at 450°C and 500°C, respectively. The 450°C demagnetization step was instituted after the pilot study had indicated that the Site A specimens were quite stable to 400°C, with a small, possibly systematic, directional change occurring at 500°C; it was therefore useful to subject all specimens to

TABLE 5.3

Mean site magnetization of the Killary Harbour  
ignimbrites, after step-wise thermal demagnetization.

Site	Band	T	$\bar{D}$	$\bar{I}$	N	R	k	$\alpha_{95}$
A	1	NRM	154	-4	3	2.608	5.1	61.1
B	3/4	NRM	98	+72	4	3.931	43.5	14.1
C	5	NRM	39	+75	4	3.949	59.0	12.1
A	1	400	149	-9	3	2.418	3.4	80.8
B	3/4	400	83	+68	4	3.924	39.7	14.7
C	5	400	49	+73	4	3.895	28.5	17.5
A	1	450	148	-18	3	2.719	7.1	50.4
B	3/4	450	88	+66	4	3.970	99.2	9.1
C	5	450	49	+73	4	3.933	45.1	13.8
A	1	500	166	+2	3	2.474	3.8	75.4
B	3/4	500	81	+60	4	3.959	72.9	10.8
C	5	500	42	+77	4	3.936	47.2	13.5
A	1	670	307	+32	3	2.200	2.5	>90
B	3/4	670	15	-65	3	2.500	4.0	72.0
C	5	670	343	+52	3	1.889	1.8	>90

$\bar{D}$  (deg.),  $\bar{I}$  (deg.) = mean declination and inclination (+ values in lower hemisphere) for N samples per site, one or two specimens being averaged per sample (Table 5.2).

T (°C) = temperature to which specimens have been demagnetized in zero field, and in air.

R, k,  $\alpha_{95}$  (deg.): Fisher (1953) statistics, as in Table 3.3.

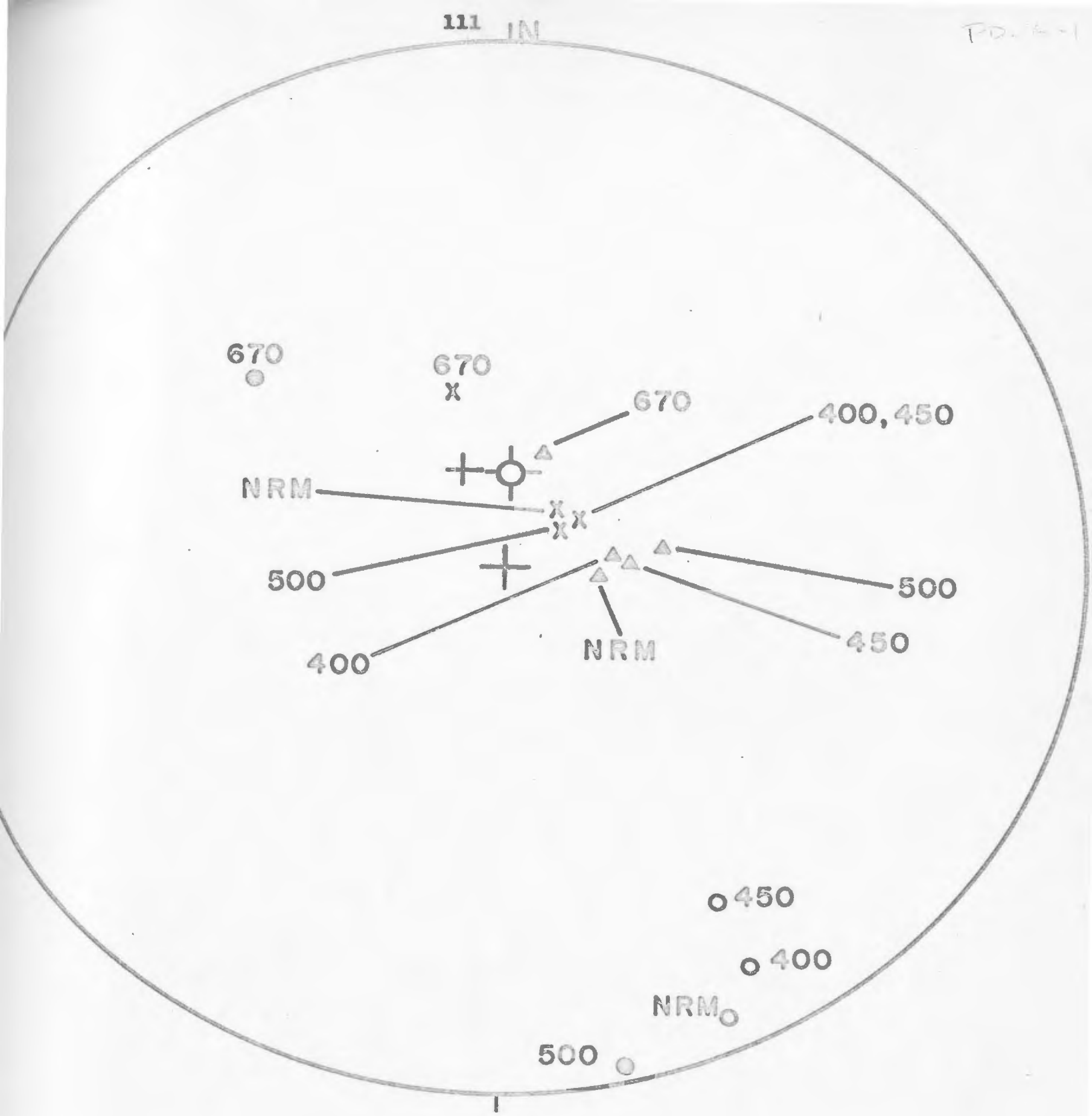


Fig 5.3. Mean directions of magnetization at the three Killary Harbour sites for NRM and after 4 steps of thermal demagnetization, relative to the present horizontal plane

Numbers refer to the demagnetization temperature (°C)

(All symbols as in Fig 3.1)

a further, intermediate step between 400 and 500°C.

After the 670°C step, the directions at all the three sites exhibit a large scatter, indicating that the main components responsible for the NRM at all sites have been demagnetized. These results are similar to the ones obtained from the pilot specimens, and the conclusions of Section 5.3 apply here as well.

Whereas the various demagnetization steps up to 500°C have made relatively little difference to the site mean directions (Fig. 5.3) and their precision, the directional groupings after the 450°C step have been preferred over the others in analyzing the results of the thermal treatment. This is partly because 450°C is intermediate in the blocking temperature range (400 - 500°C) above which the directions begin to be scattered and partly because at Site A, where the grouping is poor throughout the treatment,  $k$  attains its maximum value at 450°C. Even here  $k$  is relatively low (7.1).

#### 5.5. Fold test.

It was necessary to refer the mean site directions to the bedding planes by unfolding the structure about the strike (Table 2.2). This yields a fold test (Graham, 1949) corresponding to the one applied after alternating-field demagnetization (Section 3.5), where it gave positive evidence for a stable, possibly primary magnetization of the ignimbrites.

All but one of the specimen declinations in Fig. 5.4 are now grouped in the second quadrant, with all inclinations downward, giving a mean direction for 11 sample unit vectors (one or two specimens averaged

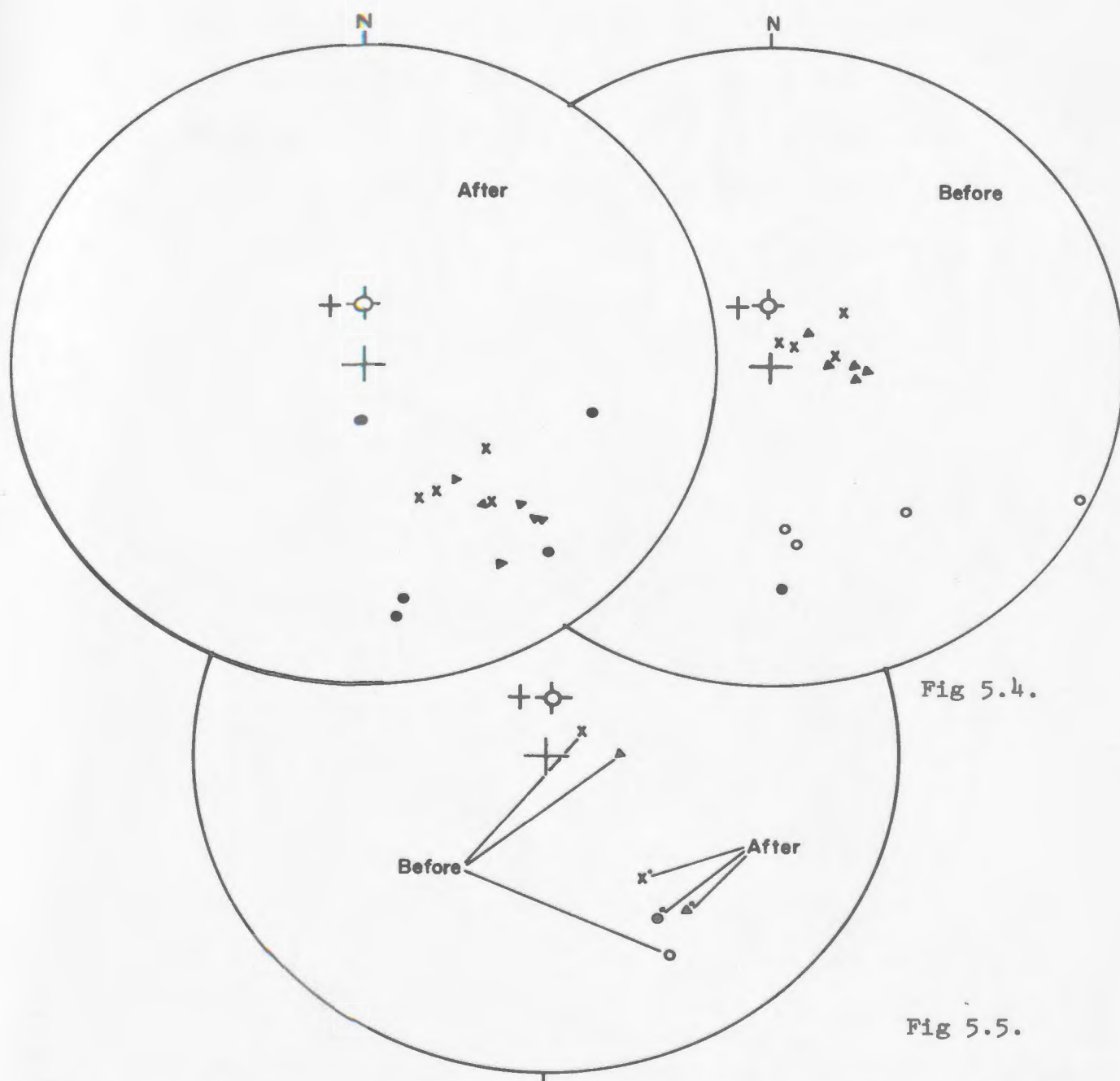


Fig 5.4.

Fig 5.5.

Figs 5.4.,5.5. Tilt correction of the directions of magnetization for the Killary Harbour ignimbrites, after demagnetization to 450°C

Equal area projections, showing 5.4. directions of magnetization of 15 specimens, before and after tilt correction; 5.5. mean site directions before and after tilt correction. For strike and dip data, refer to Table 2.2.

(All symbols as in Fig 3.1)

per sample) of  $\bar{D} = 143.5^\circ$ ,  $\bar{I} = 32.1^\circ$ ,  $k = 22.0$ , in Table 5.4. The corresponding mean direction taking  $N = 3$  sites as units is almost identical, but with increased precision ( $k = 98.4$ ). While McElhinny's (1964) performance criterion for the fold test is not applicable for the reasons stated in Section 3.5, Fig. 5.5 shows clearly the striking improvement in grouping brought about by the tilt correction. Hence the result of the fold test is regarded to be positive as in the case of the samples subjected to a.c. demagnetization, and the conclusions of Section 3.5 also apply here.

#### 5.6. Comparison of alternating-field with thermal demagnetization.

It is interesting to compare the response of the ignimbrites to the two types of demagnetizations performed. The results are based on 50 specimens (2 from each sample) in the a.c. treatment (Chapter 3), plus 21 specimens (representing 15 samples) in the more restricted thermal treatment (this Chapter).

##### 5.6.1. Comparison of pilot studies.

Pilot a.c. demagnetization results (Table 3.1) show that scattering tends to increase above 540 oe, with relatively little directional change (Fig. 3.1). Also the site mean directions (Fig. 3.4) show relatively little change up to 770 oe. The five  $(J/J_n) - H$  curves (Fig. 3.1) indicate the presence of a high-coercivity component, with 20% or more of the NRM intensity still remaining after 700 oe treatment, and over 60% remaining in the case of KH 16b from Site C.

For thermal treatment, scatter tends to increase above 450 - 500°C becoming extreme at 670°C, as shown by pilot specimens (Figs. 5.1.1 -

TABLE 5.4

Mean site magnetization of the Killary Harbour ignimbrites,  
after 450°C thermal demagnetization and tilt correction.

Site	Band	$\bar{D}$	$\bar{I}$	Fisher statistics (Fisher 1953)			
				N	R	k	$\alpha_{95}$
A	1	147°	+28°	3	2.716	7.1	50.4°
B	3/4	139°	+26°	4	3.970	100	9.1°
C	5	144°	+40°	4	3.934	45.4	13.8°
All samples		143.5°	+32.1°	11	10.526	22.0	10.2°
All sites		143.6°	+31.6°	3	2.979	98.7	12.7°

(Symbols as in Tables 3.6, 5.3)

5.1.6) and Site mean directions (Fig. 5.3). The  $(J/J_n) - T$  curves for pilot specimens show a sharp drop in  $J$  above  $400^{\circ}\text{C}$ ; they also tend to level off above  $500 - 600^{\circ}\text{C}$ , except for the erratic specimen KH 8c, and KH 7aII, which showed abnormal  $J$  increases above  $500^{\circ}\text{C}$ . The results are consistent with the main blocking temperature range being  $400 - 600^{\circ}\text{C}$ , though a small "tail" with  $J$  usually less than 20% of  $J_n$  persists above  $600^{\circ}\text{C}$ .

Intensity maxima were attained by pilot specimens KH 8a and 2bI after treatment to 25 oe and 100 oe respectively, and by 7aII after  $150^{\circ}\text{C}$ ; all three specimens are from Site A, but the Site B specimen KH 20a also showed maxima at relatively low temperature ( $275^{\circ}\text{C}$ ). While KH 7aII and 20a both show stable directions well above the temperatures concerned, the stable directions of the latter differs from those of the former by  $110 - 120$  degrees of arc. To account for these maxima by invoking a low-coercivity, antiparallel component that is removed, is therefore doubtful, as these unstable components, to be antiparallel, would have to have entirely different directions in the two specimens concerned. Again in the case of KH 8a, an antiparallel component would be consistent with the large directional changes resulting from removal in low fields of a VRM roughly in the recent Earth's field direction, whereas for KH 2bI, which showed great directional stability throughout, an antiparallel component would have to be of low inclination and quite different in direction from that invoked to be KH 8a. Hence the intensity increases noted in pilot specimens are difficult to explain. Similarity of trends on the thermal curves (notably KH 20a and 22a) suggests removal of a smaller component at  $300^{\circ}\text{C}$ ; this is possibly the

same component as the one whose removal is less distinctly suggested in the a.c. demagnetization of some pilot specimens to 350 - 400 oe (Fig. 3.1).

The pilot results suggest that a fairly "hard" component acquired between 400 and 600°C, which dominates the NRM of these specimens, becomes somewhat better isolated after thermal treatment to 450°C, and particularly, a.c. treatment to 540 oe (peak). Thermal demagnetization allows one to distinguish another component (possibly also of high coercivity with Curie point above 600°C). The two treatments differ in that thermal demagnetization has effectively demagnetized the main component at the latter temperature, whereas alternating fields to nearly 800 oe are insufficient to do so. Moreover the drop of J with temperature in the thermal demagnetization of pilot specimens begins to be appreciable only above 400°C; i.e. the blocking temperature distribution, with some exceptions, may be said to be "discrete" within the 400 - 600°C range (Irving and Opdyke, 1965) rather than thermally "distributed" over the entire NRM - 600°C range. The results depicted in both sets of J/J<sub>n</sub> curves (a.c. and thermal) are evidence for high stability in most specimens.

#### 5.6.2. Comparison of extended demagnetizations.

The demagnetization results after optimum a.c. or thermal steps at all 3 sites, showed little direction change due to treatment. The site mean changes between NRM and 540 oe (N = 9, 8, 8 samples, at Sites A, B, C, respectively; Fig. 3.4), and between NRM and 450°C (N = 3, 4, 4 samples; Fig. 5.3) were always less than 10° of arc after treatment. Also the final mean directions (equal weight for N = 3 sites or 4 bands) after tilt correction changed by less than 10° of arc, between NRM and 540 oe, as well

as between NRM and  $450^{\circ}\text{C}$ . At intermediate steps in the treatment (i.e. between NRM and 540 oe and  $450^{\circ}\text{C}$  respectively) changes in individual specimen directions are mostly small (Figs. 3.2, 5.2.1 - 5.2.5; Tables 3.2 and 5.2), and the same can be said for changes in mean direction of larger units (samples, bands, sites). These results give partial indication of relatively high stability, along with another partial stability criterion, discussed previously, i.e. the divergence by large angles of most of the Site A NRM directions from the present or axial dipole fields, and the divergence by much smaller but still significant angles of most Site B NRM directions from these fields.

### 5.6.3. Optimum demagnetization.

The above observations might explain why the optimum demagnetization steps decided upon after the pilot study (a.c. or thermal) are not sharply defined. The two sets of pilot intensity curves, i.e.  $(J/J_n) - \tilde{H}$  (Fig. 3.1) and  $(J/J_n) - T$  (Figs. 5.1.1 - 5.1.6), showed considerable similarities in trend for specimens from different sites. One would expect this, since the specimens were all ignimbrites of contemporaneous origin, and hence should have compositions that differ little from band to band. This justified demagnetizing all samples to the field or temperature chosen to be optimum ( $540$  or  $450^{\circ}\text{C}$ ), rather than making an artificial distinction on the basis of site differences. In theory, by comparing dispersions as the treatment proceeded, the optimum step could then be chosen on the basis of maximum  $k$ .

However, for a.c. demagnetization (Table 3.3)  $k_B$  (i.e. the precision for the Site B mean direction) is largest at NRM and also slightly larger at 540 oe than 310 oe; whereas  $k_A$  increases from a very

low value at NRM to a maximum at 540 oe; with  $k_A = 8.6$ , this represents still greater scatter than after 540 oe at Sites B and C ( $k_B = 44.6$ ;  $k_C = 21.0$ ).  $k_C$  increased from NRM to about equal values at 310 and 540 oe, deciding whether to adopt NRM or 540 oe directions for samples (the former based on  $k_B$  values, the latter on  $k_A$  and  $k_C$  values) one should take into account the actual directional change for Site B between NRM and 540 oe was  $< 5^\circ$ , several specimens from Site A (e.g. KH 8a) gave evidence that low-coercivity components caused some of the NRM directions to differ by large angles from the "stable", low-dip NRM directions from that site, causing the low  $k$ ; here considerable direction changes and improved precision of the mean were brought about by the treatment to 540 oe. On the other hand, the Site B and C directions showed little change in the range NRM - 540 oe. Hence in considering the overall treatment, demagnetization to 540 oe is clearly preferable to using the NRM directions.

In the case of thermal treatment the NRM grouping at Site C is better than that after  $450^\circ\text{C}$  (Table 5.3), whereas for Sites A and B the former is worse. However, the poor grouping, particularly after treatment, at Site A, is largely due to one sample (KH 9). The samples as a whole ( $N = 11$ ) are better grouped at NRM than after  $450^\circ\text{C}$  (though the precision again could have been improved in the absence of sample KH 9), whereas if the 3 sites are given equal weight in determining the mean direction, the grouping becomes somewhat closer after demagnetization to  $450^\circ\text{C}$ . The actual  $k$  values for the latter case (NRM:  $k = 100$ ;  $450^\circ\text{C}$ :  $k = 98.4$ ), which are not greatly affected by non-conforming individual sample directions, are quite high compared with the mean results

for  $N = 4$  bands in the a.c. treatment ( $k = 23$  for 540 oe).

In Figs. 5.1.1 - 5.1.6, the sharp drop of  $J/J_n$  below  $600^{\circ}\text{C}$  suggests that the Curie point of the main component is less than that temperature and consistent with magnetite or titanomagnetite. The "tail" above  $600^{\circ}\text{C}$  could be due to hematite. The fairly high coercivities suggested by the  $J/J_n - \tilde{H}$  curves (Fig. 3.1) might be consistent with titanomagnetite or the presence of both titanomagnetite and hematite. These results are compatible with those of the polished-specimen examination by Dr. N. D. Watkins (Section 5.2). However, the absolute NRM intensities of magnetization are in the range  $J_n = 1-70$  ( $\times 10^{-5}$  emu/cc), which is intermediate between typical intensities found in basic igneous rocks and in paleomagnetically useful sedimentary rocks (Nagata, 1961), so that it is difficult to associate the intensities of these ignimbrites with a particular mineral composition.

#### 5.7. The fold test and secular variation.

Both thermal and a.c. treatment gave evidence for stability, with similar site mean directions after 540 oe or  $450^{\circ}\text{C}$ ; moreover, the overall grouping was much improved by the tilt correction, using band, site or sample means for comparison. Systematic differences in the direction of magnetization for different bands are then probably due to secular variation, because of differences in field directions at the (slightly ?) different times of origin of the four bands. In concluding that the fold test was "successful", it has been assumed that the secular variation in this case involved significantly smaller

directional differences between different sites than the geometrical differences between different limbs of the syncline.

The assumption that the secular variation during Ordovician was not drastically greater than Recent times has not been proven, but is plausible (Khranov et al, 1965). Thus a modest amount of secular variation would be consistent with the interpretation that the fold test was successful, and this has been assumed here. In turn, the positive result of the fold test is strong evidence that the mean direction of magnetization of the ignimbrites is pre-Silurian (Chapter 2), and hence is either primary or was acquired within the Ordovician a relatively short time after the rocks were laid down.

#### 5.8. Ordovician pole positions.

Adopting the mean north pole direction of magnetization for  $N = 4$  bands after the 540 oe (peak) a.c. treatment and tilt correction ( $\bar{D} = 134.1^\circ$ ,  $\bar{I} = +32.0$ , Table 3.6), the corresponding pole position was calculated (Table 5.5, second row). Since the a.c. demagnetization involved all 25 samples this pole position ( $9^\circ\text{S}$ ,  $34^\circ\text{E}$ ) is here considered to be more reliable than the pole ( $13^\circ\text{S}$ ,  $26^\circ\text{E}$ ) corresponding to  $N = 3$  sites after  $450^\circ\text{C}$  treatment, though the two poles are very close. The pole corresponding to the mean (first row, is shown for comparison), is quite close the other poles, illustrating that the laboratory treatment, while confirming stability in the NRM directions, did not make much difference in the final results. Pole positions corresponding to mean directions in which samples were given unit weight are shown in rows 4 and 5, and while these are close to the other three results, it is generally more reliable to adopt a pole position based

TABLE 5.5

Paleomagnetic pole positions for the Killary Harbour ignimbrites,  
from the mean directions of magnetization after laboratory  
treatment and tilt correction.

(Tables 3.6, 5.4)

Unit	Treatment	N	Pole position		Antipole position		dp	dm
Bands	NRM	4	9°S	30°E	9°N	150°W	9°	15°
Bands	540 oe	4	9°S	34°E	9°N	146°W	12°	22°
Sites	450°C	3	13°S	26°E	13°N	154°W	8°	14°
Samples	540 oe	25	7°S	33°E	7°N	147°W	6°	10°
Samples	450°C	11	13°S	26°E	13°N	154°W	7°	11°

N number of units averaged

dp, dm semi-axes of the 95% oval of confidence

Pole (antipole) positions correspond to mean north (south)  
 pole directions for the rock units concerned.

upon directions in which bands or sites, rather than samples, have been given unit weight (Irving, 1964, p. 64). Although the error assigned to the adopted pole position (Table 5.5, second row,  $dP = 12^\circ$ ,  $dm = 22^\circ$ ) is larger than for the other four poles listed, it is probably the most realistic.

While the inferred pole is considered to be a "geographical" one, in accordance with the axial dipole assumption (Chapter 1), it should be noted that the total number of bands on which it is based ( $N = 4$ ) is rather small, and may have been insufficient to average out the secular variation.

Comparison with published polar wandering curves relative to Europe (Irving, 1964, p. 137) suggest that in Table 5.5 the antipoles rather than the pole corresponds to an Ordovician geographical north pole; this implies that the Earth's field responsible for the stable magnetization of the ignimbrites was "reversed" compared with the present field.

The two antipole positions corresponding to alternative laboratory treatment (2A:  $9^\circ\text{N}$ ,  $146^\circ\text{W}$ ; 2B:  $13^\circ\text{N}$ ,  $154^\circ\text{W}$ ) are compared in Fig. 5.6 with published Ordovician pole positions inferred from sites in North America, Europe and Siberia, most of which are in the present Pacific Ocean. The present poles are located between Poles 3, 4, based on Ordovician volcanic rocks in Britain (Nesbitt, 1967), and Poles 5, 6, inferred from Lower and Upper Ordovician sediments in Bohemia (Bucha, 1965).

Despite the small number of samples and bands in the present

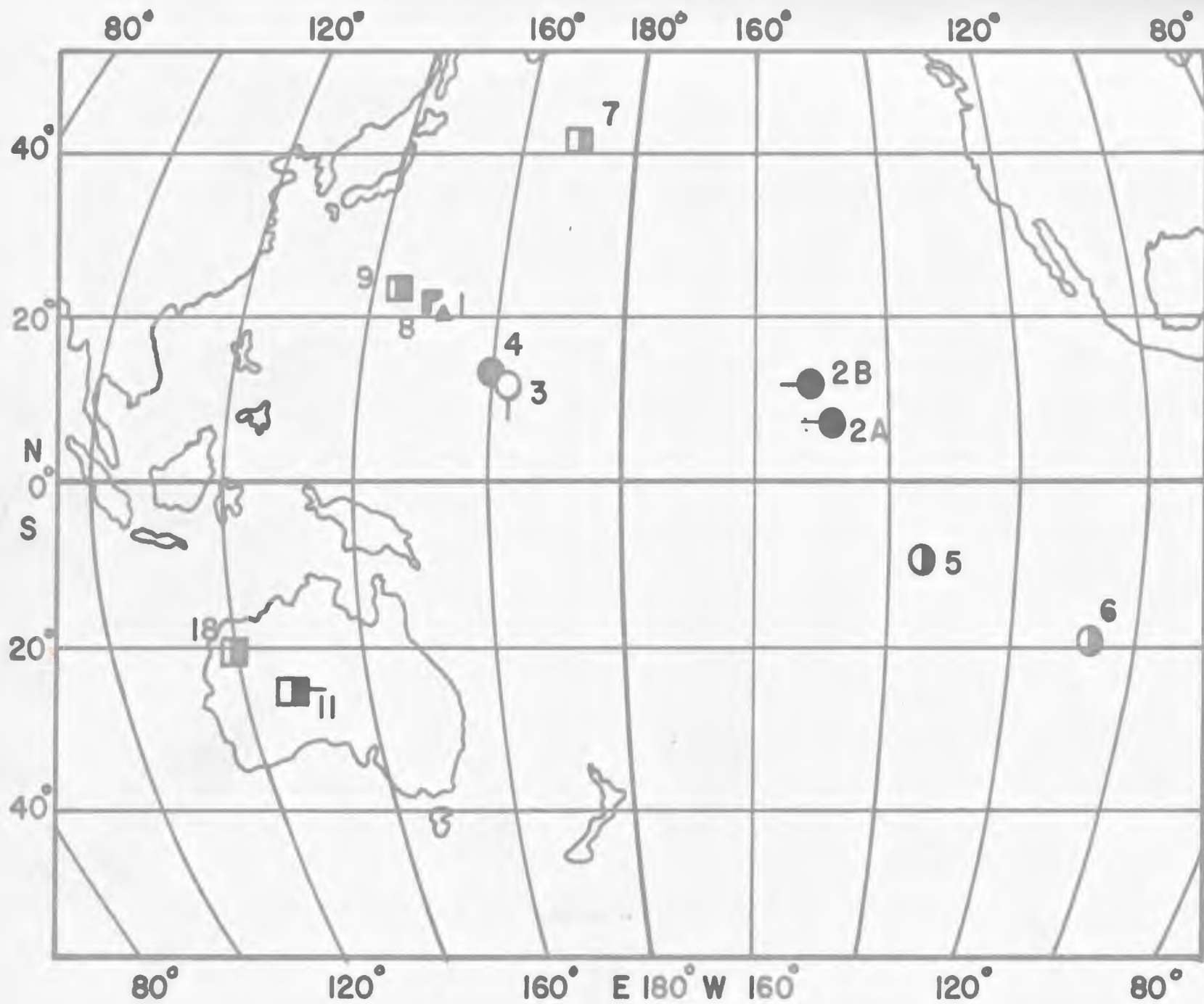


Fig 5.6. Paleomagnetic pole positions from rocks in N.America and northern Eurasia  
 (caption on next page)

125

Caption for Fig. 5.6

Sampling sites in:     △ Mainland North America;  
                          ○ Ireland;     ○ Britain;  
                          ○ Europe west of 25°E;  
                          □ Europe east of 25°E;  
                          □ Siberia

Poles shown correspond to the following polarities in the rock:

Open symbols: "Normal" polarity (i.e. the remanent magnetization is believed to have the same sense as the present field.

Solid symbols: "Reversed" polarity,

Half-solid symbols: "Mixed" (i.e. alternately normal and reversed) polarity.

Numbers refer to results of paleomagnetic surveys (numbers in brackets are from the tabulation by Irving, 1964):

1. Juniata Formation, U.S.A. (3.06);
- 2A. Killary Harbour ignimbrites (present study), 4 bands after a.c. demagnetization;
- 2B. Present study, 3 sites after thermal demagnetization;
3. Borrowdale volcanics (Nesbitt, 1967);
4. Builth volcanics (Nesbitt, 1967);
5. Central Bohemian sediments, Lower Ordovician (Bucha, 1965);
6. Central Bohemian sediments, Upper Ordovician (Bucha, 1965);
7. Tremadocian Sediments, U.S.S.R. (3.01);
8. Asha Stage, U.S.S.R. (3.04);
9. South Urals and Baltic sediments (Khramov et al, 1965);
10. Lugov Suite, U.S.S.R. (3.10);
11. Sediments from Siberian Platform (Khramov et al, 1965; Rodionov, 1966).

study, giving rise to some uncertainty as noted above, a fair measure of confidence in the pole position relative to Killary Harbour is justified by the excellent evidence for stability, compared with most of the earlier results depicted in Figure 5.6.

CHAPTER 6DEMAGNETIZATION STUDY OF SINGLE LAVAS FROMNEWFOUNDLAND AND LABRADOR.6.1. Previous work.

The first paleomagnetic results from Newfoundland were obtained from late Precambrian sandstones on the Avalon Peninsula by Nairn et al, (1959). Comparing the pole positions with those obtained from Precambrian paleomagnetic results in Arizona, they inferred a  $20^{\circ}$  anticlockwise rotation of Newfoundland; however, the significance of this conclusion was questioned by DuBois (1959). Later, a  $30^{\circ}$  anticlockwise rotation [similar to that proposed by Wegener (1929; Transl. 1966)] was inferred by Black (1964) from comparisons of Cambrian and Devonian paleomagnetic results in Newfoundland and New Brunswick, as well as a comparison of Carboniferous rocks in Newfoundland and on the eastern Canadian mainland. Black concluded that the rotation occurred in the Devonian, and had been completed by the Carboniferous. Black's data appears to be inconclusive, as the Cambrian magnetic directions in Newfoundland and New Brunswick are not significantly different at the 95% level, while the fields responsible for the "Devonian" direction in the two sampling regions were not necessarily contemporaneous (Robertson et al, 1968). Hence the rotation of Newfoundland cannot be regarded as established, and further paleomagnetic data from Paleozoic rocks in Newfoundland and the North American mainland are necessary to test this hypothesis. In this context it is interesting to compare

contemporaneous rocks from the Lower Paleozoic on the two sides of the Strait of Belle Isle.

## 6.2. Geological setting.

During the summer of 1966, Dr. E. R. Deutsch and Dr. P. S. Rao of the Physics Department collected 33 oriented hand samples of basalt from a single flow exposed on Cloud Mountain near Roddickton on the Great Northern Peninsula of Newfoundland (Fig. 6.1) and also sampled the nearby exposures of red and grey sedimentary rocks of the Cloud Mountain and Devil's Cove formations, which are of known Cambrian age. A further collection of a single basalt flow, along with underlying red sediments, was made at Table Head along the Labrador coast north of the Strait of Belle Isle. This completed a collection begun during the summer of 1965 (Murty, 1966) at Table Head and at Henley Harbour, 10 miles south of Table Head, where an 80-foot section of basalt probably representing a single flow is exposed at two offshore islands (Christie, 1951; Douglas, 1953; Eade, 1962). The number of basalt hand samples collected at Henley Harbour and Table Head is 33 and 26 respectively. The basalts of Labrador and Cloud Mountain are regarded as contemporaneous and probably post-Precambrian (Clifford, 1965) since in Labrador they rest upon red sedimentary rocks believed to be equivalent to the Lower Cambrian Bradore formation (Christie, 1951) which is exposed further south along the Labrador coast, whereas at Cloud Mountain they are associated with the aforementioned sedimentary formations of Cambrian age. Moreover, the flows at all three sites form the upper members of a structurally similar gneiss-red sediment - basalt

association, and in all cases the flows have low eastward dips (Fig. 6.1 and Sections 6.4.1, 2, 6.5). While the above considerations would suggest a likely Cambrian origin for the Labrador and Cloud Mountain flows, this disagrees with the Devonian ages obtained by the Geological Survey of Canada from one K-Ar determination each on basalt at Table Head (345 m.y.) and Cloud Mountain (334 m.y.), respectively. The former date is from Wanless et al, (1965), while the latter is quoted by Clifford (1965), who concludes that the age of the Labrador and Cloud Mountain flows is anywhere in the range from Lower Cambrian to Devonian.

Preliminary NRM measurements and some a.c. demagnetization data from two Henley Harbour sites and Table Head are reported by Murty (1966), and summarized in Table A4-1. In the current work on these single lavas, Henley Harbour will be treated as a single site, with Table Head and Cloud Mountain constituting the other two sites; studies on the sedimentary samples collected at these sites will not be discussed here. The single lava studies may yield a useful comparison regarding the stability and thermomagnetic properties of these superficially similar but widely separated exposures. As in the case of the Killary Harbour ignimbrites, the basalts are strongly oxidized (Oxidation Index VI: Wilson et al, 1968) so that the present study should also enable one to compare the same magnetic behaviour of two types (ignimbrite, basalt) of Lower to Middle Paleozoic oxidized volcanic rocks, exposed at opposite sides of the North Atlantic. Since only one flow is represented at each site in the present investigation, the results are unsuitable for paleomagnetic interpretation, but might give an initial idea about the direction of the Lower to Middle Paleozoic field.

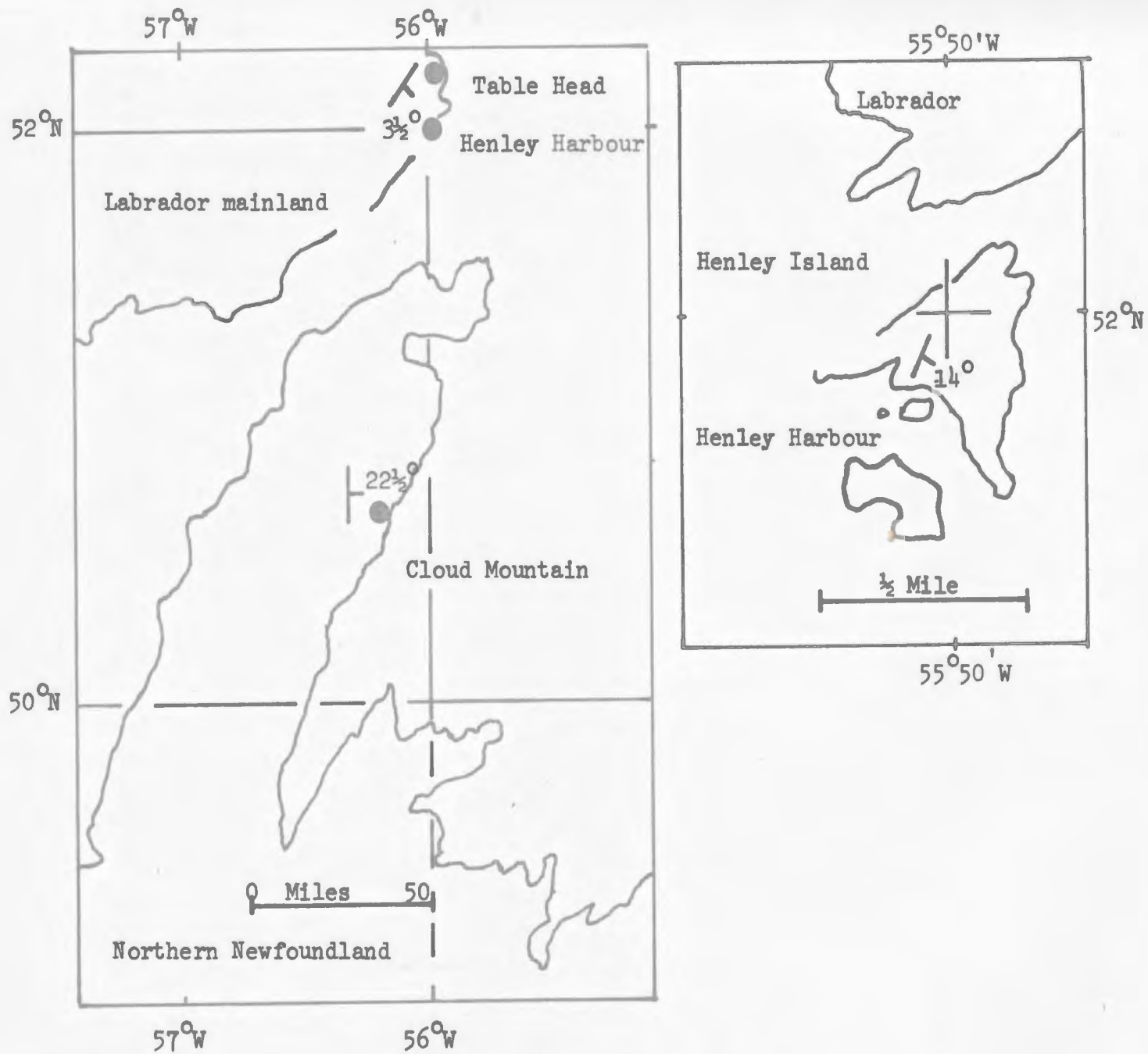


Fig 6.1. Sites for collections of single basalt flows at Table Head and Henley Harbour, Labrador, and Cloud Mountain, Northern Newfoundland.

### 6.3. Earlier measurements of the Labrador Basalts.

The primary study of the single lavas from Henley Harbour and Table Head (Murty, 1966; P. 96-110) showed that the NPM intensities of magnetization ranged mostly from  $10^{-4}$  to several times  $10^{-3}$  emu/cm<sup>3</sup>, which is typical of many basalts. The mean directions of magnetization at the two sites, both before and after tilt correction, have relatively steep inclinations tending towards the east. These NRM directions are close to, but (at the 95% confidence level) still significantly different from the present direction and axial dipole direction of the Earth's field. While the poles corresponding to these sites represent spot readings of a Paleozoic field and have little paleomagnetic significance, one would expect (on the unproven but perhaps reasonable assumption that the magnitude of the secular variation was not drastically greater than today), that paleomagnetic poles of Cambrian to Devonian age should be closer to pole positions for that time span reported in the literature than the "virtual" poles (Cox and Doell, 1960) actually obtained from the Labrador flows. The latter are in the present location of Western Europe (Murty, 1966) and far from the published polar wandering curves relative to North America (e.g. Runcorn, 1965).

The Cloud Mountain basalts are also quite strongly magnetic, having their intensities between  $1 \times 10^{-3}$  to  $7 \times 10^{-3}$  emu/cc with a few exceptions (Table 6.3). The steep positive (downward) magnetizations found with respect to all three sites (except Samples CM 2, 4, 13) may reflect the presence of a superimposed component relatively close to the present earth's field. Possible causes of the steep upward directions in Samples CM 2, 4 and 13, will be discussed in Section 6.5. In any case,

it appears likely that significant unstable components are contributing to the observed magnetization, at all three sites, and hence it is necessary to provide some independent stability tests before drawing conclusions from the NRM measurements.

Four specimens from Henley Harbour and two from Table Head were demagnetized at successively higher fields by G. W. Pearce (1967). The mean NRM directions of the six specimens are closely aligned ( $k = 486$ ; Table A4-2) with somewhat diminished but still excellent grouping in fields up to 324 oe peak. These a.c. demagnetization resulted (Pearce, 1967) in a relatively little directional change, confirming at least partial stability of the basalt, and indicating the presence of a hard component that may or may not have been of primary origin.

Studies of thin sections from Henley Harbour and from Table Head indicate the presence of altered hematite in local concentrations, often in association with magnetite (Murty, 1966); in some cases secondary hematite is found replacing olivine. Polished section studies by Dr. N. D. Watkins of Florida State University (Appendix 3) made on five basalt specimens from Henley Harbour and one each from Table Head and Cloud Mountain, revealed the common occurrence of secondary hematite replacing part of the olivine or titanomagnetite, the latter being the probable carrier of the primary magnetization. Three of the Henley Harbour specimens were in the highest oxidation state (Index VI) according to the notation of Watkins (Wilson et al, 1968). This oxidation may have been produced during the late stages of the cooling of the lava. The alternative explanation of heating caused by subsequent metamorphism is perhaps less likely, since the gentle folding of the lavas at all three

sites suggests the absence of major tectonic events affecting these rocks since they were laid down in the Lower to Middle Paleozoic.

The presence of significant magnetization components residing in secondary hematite, which one would expect to occupy a high range in the coercivity spectrum, is consistent with the evidence for relatively high stability from the a.c. demagnetization (Table A4-2). Since this stability is associated with secondary components, the isolation of any primary component was likely to be accomplished, if at all, only through application of thermal demagnetization, requiring that the primary component be associated with significantly higher blocking temperatures than the high-stability secondary components. Progressive thermal demagnetization on some selected samples from all the sites was undertaken. It was hoped that these measurements might give some useful results regarding stability. Such data, however, could not be expected to lead to final paleomagnetic conclusions, in view of the small number of samples involved, and the fact that the collections involved single lava flows.

#### 6.4. The basalts from Southern Labrador.

Nine and six samples from Table Head and Henley Harbour respectively, were selected for thermal demagnetization. The specimens were randomly arranged inside the oven as discussed in Section 4.8. All NRM directions (Tables 6.1, 6.2; Fig. 6.2) had positive (downward) inclinations, and all declinations except for TH 4aI and TH 20c were in the first or second quadrants. The NRM vectors generally made small angles with the present field or axial dipole directions, with some

N



Fig 6.2. Equal area plot of NRM directions relative to the present horizontal plane at the sampling site, of 13 Table Head and 6 Henley Harbour specimens from Labrador.

North pole in:      Lower hemisphere                      Upper hemisphere

- Table Head                      ▲    ▲
- Henley Harbour                ⬡    ⬡
- ⊙      Axial dipole field

exceptions (mainly HH 24dI, Th 5cIV, TH 18a, TH 18b). At both sites the intensities tend to fall fairly sharply up to 350 - 400°C and then level off (see also Fig. 6.7); for Henley Harbour, the arithmetic mean of the normalized intensity (N = 6 specimens) is  $J_T/J_n = 0.2$  in the range  $T = 350 - 500^\circ\text{C}$ , with a minimum value of 0.18 at 500°C. For Table Head (N = 12) the corresponding minimum is  $J_{450}/J_n = 0.41$  at 450°C.

At both sites the intensity increased again after further demagnetization, this being accompanied by an increase in the directional scatter. Thus, in Table 6.4 the grouping is seen to be far closer before treatment ( $k_{\text{NRM}} = 7.5$  and 29 for Table Head and Henley Harbour, respectively) than afterwards, though smaller precision maxima<sup>1</sup> are reached at intermediate steps, i.e.  $k_{450} = 3.3$  and  $k_{350} = 3.0$  at the respective sites. Since the latter temperatures (450 and 350°C) were also associated with intensity values close to their minima at the respective sites (Tables 6.1, 6.2), it is reasonable to suppose that the NRM magnetizations may have incorporated a strong viscous component, perhaps acquired in quite recent geological time, which has been removed by the treatment to 450 or 350°C. That this would not be a "soft" component (e.g. of laboratory origin) is indicated by the results of the previously quoted a.c. treatment (Pearce, 1967).

---

<sup>1</sup>Very small values of the precision parameter (say,  $k \leq 3$ ), apart from indicating very large scatter, have little statistical significance, since the requirement of a vector distribution corresponding to a normal population then tends to be violated (e.g. Larochelle, 1968). Whereas the values of  $k = 3.3$  and 3.0 quoted here may be taken to represent real maxima, the  $k$  value between 1 and 3 quoted for most of the other temperatures in Tables 6.4, 6.5 are listed only as rough indicators of a large scatter, and their use in quantitative comparisons is not justified.

TABLE 6.1

Systematic thermal demagnetization of the Table Head basalts.

Specimen	NRM			400°C			450°C			550°C			600°C			650°C		
	D	I	Jx10 <sup>-4</sup>	D	I	Jx10 <sup>-4</sup>	D	I	Jx10 <sup>-4</sup>	D	I	Jx10 <sup>-4</sup>	D	I	Jx10 <sup>-4</sup>	D	I	Jx10 <sup>-4</sup>
TH 4aI	269	+56	62	194	+79	60	132	+42	14	133	-1	31	113	-9	25	109	-23	32
5cI	73	+75	51	103	+51	15	155	+46	24	266	+9	35	148	-32	29	228	-32	36
5cIV	70	+36	30	105	+63	17	134	+37	21	179	+7	20	188	-33	23	197	-39	19
6aIII	26	+69	4.5	12	+73	0.7	86	+36	26	238	-10	23	62	-31	35	313	+56	62
6bII	28	+83	40	*	*	*	*	*	*	246	+8	39	341	-19	27	13	-58	30
16aVI	145	+76	29	122	+53	3.4	180	-14	15	242	-4	13	219	-4	14	230	-49	15
17b	119	+54	38	129	-26	6.2	175	-67	3.6	185	-2	9.7	184	+21	9.1	174	-60	16
18a	135	+28	11	too weak to measure			125	+15	3.5	174	+13	6.9	152	+31	20	126	+70	17
18b	120	+47	13	116	-66	5.5	121	+3	12	112	-5	16	268	+59	17	125	+77	14
19a	81	+69	13	138	+54	8.4	154	+68	12	144	+7	0.4	234	+12	20	166	-36	13
19b	72	+54	55	99	+80	27	185	+35	14	164	+28	16	184	-33	13	196	-47	31
20c	337	+68	56	*	*	*	275	+72	11	163	+38	17	236	+44	27	236	+83	33
21a	103	+57	41	101	+24	14	141	+33	11	211	+34	19	157	+45	42	81	+82	24

Symbols as in Table 3.1

\*Indicates no measurement was made.

TABLE 6.1 (Continued)

680°C		
D	I	Jx10 <sup>-4</sup>
119	-87	6.5
214	+31	13
130	-77	58
87	-45	14
343	-29	15
203	-78	11
179	+47	7.1
169	+35	18
180	+33	11
170	+20	5.7
214	+79	3.5
98	+34	20
248	+48	23

TABLE 6.2

Systematic thermal demagnetization of the Henley Harbour basalts.

Specimen	NRM			100°C			250°C			295°C		
	D	I	Jx10 <sup>-4</sup>	D	I	Jx10 <sup>-4</sup>	D	I	Jx10 <sup>-4</sup>	D	I	Jx10 <sup>-4</sup>
HH 3CII	116	+83	8.5	129	+73	6.8	123	+62	3.6	136	+62	4.8
12dI	9	+73	19	*	*	*	273	+88	2.1	262	+50	2.2
16bIV	66	+74	27	200	+87	14	227	+84	8.4	*	*	*
17bI	30	+67	18	14	+32	8.8	42	+11	4.2	79	+8	3.6
24dI	64	+48	15	174	+73	6.2	153	-32	4.1	154	-20	3.9
25bII	50	+77	15	21	+75	9.2	14	+49	5.8	350	+52	6.5

Symbols as in Table 3.1.

\*Indicates no measurement was made.

TABLE 6.2 (Continued)

Specimen	350°C			450°C			500°C			590°C		
	D	I	Jx10 <sup>-4</sup>									
HH 3cII	194	+54	2.2	90	+70	2.8	84	+61	1.9	209	-25	5.1
12dI	62	+65	0.9	241	+68	2.1	229	+56	0.4	137	-82	7.1
16bIV	126	+76	5.8	236	+87	6.9	301	-63	4.0	-	-90	19
17bI	84	+21	3.3	66	+3	2.9	189	-70	5.3	261	-54	7.2
24dI	151	-9	4.6	153	-18	4.9	125	-55	5.3	165	-41	6.8
25bII	10	+65	3.4	352	+77	2.9	262	-20	2.0	289	-72	6.1

#### 6.4.1. Table Head.

The mean declination for Table Head (Table 6.4; see also Figs. 6.3.1 - 6.3.3), changed from east to south upon heating to 680°C, while the mean inclination gradually decreased from its large NRM value (+70°) to low values. The mean direction at 450°C (D = 143°, I = +33°, k = 3.3, N = 12, specimens) may be compared with the mean Henley Harbour directions (Table 6.4) at 350°C (D = 114°, I = +61°, k = 3.0, N = 6); these directions are quoted prior to the tilt correction, which brought the two mean vectors somewhat closer together (Table 6.5). The temperatures for which the above site mean directions are quoted correspond to near-minima of the respective arithmetic-mean intensities and to slightly improved (though still very poor) vector grouping, as discussed under Section 6.4. For the respective temperatures, before or after tilt correction, the declinations are roughly comparable at the two sites, though the Henley Harbour inclination is steeper. The direction for 450°C at Table Head may be interpreted in the same way as the 350°C direction at Henley Harbour, i.e. as probably representative of a partially stable component with blocking temperatures below 450°C. Directional changes for one representative specimen is plotted in Fig. 6.5.1.

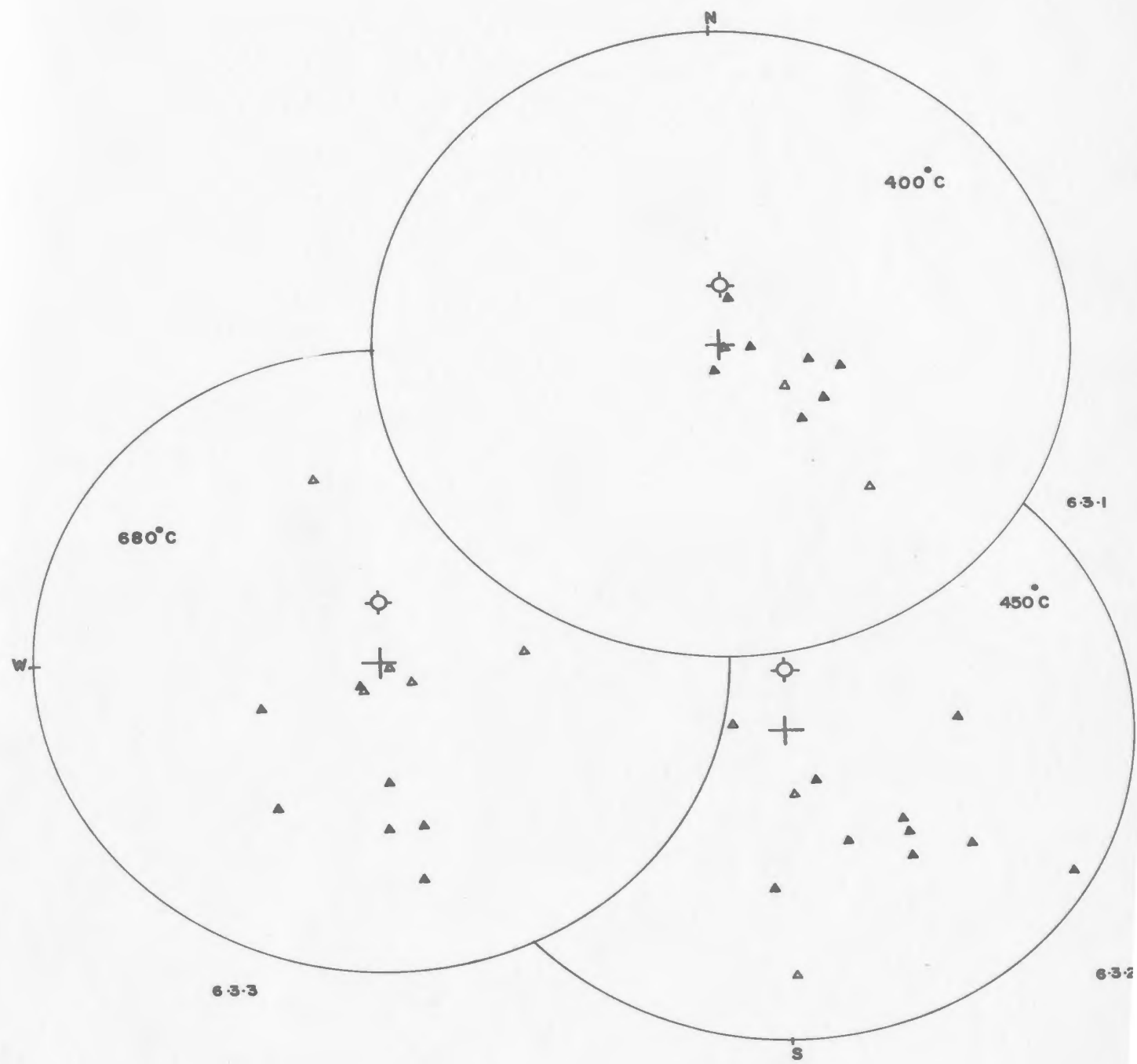
Intensity values for Table Head (Table 6.1; Fig. 6.7) tend to rise again sharply between 450 - 650°C, with the arithmetic mean intensity finally dropping again to just below 50% of the mean of  $J_n$  at 680°C. Even at minimum (450°C), the mean intensity was still over 40% of its NRM value, compared with 18% at 500°C for Henley Harbour.

TABLE 6.4

Mean magnetization of basalt specimens from Table Head and  
Henley Harbour, Labrador after stepwise demagnetization.

(T = demagnetization temperature. Other  
symbols as in Table 3.3)

Site	T	$\bar{D}$	$\bar{I}$	N	k
<u>Table Head</u>	NRM	92°	+70°	13	7.5
	400°C	117°	+51°	11	2.1
	450°C	143°	+33°	12	3.3
	550°C	188°	+13°	13	2.9
	600°C	183°	+7°	13	1.6
	650°C	183°	-10°	13	1.3
	680°C	171°	+11°	13	1.4
<u>Henley Harbour</u>	NRM	50°	+72°	6	29
	100°C	44°	+80°	5	7.3
	250°C	79°	+66°	6	2.1
	295°C	115°	+64°	5	1.6
	350°C	114°	+61°	6	3.0
	450°C	108°	+69°	6	2.3
	500°C	223°	-46°	6	1.2
	590°C	213°	-68°	6	6.1



Figs 6.3.1.- 6.3.3. Systematic thermal demagnetization of basalt specimens from Table Head, Labrador

Equal area projections, showing 6.3.1. directions after demagnetization to 400°C (10 specimens); 6.3.2. directions after demagnetization to 450°C (12 specimens); 6.3.3. directions after demagnetization to 680°C (13 specimens), relative to the present horizontal plane at the sampling site.

△ North pole in upper hemisphere  
(Symbols as in Fig 6.2)

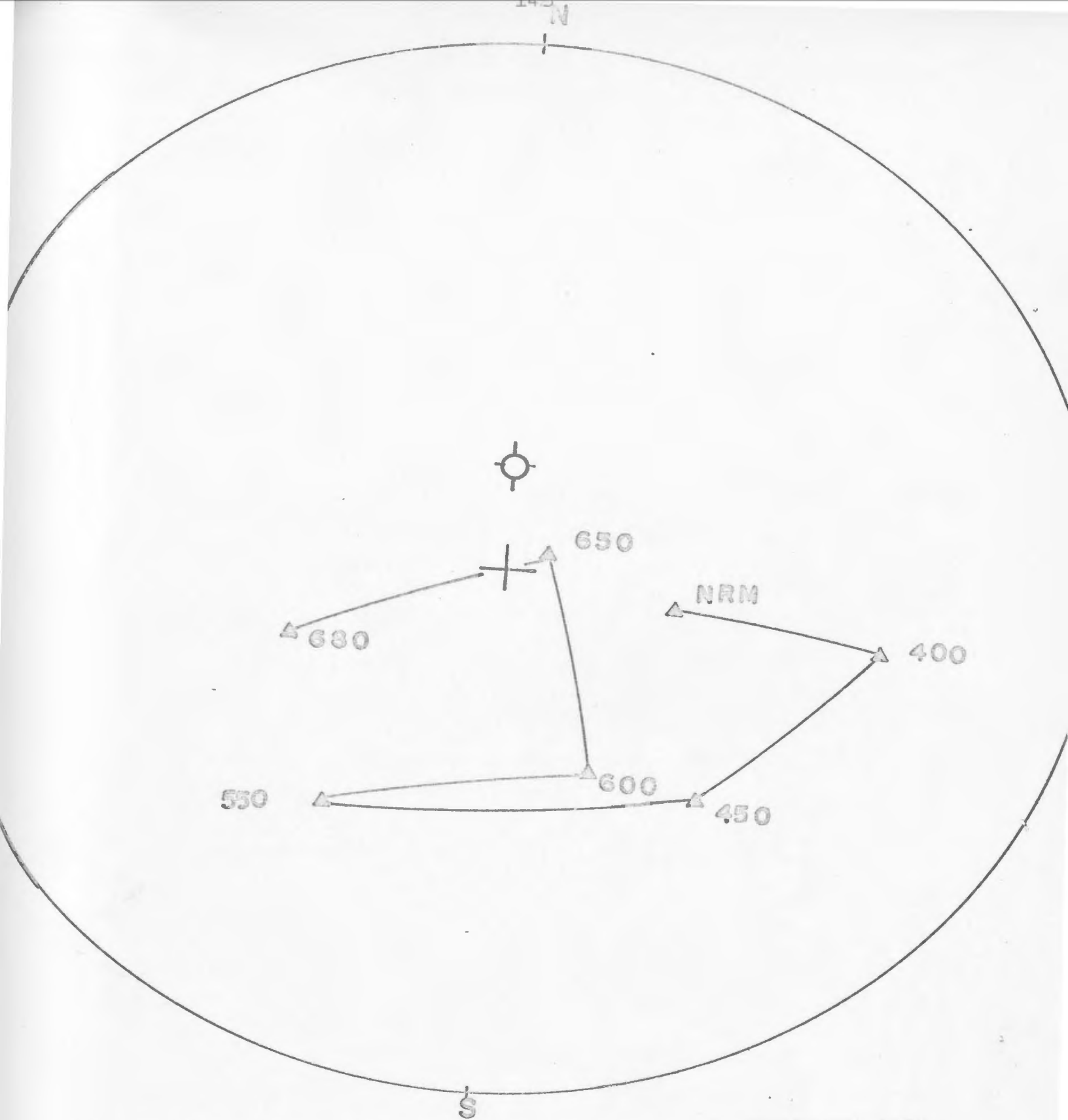


Fig 6.5.1. Directions of magnetization of specimen TH 21a, after stepwise demagnetization

Equal area plot. Numbers refer to the demagnetizing temperature ( $^{\circ}\text{C}$ )

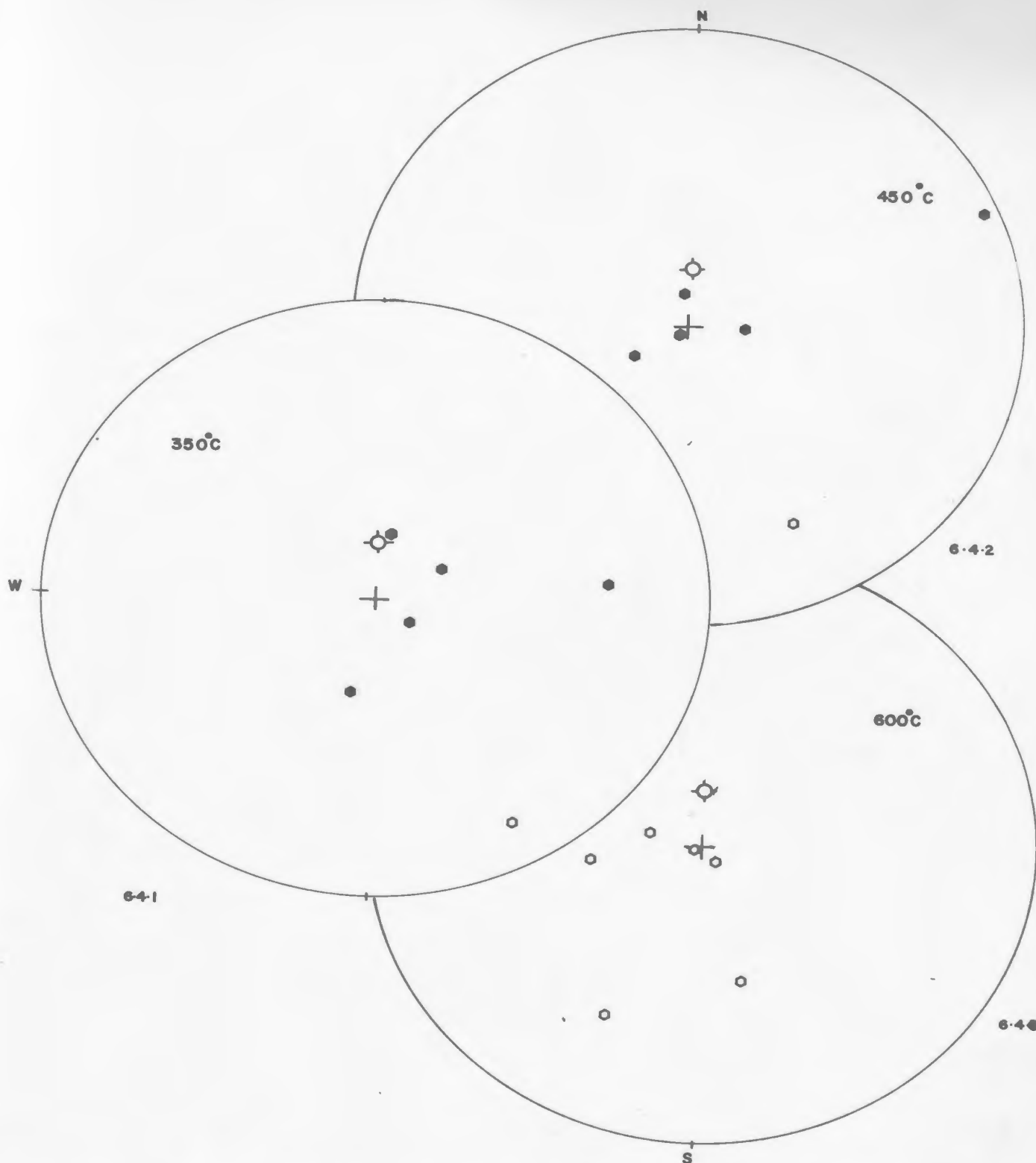
(Symbols as in Fig 6.2)

It is puzzling why heat treatment to  $680^{\circ}\text{C}$  failed so completely to demagnetize the Table Head specimens. However, while the  $(J_T/J_n) - T$  curves for Henley Harbour at first tend to drop much more sharply with increasing temperature than the Table Head curves (Fig. 6.7), the trend in both cases is broadly similar, indicating the presence of components having widely distributed blocking temperatures below  $350$  to  $450^{\circ}\text{C}$ . The intensity increase above  $450 - 500^{\circ}\text{C}$  is again common to both sets of curves, though at Table Head there is only a gradual change in mean direction up to  $680^{\circ}\text{C}$  ( $D = 171^{\circ}$ ,  $I = +11^{\circ}$  in Table 6.4, compared with  $D = 213^{\circ}$ ,  $I = -68^{\circ}$  at  $590^{\circ}\text{C}$  for Henley Harbour). At both sites the scatter was extreme at the highest temperatures, and no further discussion of the origin of the magnetizations above  $450^{\circ}\text{C}$  will be attempted.

At Table Head the flow and underlying sediments are nearly horizontal necessitating only a small tilt correction ( $3\frac{1}{2}^{\circ}\text{SE}$ ; E. R. Deutsch and P.S. Rao; unpublished field notes, 1966). Corrected mean directions for NRM,  $400$ ,  $450$ , and  $680^{\circ}\text{C}$ , are given in Table 6.5.

#### 6.4.2. Henley Harbour.

The Henley Harbour specimens ( $N = 6$ ) retained a fairly steep downward inclination up to  $450^{\circ}\text{C}$ , but their mean NRM declination, which was in the first quadrant, changed to a direction in the second quadrant (Table 6.4; see also Figs. 6.2, 6.4.1 - 6.4.3) that was nearly constant over the range  $295 - 450^{\circ}\text{C}$ . At  $350^{\circ}\text{C}$ , where  $k$  attains its small maximum<sup>1</sup>, the mean direction is  $D = 114^{\circ}$ ,  $I = +61^{\circ}$ . Hence the latter values may be representative of a partially stable component



Figs 6.4.1.- 6.4.3. Systematic thermal demagnetization of basalt specimens from Henley Harbour, Labrador

Equal area projections, showing 6.4.1. directions after demagnetization to 350°C (6 specimens); 6.4.2. directions after demagnetization to 450°C (6 specimens); 6.4.3. directions after demagnetization to 600°C (6 specimens), relative to the present horizontal plane at the sampling site.

○ North pole in upper hemisphere  
(All symbols as in Fig 6.2)

TABLE 6.5

Mean magnetization of Table Head and Henley Harbour basalts,  
after stepwise demagnetization and tilt correction.

(Symbols as in Tables 3.3, 6.4)

Site	T	$\bar{D}$	$\bar{I}$	N	k
<u>Table Head</u>	NRM	97°	+67°	13	7.5
	400°C	117°	+48°	11	2.1
	450°C	143°	+29°	12	3.3
	600°C	171°	+8°	13	1.4
<u>Henley Harbour</u>	NRM	74°	+62°	6	28
	350°C	113°	+47°	6	3.1
	450°C	109°	+55°	6	2.3
	590°C	239°	-61°	6	6.0

with blocking temperatures below  $450^{\circ}\text{C}$ . Whether this represents a primary magnetization is difficult to determine from these limited data: above  $450^{\circ}\text{C}$ , a progressive upward change of the inclinations which is completed at  $590^{\circ}\text{C}$  (all inclinations negative), appears to be systematic. Directional changes for one specimen is plotted in Fig. 6.6.1.

Since most of the temperature range  $450 - 590^{\circ}\text{C}$  is below the Curie point of magnetite, it is possible that these upward-directed vectors reside in magnetite or titanomagnetite, and represent a stable component pre-dating the one that was prominent at  $295 - 450^{\circ}\text{C}$ . However, the intensities of all specimens had increased sharply after the final step, the mean value ( $N = 6$ ) of  $J_{590}/J_n$  being 0.5 (see also Fig. 6.7). Hence it is alternatively possible that the major directional changes above  $450^{\circ}\text{C}$  are due to a chemical modification during heating (compare Section 5.3), or possibly they were caused by some spurious field present in the oven, resulting from incomplete field cancellation. In the latter case, it had been estimated from the oven calibration that the value of any stray field in the region occupied by specimens is always within  $50 - 100 \gamma$  in a properly conducted demagnetization run (Chapter 4). Even smaller fields, however, would be capable of inducing stable PTRM components into a specimen above the temperatures at which its NRM has been effectively demagnetized.

A correction for the small geological dip ( $14^{\circ}\text{ESE}$ ; Murty, 1966), obtained by rotating the mean direction about strike ( $20^{\circ}$ ) is shown in Table 6.5 for the cases: NRM,  $350$ ,  $450$ , and  $590^{\circ}\text{C}$ . At both

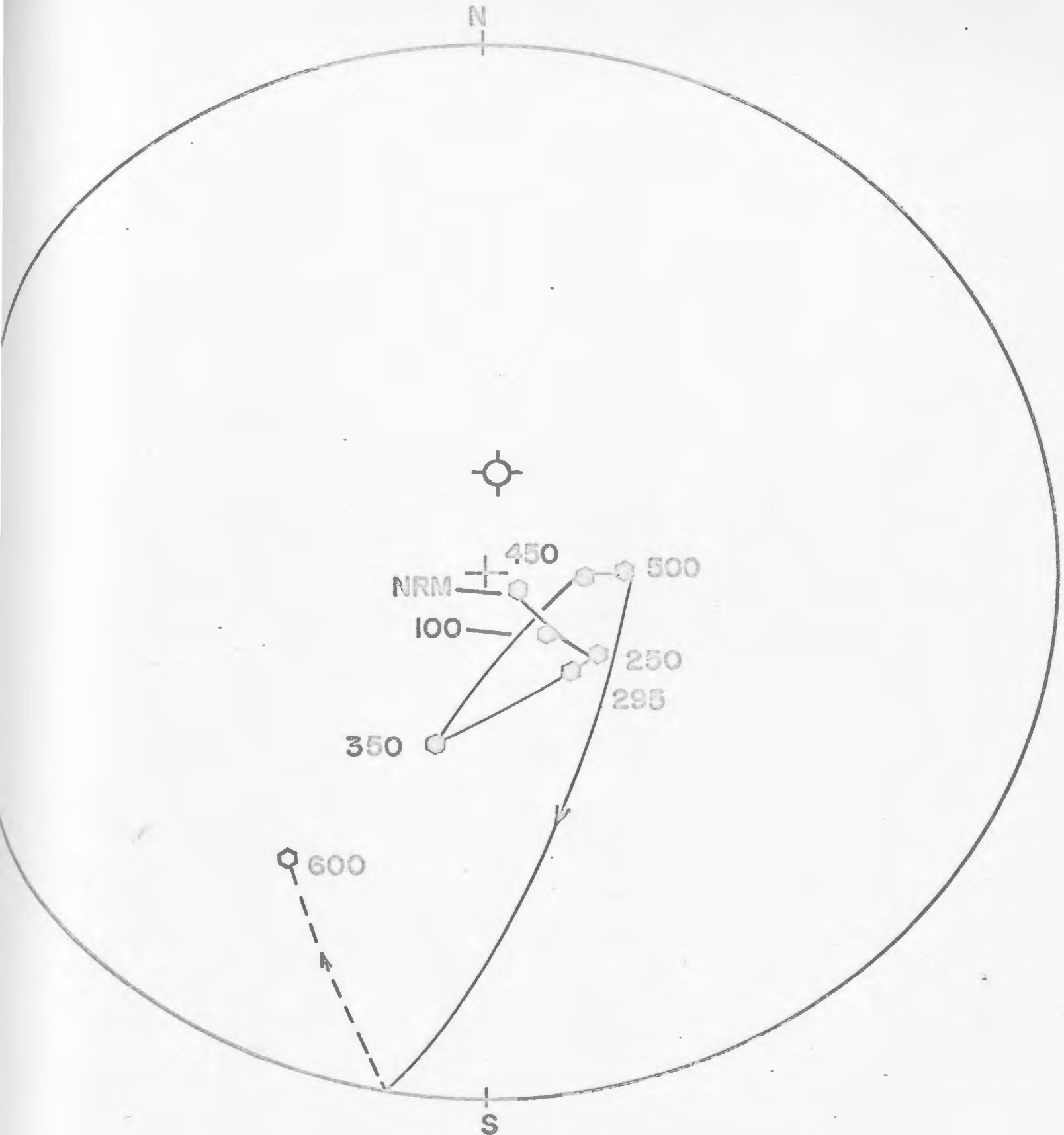


Fig 6.6.1. Directions of magnetization of specimen HH 3011, after stepwise demagnetization

Equal area plot. Numbers refer to the demagnetizing temperature (in °C)  
(Symbols as in Fig 6.2)

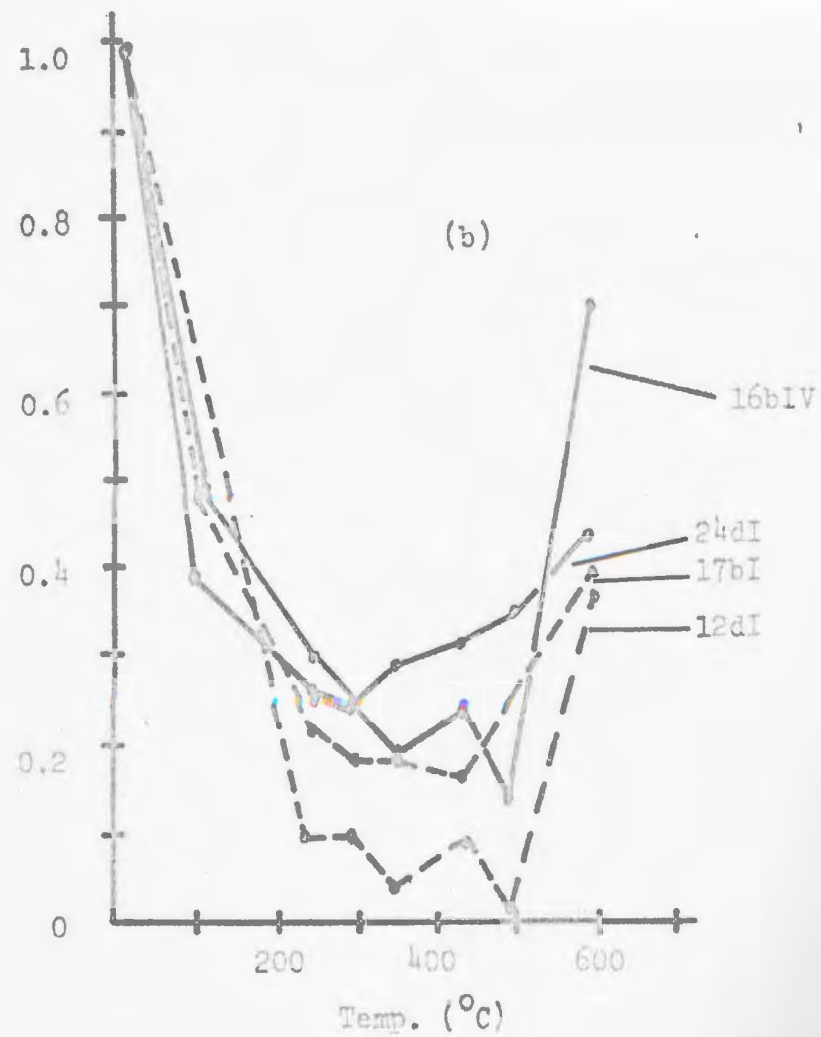
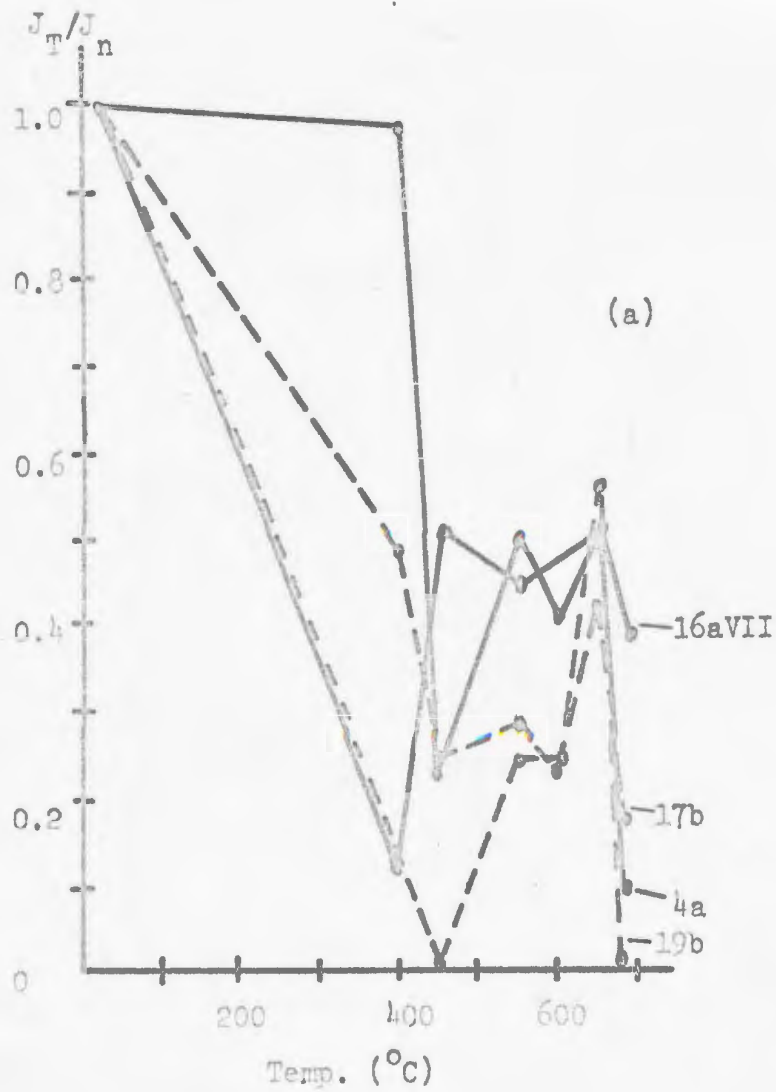


Fig 6.7. Variation of intensity (in normalized units with demagnetizing temperature for certain basalt specimens from: (a) Table Head. (b) Henley Harbour

Labrador sites, as well as Cloud Mountain, a simple rotation about strike is probably sufficient for referring the magnetic directions to the ancient horizontal plane, since the geological deformation of the lavas and underlying sediments seems to be confined to a gentle, eastward tilt of the beds at all three sites. In making the tilt correction one implies, however, that the lavas were laid down on a perfectly horizontal surface, an assumption which may be in error by a few degrees.

#### 6.5. Cloud Mountain.

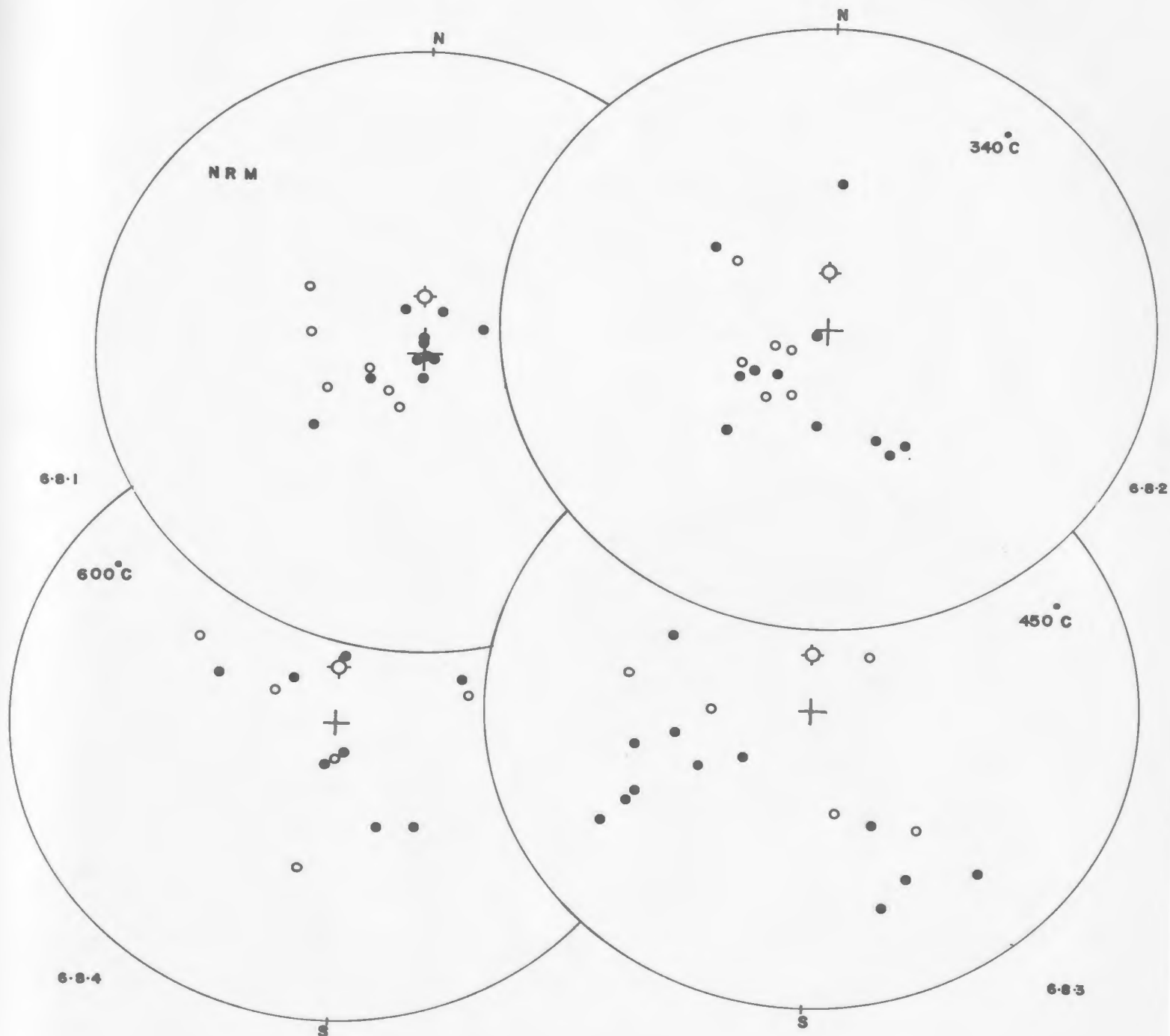
Whereas the NRM directions of all Table Head and Henley Harbour specimens (Tables 6.1, 6.2) had positive polarities (north pole downwards), the 17 Cloud Mountain specimens included six having intermediate to steep negative inclinations, compared with the (mostly steep) positive ones of the remainder (Table 6.3; Fig. 6.8.1). An unstable VRM, such as might have been acquired during laboratory storage, can be ruled out as a significant factor in causing these negative polarities, since the polarity grouping persisted to 450°C for all specimens (Figs. 6.8.2 - 6.8.4). Moreover, in either polarity group the agreement between the mean NRM directions of different samples tended to be poorer than the within-sample agreement in those cases where two specimens had been cut from the same sample: e.g. the two specimen directions in each "negative" sample (CM 2, 4, and 13) were moderately well aligned. While this within-sample alignment tended to become poorer at 450°C, the directional differences between specimens from opposite polarity groups clearly remained systematic, and it seems improbable that a spurious laboratory field would have remagnetized both specimens in

TABLE 6.3

## Systematic thermal demagnetization of the Cloud Mountain basalts.

Specimen	NRM			100°C			340°C			450°C			525°C			600°C		
	D	I	Jx10 <sup>-4</sup>	D	I	Jx10 <sup>-4</sup>	D	I	Jx10 <sup>-4</sup>	D	I	Jx10 <sup>-4</sup>	D	I	Jx10 <sup>-4</sup>	D	I	Jx10 <sup>-4</sup>
CM 1a	236	+45	0.6	235	75	0.2	*	*	*	241	+16	0.1	230	-61	0.1	*	*	*
1b	243	+69	0.3	*	*	*	7	+40	0.1	137	+17	0.2	148	+35	0.3	158	+50	0.6
2a	283	-50	67	272	-47	48	240	+55	16	141	-36	10	157	-46	21	304	-37	30
2c	300	-45	68	301	-43	54	309	-51	14	168	-54	6.3	85	-21	14	316	+69	19
4a	220	-72	42	218	-74	35	207	-63	14	44	-61	6.3	55	+17	4.6	4	+66	5.8
4c	253	-71	79	251	-71	65	251	-70	28	272	-56	9.1	273	-24	3.4	*	*	*
13a	211	-69	11	208	-63	15	218	-57	10	258	-33	10	273	-22	11	299	-66	6
13b	248	-55	11	223	-70	13	248	-57	6.3	283	-31	5.6	279	+36	9.9	294	+50	7
16a	3	+87	17	143	+83	22	226	+65	8.9	260	+45	9.9	313	+18	19	*	*	*
16b	217	+88	29	210	+88	20	239	+60	9.5	234	+61	6.6	252	+42	23	69	+46	26
19b	182	+80	43	185	+62	28	157	+41	15	153	+26	19	189	+4	12	*	*	*
26a	65	+68	17	141	+66	12	186	+54	5.9	243	+28	2.9	295	-37	14	166	+77	15
28a	112	+86	24	133	+74	21	159	+48	15	154	+45	14	159	+31	23	191	-37	9.5
28c	104	+89	21	148	+68	17	149	+43	1.2	163	+20	18	98	+42	12	145	+45	16
32a	1	+87	14	297	+88	9.4	238	+86	5.1	242	+49	3.7	313	-12	5.1	193	+74	17
32c	338	+72	14	344	+67	10	307	+43	2.9	302	+37	2.2	302	-13	10	85	+42	19
33a	23	+74	63	146	+80	36	223	+41	6.7	242	+25	8.9	277	+5	22	176	-75	*

Symbols as in Table 3.1



Figs 6.8.1.-6.8.4. Systematic thermal demagnetization of basalt specimens from Cloud Mountain, Northern Newfoundland

Equal area projections, showing 6.8.1. NRM directions of 17 specimens; 6.8.2. directions after demagnetization to  $340^{\circ}\text{C}$  (17 specimens); 6.8.3. directions after demagnetization to  $450^{\circ}\text{C}$  (17 specimens); 6.8.4. directions after demagnetization to  $600^{\circ}\text{C}$  (13 specimens, excluding weakly magnetized specimens), relative to the present horizontal plane at the sampling site.

North pole in: ● Lower hemisphere      ⊙ Axial dipole field  
○ Upper hemisphere

some of the samples in drastically different directions from those of the remaining samples (Storetvedt, 1968).

It could still be argued that if the "negative" samples were very different petrologically from the others, they would have been capable of acquiring the observed discordant magnetization either in situ or in the laboratory before the specimens were cut. One polished section (Specimen CM 20CI, with positive NRM polarity), examined by Dr. N. D. Watkins of Florida State University (Appendix 3), gave evidence of partial oxidation of titanomagnetite grains to hematite, with Oxidation Index IV (Wilson et al, 1968). This agrees qualitatively with the observed occurrence of low to extreme oxidation states (Indices II - VI) in the 6 polished sections from basalt at Table Head and Henley Harbour (Section 6.3; Appendix 3).

While no further petrological study of the Cloud Mountain basalts was made, a comparison of the thermal demagnetization curves for different sets of specimens can often lead to useful inferences regarding petrological relationships between the sets as it affects magnetic behaviour. In Fig. 6.9, the arithmetic mean of N specimen intensities has been plotted (in normalized units,  $\bar{J}_T/\bar{J}_N$ ) against temperature T, for (1) all Cloud Mountain specimens; (2) positive NRM polarities only; (3) negative polarities only.

The three curves nearly coincide up to 340°C, where two-thirds of the NRM has been destroyed, and where the curve (2) shows minimum relative intensity. Between 340 and 450°C, this curve rises slightly, whereas curves (1) and (3) continue to drop, reaching their minima

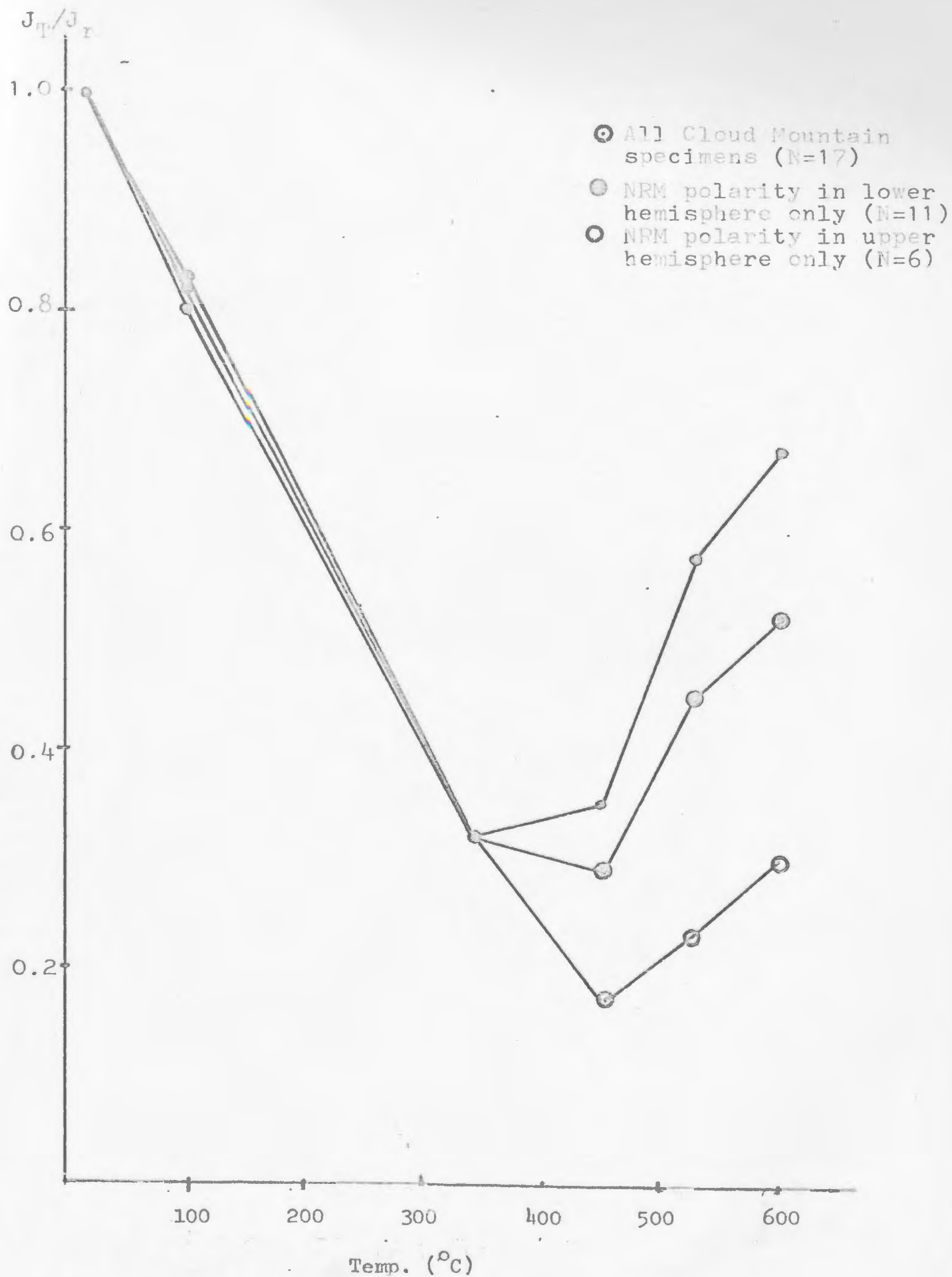


Fig 6.9. Arithmetic mean of N specimen intensities, Cloud Mountain (in normalized units)

at 450°C. However, at this temperature, the  $\bar{J}_T/\bar{J}_n$  of the "negative" specimens (0.17) is about half that of the "positive" ones (0.35), and since the arithmetic mean of the absolute intensities at NRM was about twice as large for the "negative" set ( $J_T = 46.3 \times 10^{-4}$  emu/cm<sup>3</sup>) as for the "positive" one ( $22.2 \times 10^{-4}$ ), this implies that any "excess" magnetization imposed on the former set has been effectively removed at 450°C. Above that temperature, the trend of the three curves is again similar, the absolute mean intensities of the two polarity sets being comparable up to 600°C. All the above findings strongly support the supposition that the samples exhibiting opposite polarities have a very similar ferromagnetic petrology. Moreover a comparison of the combined Cloud Mountain curve (1) with the selected  $J_T/J_n$  curves for the other two sites (Fig. 6.7) again reveals close similarities in trend, the intensity minima of these curves again occurring mostly at or near 450°C.

Self-reversal is unlikely to explain the negative NRM polarities at Cloud Mountain, partly in view of the suggested petrological similarities with the "positive" group, and also because self-reversal would not be likely to occur in basalts (Wilson and Watkins, 1967). That the opposite polarities reflect a reversal of the Earth's field is also unlikely, since all Cloud Mountain samples are from a single flow. A more plausible cause of the discordant (-) polarities might be magnetization by lightning, as samples CM 2 and 4 had been collected from the top of Cloud Mountain. (though CM 13, along with some positively polarized samples was collected 200 feet below the top). The observed

large intensities of "negative" Samples CM 2 and 4 (attaining  $8 \times 10^{-3}$  emu/cm<sup>3</sup> in the case of Specimen 4 C), along with the persistence of the polarity grouping of all six specimens up to 450°C, would be consistent with the imposition of a fairly stable, strong IRM by lightning, as observed by several workers.

Regardless of the cause of the polarity difference, it was convenient to divide the Cloud Mountain specimens into two sets based on their polarity at NRM. For the "positive" specimens only the mean directions and precision constants are given in Table 6.6 for NRM and after treatment. Direction changes for single "positive" and "negative" specimens (at NRM) are shown in Figs. 6.10.1 - 6.10.2.

The mean declination of the positive Cloud Mountain specimens changed from west to southeast upon heating to 600°C, while the mean inclination gradually decreased from its large NRM value (+87°). The mean direction before tilt correction after 450°C ( $D = 214^\circ$ ,  $I = +46^\circ$ ,  $k = 3.4$ ,  $N = 11$  specimens) may be compared with the mean directions after 450°C for Table Head and 350°C for Henley Harbour (Table 6.4). Whereas the above mean directions for these Labrador sites correspond to minima of the arithmetic intensities and to small precision maxima (Sections 6.4, 6.4.1, 6.4.2), the mean intensities of the positive Cloud Mountain specimens has a minimum at 340°C (see this Section), whereas  $k$  continuously decreases between 100 and 525°C, so that  $k_{340}$  (4.6) is larger than  $k_{450}$  (3.4). Hence the most appropriate comparison of the mean directions at the three sites (omitting "negative" CM specimens) is likely to correspond to the

TABLE 6.6

Mean magnetization of basalt-specimens from  
Cloud Mountain, Northern Newfoundland after  
stepwise demagnetization

(symbols as in Tables 3.3, 6.4)

T	$\bar{D}$	$\bar{I}$	N*	k
NRM	272°	+87°	11	18.7
100°C	162°	+82°	10	24.8
340°C	201°	+71°	10	4.6
450°C	214°	+46°	11	3.4
525°C	258°	+14°	11	1.4
600°C	141°	+46°	8	1.9

\*Six specimens with negative NRM polarity have been excluded.

Figs 6.10.1.-6.10.2. Directions of magnetization of specimens CM 26a, and CM 2c, after stepwise demagnetization

Equal area plot. Numbers refer to the demagnetizing temperature (in °C)

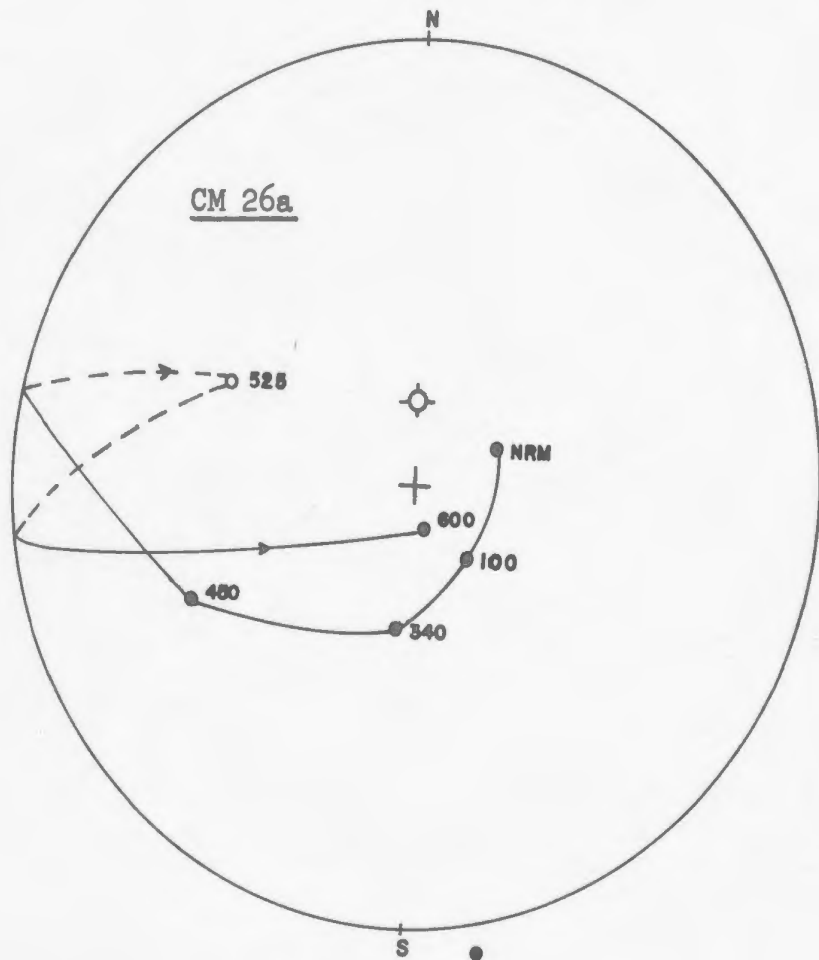


Fig 6.10.1.

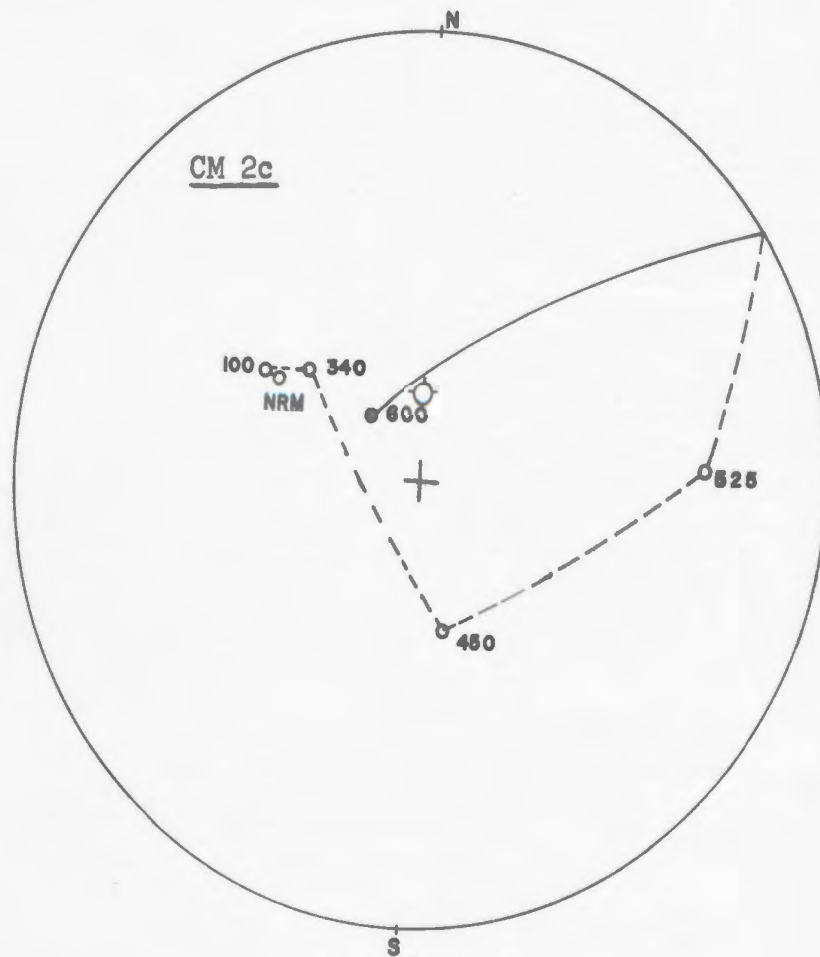


Fig 6.10.2.

(Symbols as in Figs 6.8.1.-6.8.4)

350, 450, and 340°C steps at Henley Harbour, Table Head, and Cloud Mountain respectively.

A correction for the geological dip (22.5°E; Clifford, 1965), is shown in Table 6.7 for the cases: NRM, 340, 450, and 600°C. The mean direction corresponding to 340°C is  $D = 140^\circ$ ,  $I = +66^\circ$ , compared with  $D = 113^\circ$ ,  $I = +47^\circ$  and  $D = 143^\circ$ ,  $I = +29^\circ$ , for Henley Harbour (350°C) and Table Head (450°C) respectively. Despite the large difference in  $I$  values and low precision in all cases, the three site mean directions show some similarities, all declinations being in the second quadrant.

From the above mean directions, the "virtual" pole positions for the three sites were calculated and are shown in Table 6.8. These "virtual" poles have no paleomagnetic significance because of the reasons stated in Section 6.3, and are only quoted to indicate roughly whether these heat-treated specimens from single lava flows give directions anywhere near those one might expect from Lower to Middle Paleozoic rocks. A comparison of Table 6.8 with Fig. 5.6 shows that there is indeed some rough correlation which may, or may not, be fortuitous.

Further paleomagnetic collections from suitable exposures of sediments or multiple flows of that age and from similar area might give promising results; ultimately such data could prove useful in providing evidence on "pre-Wegenerian" drift.

The present work was confined to thermal demagnetization of the single-flows specimens under study. Future paleomagnetic work on basalts and contemporaneous sediments should be accompanied by additional a.c. demagnetizations, petrological examination, susceptibility and coercivity studies, along with extensive thermal demagnetization.

TABLE 6.7

Mean magnetization of Cloud Mountain basalts after stepwise demagnetization and tilt correction.

(Symbols as in Tables 3.3, 6.4)

T	$\bar{D}$	$\bar{I}$	N*	k
NRM	90°	+70°	11	18.5
340°C	140°	+66°	10	4.6
450°C	188°	+54°	11	3.4
600°C	129°	+30°	8	1.9

\* Six specimens with negative NRM polarity have been excluded.

TABLE 6.8

Paleomagnetic pole positions (virtual) for basalts from Table Head, Henley Harbour, and Cloud Mountain, from the mean directions of magnetization (N specimens) after laboratory treatment and tilt correction

Unit	Treatment	N	Virtual Pole Positions	
			Pole	Anti pole
Table Head	450°C	12	15°S 19°W	15°N 161°E
Henley Harbour	350°C	6	9°N 1°W	9°S 179°E
Cloud Mountain	340°C	10	15°N 30°W	15°S 150°E
Henley Harbour*	NRM	15	56°N 2°E	56°S 178°W

\*Virtual pole position from NRM measurement and after tilt

(Murthy, 1966).

APPENDIX 1EXISTING APPARATUSAl.1. Astatic Magnetometer.

Measurements of the magnetization before and after each demagnetization step were carried out with the astatic magnetometer at the Physics Department (Murty, 1966; Deutsch et al, 1967), the characteristics of which are given in Table Al.1; the sensitivity figure quoted corresponds to the use of a suspension used until 1967. A recalibration of the instrument constants by the present author (Table Al.2), undertaken prior to the measurements described in this thesis, gave a reciprocal sensitivity  $1.65 \times 10^{-7}$  oe per mm deflection, compared with  $3.9 \times 10^{-7}$  oe/mm deflection originally obtained by Murty (1966) for the same mirror-scale distance (180 cm). The improvement resulted from substitution of a new gold ribbon suspension for the original suspension of the same material, having about the same length (10 cm) and quoted cross-section (0.002 cm x 0.0002 cm). Presumably the new suspension was in fact thinner than the previous one, thus producing a reduced torsion constant.

Al.2. Alternating-field demagnetization unit.

Alternating-field demagnetizations of the ignimbrites from Killary Harbour were carried out with the unit at the Physics Department (Pearce, 1967), having the constants given in Table Al.3. The unit produces a field of 257 oe (peak) per r.m.s. ampere, with maximum attainable field strength of 800 oe (peak). The specimens were demagnetized while tumbling about three axes with the gear ratio

TABLE A1.1Constants of the astatic magnetometerMagnets

Material	Magnadur III
Magnetization	transverse
Height h (cm)	0.75
Length l (cm)	0.25
$\beta = l/h$	0.33
Dipole moment per magnet, p (cgs)	10.1
Separation between magnets L (cm)	6.00
Moment of Inertia per magnet, $I_1$ (g-cm <sup>2</sup> )	0.0022

System

Moment of Inertia of holder without magnets, $I_2$ (g-cm <sup>2</sup> )	0.0031
Moment of Inertia of system: $I = 2I_1 + I_2$ (g-cm <sup>2</sup> )	0.0075
p/I (cgs)	$1.35 \times 10^3$
Mean reciprocal sensitivity (oe/mm deflection at 180 cm scale distance)	$3.90 \times 10^{-7}$
Reciprocal sensitivity for T = 20 sec (oe/mm at 5.0 m), calculated	$0.73 \times 10^{-8}$
Period, T for reciprocal sensitivity = $1.0 \times 10^{-8}$ oe/mm at 5.0 m (secs), calculated	17.1

Suspension

Material	Ribbon of gold alloy
Length (cm)	10.0
Cross-section (cm x cm)	0.002 x 0.0002

TABLE A1.1 (Continued)Data for the Helmholtz coils

## Vertical coils:

Radius (cm)	45.4
Number of turns/coil	50
Resistance/coil (ohms)	4.8

## North-South coils:

Radius (cm)	50.2
Number of turns/coil	50
Resistance/coil (ohms)	5.2

## East-West coils:

Radius (cm)	55.1
Number of turns/coil	15
Resistance/coil (ohms)	1.6

TABLE A1.2

Recalibration of the astatic system (1968)

Magnetic moment of the calibrating coil for one ampere of current,  
 $M = 45.9$  ergs/oe

Distance from center of calibrating coil to center of astatic system,  
 $z$  (cm)

Distance between mirror and scale,  
 $D = 180.0$  cm  $\pm$  0.5

Scale deflection,  
 $d$ (mm)

Net field on magnetometer due to calibrating coil,  
 $H$  (oe  $\times 10^{-7}$ )  
 Where  $H = \frac{3LM}{z^3}$ ; with  $L = 6.00$  cm

Reciprocal sensitivity,  
 $H/d$  (oe/mm deflection  $\times 10^{-7}$ )

$z$	$d$	$H$	( $H/d$ )
102	46	$M \times 1.66$	1.66
100	50	$M \times 1.80$	1.65
98	54	$M \times 1.95$	1.66
96	60	$M \times 2.13$	1.63
92	71	$M \times 2.53$	1.63
		<u>Mean</u>	<u><math>1.65 \pm 0.02</math></u>

100  
TABLE A1.3

Constants of the a.c. demagnetization unit

Demagnetizing coils:

Parameter	Coil 1	coils in series	Coil 2
Dimensions of wiring cross section, width x height (cm x cm)	11.0 x 6.7	--	11.0 x 6.5
Number of turns	2550	5089	2539
Total inductance (henries)	--	2.90	--
Specific field $\frac{(\text{oe/peak})}{(\text{amp.rms})}$	--	257	--

Helmholtz coils: (for d.c. field nulling)

As in the set of Helmholtz coils described in Table A1.1.

Gear ratio of the tumbling system about the inner, middle and outer axes respectively: 1.61 : 1.21 : 1.00

Maximum speed of tumbling of the specimen (inner tumbling axis), r.p.s. 5.0

shown. This was demonstrated by Pearce (1967) to be more effective than 2-axis tumbling in suppressing unwanted ARM components during demagnetization. The a.c. fields were smoothly reduced by using a variable electrolytic resistance in series with the demagnetizing coils.

APPENDIX 2AUXILIARY EQUIPMENT FOR THERMAL DEMAGNETIZATIONA2.1. Thermocouples.

During the demagnetization experiments, the temperature at the oven center was measured by a platinum-platinum/10% rhodium thermocouple inserted through the base of the oven (Fig. 4.2). The cold junction was placed in a dewar flask containing ice at 0°C. The thermocouples had been calibrated at the National Research Council in Ottawa with a quoted accuracy of  $\pm 0.3^{\circ}\text{C}$  (Table A2.1).

A second calibration was required to convert  $^{\circ}\text{F}$  scale values in the direct-reading Leeds-Northrup temperature potentiometer into corrected centigrade values corresponding to the N.R.C. standardization. A Leeds-Northrup K-2 potentiometer was used with the arrangement and circuit diagram shown in Fig. A2.1.

The hot junction was placed along the oven axis, at the center of the region normally occupied by specimens. The temperature was then raised to progressively higher levels, at each of which it was maintained by a thermostat (A2.2) for at least 20 minutes to ensure equilibrium conditions. At each level repeated readings were taken alternately with the K-2 potentiometer and the temperature potentiometer, the former readings being directly converted into true centigrade values by means of the N.R.C. calibration. The data are shown in Table A2.2 and the final calibration curve in Fig. A2.2.

A2.2. Thermostat.

The temperature at each step was maintained at a constant

TABLE A2.1Calibration of platinum-platinum10% rhodium thermocouples

(by National Research Council, Ottawa)

Temperature (°C)	E.m.f. (mv)
0	0.000
100	0.645
200	1.439
300	2.321
400	3.257
500	4.229
600	5.233
700	6.271
800	7.342
900	8.446
1000	9.585
1100	10.747

The reference junctions were held at 0°C.

The thermocouples were calibrated in a tube furnace by comparison with standard platinum-platinum/10% rhodium thermocouple C-6.

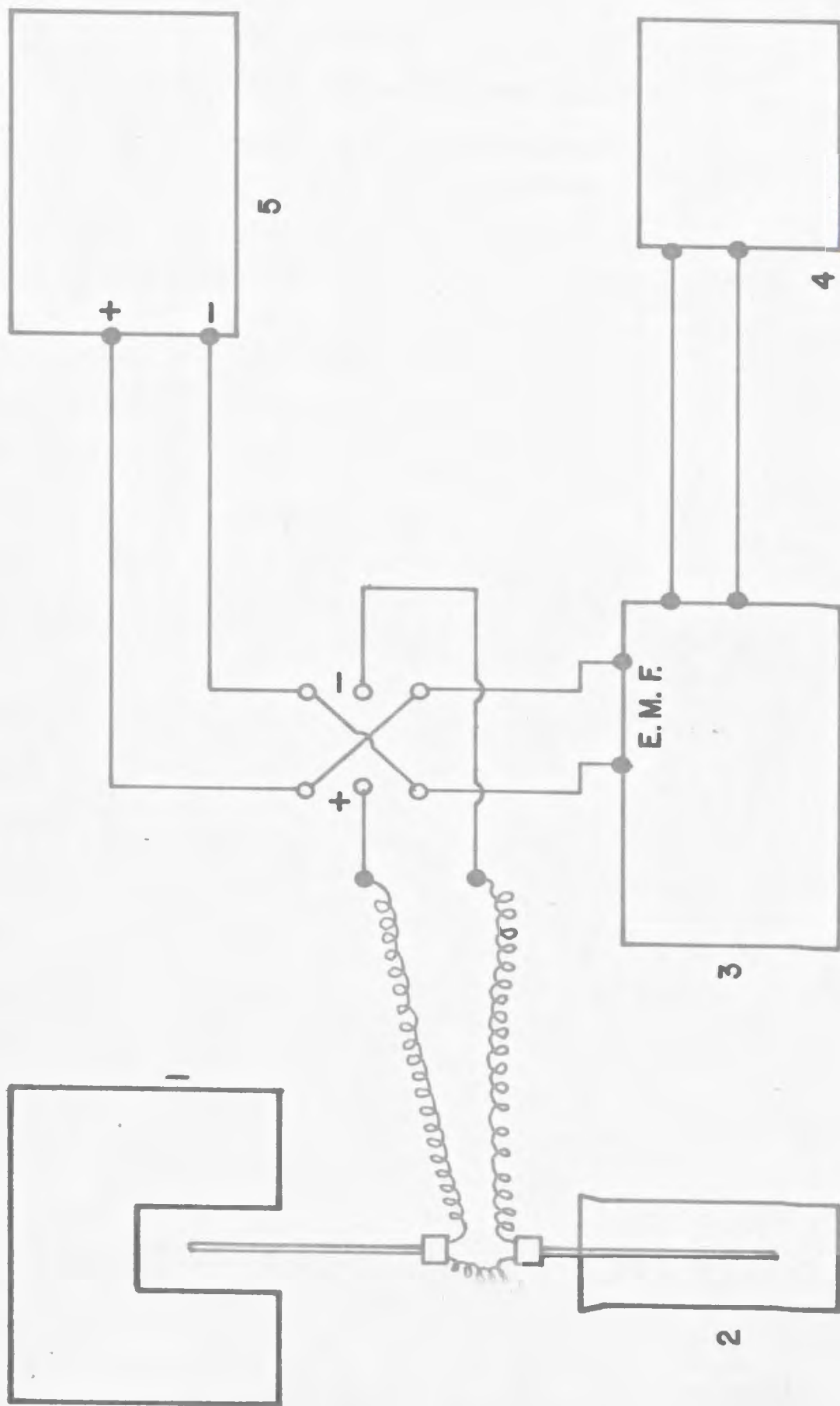


FIG A2.1. Schematic view of arrangement and circuit used in the temperature potentiometer calibration

1. Hot junction at the oven; 2. Cold junction; 3. Leeds-Northrup K-2 potentiometer; 4. Leeds-Northrup temperature potentiometer; 5. Leeds-Northrup potentiometer

TABLE A2.2

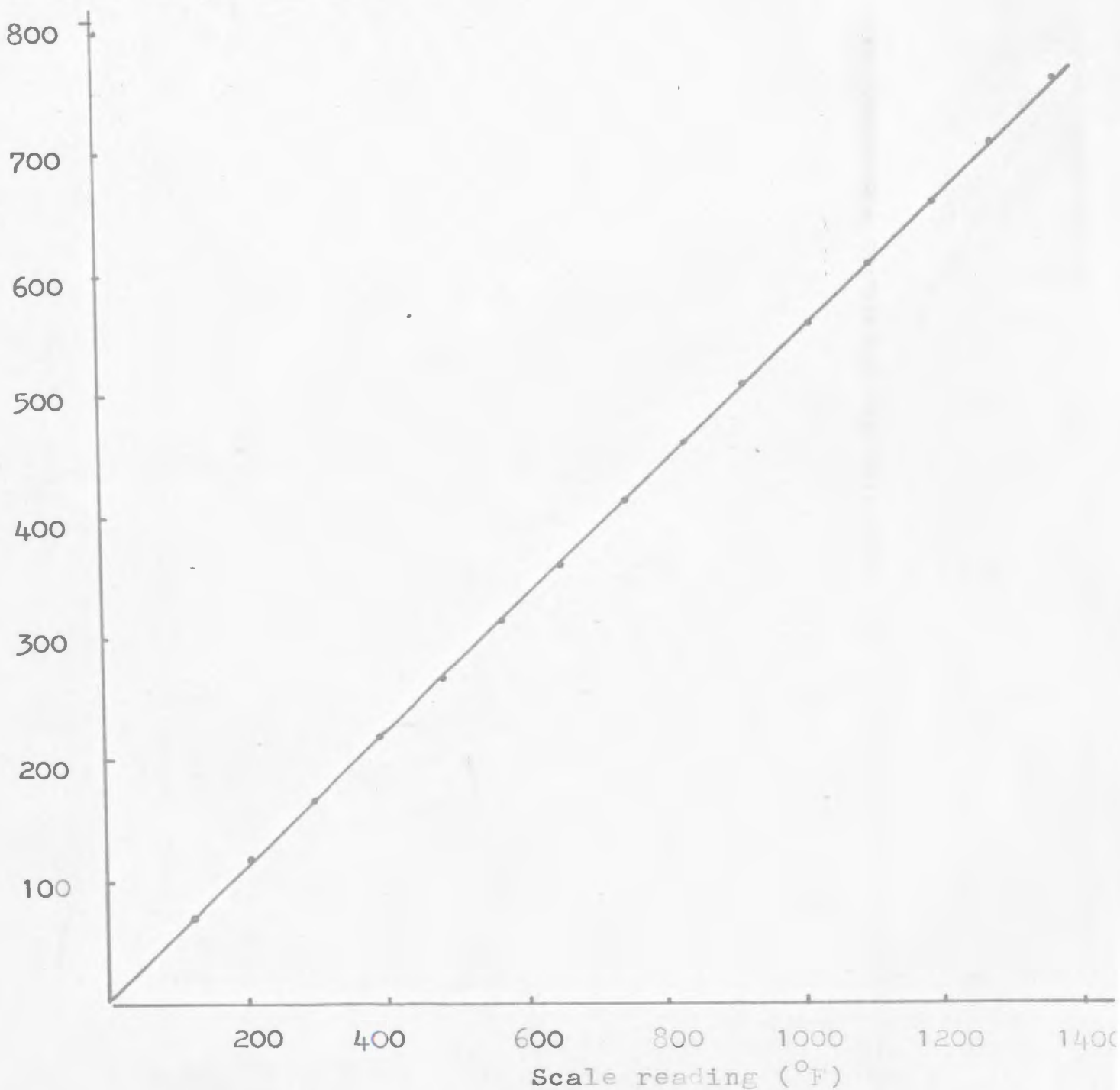
Calibration table for Leeds-Northrup  
temperature potentiometer  
 (actual data - not smoothed)

Reading on potentiometer scale		Corrected temperature in °C
°F	Corresponding °C	°C
122	50	68
212	100	121
302	150	169
392	200	218
482	250	264
572	300	313
662	350	360
752	400	412
842	450	460
932	500	509
1022	550	559
1112	600	609
1202	650	660
1292	700	709
1382	750	760

Fig A2.2. Calibration curve for Leeds-Northrup temperature potentiometer used with calibrated platinum-platinum/10% rhodium thermocouples

(The corrected temperature corresponds to standards obtained at the National Research Council, Ottawa. Calibration data are from Table A2.2).

Corrected temperature( $^{\circ}$ C)



pre-set value for 20-25 minutes by a "Resistotrol" thermostat made by Hallikainen Instruments Inc. This unit was capable of controlling the predetermined temperature to  $\pm 10^{\circ}\text{C}$  at 100-200 $^{\circ}\text{C}$  and  $\pm 5^{\circ}\text{C}$  at 200-500 $^{\circ}\text{C}$ . A resistance thermometer sensing element for the thermostat was inserted through the base of the oven next to the thermocouple. The thermostat was operable in the range 100-600 $^{\circ}\text{C}$ , the higher temperature designating the limit above which the required voltage (115 volts) may be insufficient to cause further heating. Incorporation of the thermostat circuit into the heating circuit greatly increases the time required to heat the oven to 500 $^{\circ}\text{C}$ ; hence an alternative procedure was adopted for demagnetization at higher temperature ranges. The heating coils were then connected directly to the 220-volt mains through a Variac, and the heating current was continuously controlled at the desired elevated temperature through manual adjustment.

### A2.3. Thermal gradient measurement.

Thermal gradients were measured with a movable platinum-platinum/10% rhodium thermocouple at various fixed mean temperatures in the central part of the oven normally occupied by the specimen stand. During these measurements, and also during actual demagnetization runs, this region was enclosed by an inverted copper pot acting as a secondary radiator of heat; this arrangement greatly reduces the thermal gradients in the working space, particularly at high temperatures.

Results are shown in Fig. A2.3 and (for a more detailed determination) in Table A2.3. The excess temperature,  $\Delta T$ , at a radial distance  $r$  from the oven center is quite large at temperatures  $T_0$  up to

Fig A2.3. Horizontal temperature gradients in the central region of the oven, as a function of temperature at the oven center

( $r$  is the radial distance from oven center to observation point in a horizontal plane through the oven center;  $T_0$ ,  $T_r$ , : temperature at oven center and at distance  $r$ , respectively).

Excess temperature,  
 $\Delta T = T_r - T_0$  ( $^{\circ}\text{C}$ )

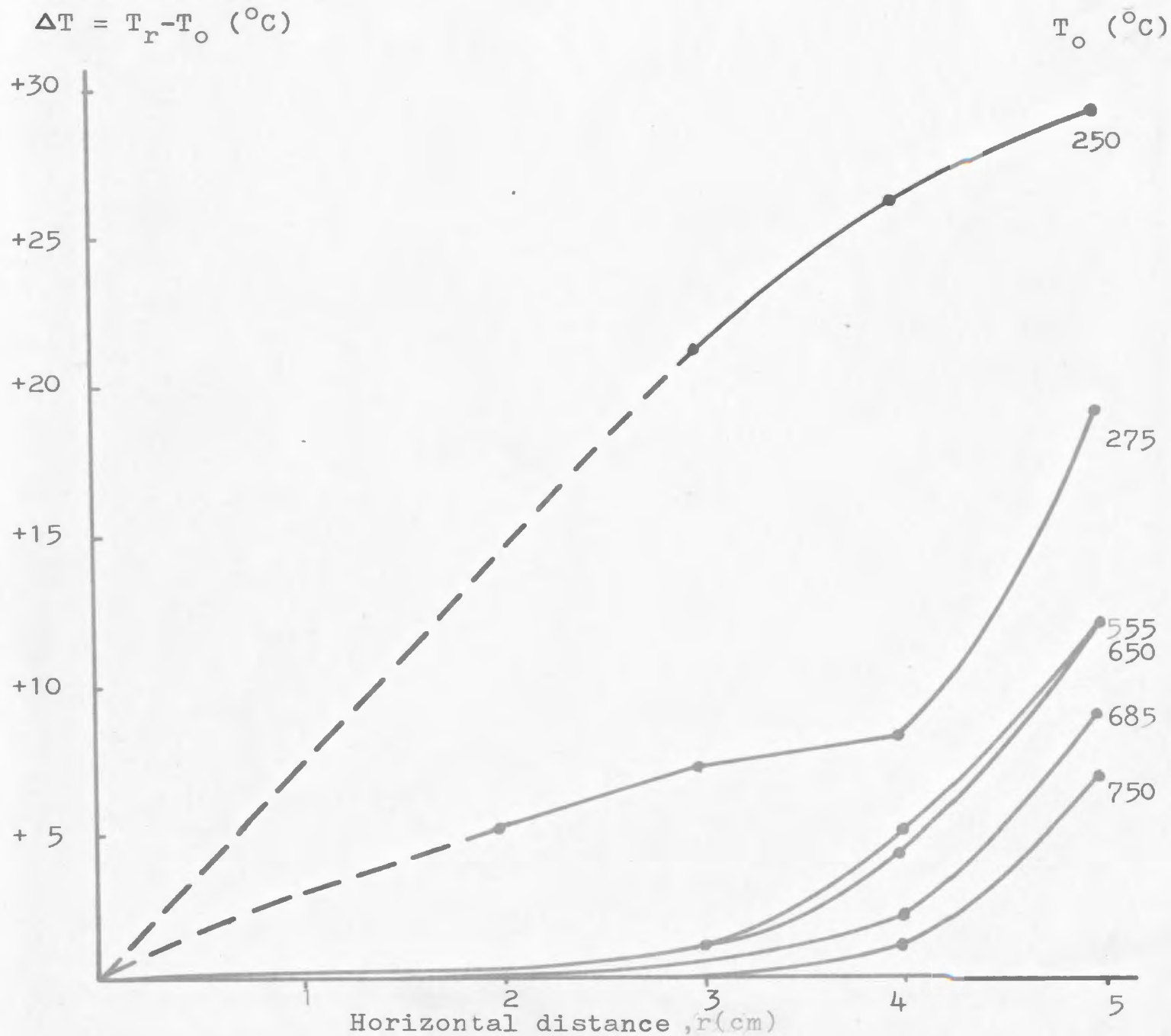


TABLE A2.3

Calibration of temperature variation in  
the working space of the oven

$T_o$  ( $^{\circ}\text{C}$ ) = temperature at oven center;

$T_r$  ( $^{\circ}\text{C}$ ) = temperature at radial distance  $r$  (cm) from oven center,

$\Delta T$  ( $^{\circ}\text{C}$ ) =  $T_r - T_o$

$r$  is measured in a horizontal plane through the oven center.

$T_o$	$\Delta T$ (all non-zero values are positive)				
	$r = 2.0$	3.0	4.0	5.0	6.0
250	*	21	26	29	*
293	5	7	8	19	*
352	0	1	1	12	*
365	0	2	2	15	*
492	1	1	1	16	*
510	1	1	2	15	*
555	0	1	5	12	*
567	0	0	4	9	*
646	0	0	4	12	*
666	0	0	2	9	*
696	0	0	2	9	*
705	0	0	2	10	11
750	0	0	1	7	8

\* no measurement

250°C and  $r$  several cm; e.g.  $\Delta T = +26^\circ\text{C}$  at  $r = 4.0$  cm and  $T_0 = 250^\circ\text{C}$ . At 275°C, the excess temperature at that distance has been reduced to +8°C, and at higher temperatures all  $\Delta T$  values become quite small at distances up to 4.0 cm. At 555°C and above, mean temperature gradients over the distance  $r = 0$  to  $r \leq 4.0$  cm are always  $+1^\circ\text{C}/\text{cm}$  or less, though between  $r = 4.0$  cm and 5.0 cm, the gradients tends to increase sharply, varying from  $+12^\circ\text{C}/\text{cm}$  at  $T_0 = 275^\circ\text{C}$  to  $+6^\circ\text{C}/\text{cm}$  at  $T_0 = 750^\circ\text{C}$ .

The gradient measurement was carried out at the central plane between the two compartments, on either of which specimens are mounted during demagnetization runs. As the separation between the two compartments is only 4.5 cm (Fig. 4.2), i.e. 2.3 cm above and below the calibrated central plane, one would not expect large thermal gradients to exist between the upper and lower compartments; the absence of a significant calibration error due to such a cause was confirmed by an additional test.

In actual demagnetization runs, the specimens were distributed at mean distances of  $r = 4.0$  or 4.5 cm from the oven center, or at the center itself. Except in the latter case, all temperatures quoted in Chapters 4-6 incorporate a  $\Delta T$  correction obtained from graphs such as shown in Fig. A2.3, and amounting to some temperature increase over that obtained from the centrally mounted thermocouple.

APPENDIX 3POLISHED SECTION STUDY OF KILLARY HARBOUR IGNIMBRITESAND BASALTS FROM NEWFOUNDLAND AND LABRADOR.

Polished sections of some ignimbrite and basalt samples used in the present study have been examined by Dr. N. D. Watkins of Florida State University. The comments (in quotation marks) by Dr. Watkins on microphotographs (not reproducible here) are given in Table A3.1.

TABLE A3.1

Microphotographs of polished sections from  
igneous rocks used in the present study

(Comments in quotation marks are by Dr. N.D. Watkins,  
who made the analysis)

Microscope field of view: 130 x 100 microns

- Plates 1 - 4: Ignimbrite from Killary Harbour, Eire  
 Plates 5 - 10: Basalt from Henley Harbour, Labrador  
 Plates 11, 12: Basalt from Table Head, Labrador  
 Plates 13, 14: Basalt from Cloud Mountain, Island of Newfoundland

- Plate 1. KH2aII. "Hematite with darker titanohematite laths and small patches of pseudobrookite, both after original titanomagnetite".
- Plate 2. KH2aII. Similar to Plate 1.
- Plate 3. KH21aI. "Irregular hematite patches, probably after ilmenite intergrowths in large titanomagnetite grain".
- Plate 4. KH21aI. "Regular development of wide laths of hematite partially replaced by pseudobrookite".
- Plate 5. HH8dII. "Unoxidized titanomagnetite grain".
- Plate 6. HH12eII. "Secondary hematite in olivine, with development clearly concentrated on cracks in the grain".
- Plate 7. HH12eII. "Top half shows secondary hematite in olivine, but lower half shows apparently low oxidation state titanomaghemite grain".
- Plate 8. HH12eII. "Secondary hematite in olivine".
- Plate 9. HH16dIII. "Skeletal titanomagnetite, probably representing grains which are quenched: that is, frozen before complete growth possible, as is frequently the case in the exteriors of pillow basalts".

TABLE A3.1 (Continued)

- Plate 10. HH25hI. "Secondary hematite in olivine, showing development of radial and parallel rods".
- Plate 11. TH6bIII. "Very regular elongate titanomagnetite skeletal grains".
- Plate 12. TH6bIII. "Another set of examples of skeletal titanomagnetite, but also featuring a relic olivine grain replaced in part by hematite (upper left center). This is an unusual example of coexisting low and high oxidation states, respectively.
- Plate 13. CM20cI. "Fine lamellae in titanohematite host, both after titanomagnetite. The lamellae have been replaced by a dark amorphous mineral".
- Plate 14. CM20cI. "Titanohematite pseudomorph of titanomagnetite, with irregular magnetization along conchoidal fractures which is replaced by a dark grey amorphous Fe-Ti oxide".

APPENDIX 4INITIAL NRM AND DEMAGNETIZATION MEASUREMENTSOF THE LABRADOR BASALTS

The NRM measurements of 21 Henley Harbour and 4 Table Head basalts from Labrador were measured by Murty (1966). Direction and intensity of the mean magnetization at each of the two sites is quoted in Table A4.1. The initial a.c. demagnetizations were carried out on 6 specimens by Pearce (1967), using four demagnetization steps. Results are shown in Table A4.2 and Fig. A4.1.

TABLE A4.1

Mean natural remanent magnetization of Table Headand Henley Harbour basalts

(from Murthy, 1966)

Site	$\bar{D}$	$\bar{I}$	$\bar{J} \times 10^{-4}$	N	k	$\alpha_{95}$
Table Head	72.6	72.8	17.89	4	5	31.9
Henley Harbour:						
Henley Island	13.1	76.1	6.55	15	16	9.0
Castle Island	9.3	73.9	7.45	6	42	8.8

Symbols as used in Chapters 3-6, with unit weight (N = 1) given to samples.

TABLE A4.2

Mean direction of magnetization of selected specimens of  
Labrador basalts after a.c. demagnetization  
 (from Pearce, 1967)

Treatment (oe, peak)	$\bar{D}$	$\bar{I}$	N	k	$\alpha_{95}$
Before treatment	31.8	70.6	6	336	9.9
108 (except HH 16aI)*	42.5	70.7	5	404	9.0
243 (except TH 2bI)*	36.4	72.6	5	486	8.2
324 (except TH 2bI)*	23.8	75.9	5	176	13.6

The NRM measurements included 4 and 2 specimens from Henley Harbour and Table Head, respectively. (See Fig. A4.1)

Symbols as used in Chapters 3-6, with unit weight (N = 1) given to specimens.

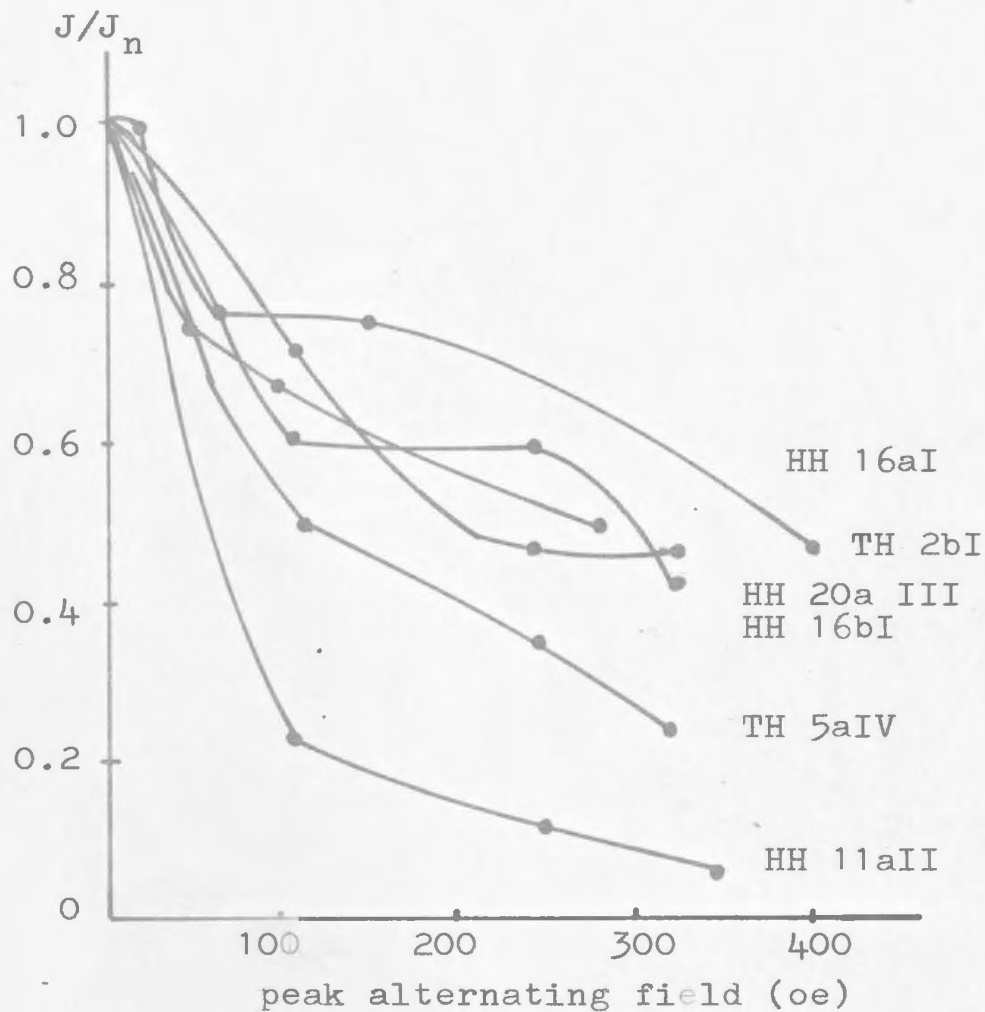


Fig A4.1. Variation of normalized intensity of magnetization with the demagnetizing field for basalt specimens from Henley Harbour and Table Head

(from Pearce, 1967; see also Table A4.2)

$J_n$  = Intensity before treatment (NRM)

APPENDIX 5MAGNETIC SHIELDING

A can made of three concentric cylindrical shields of the highly permeable materials "Netic" and "Co-Netic" (Fig. A5.1) was used to store the specimens between steps in the a.c. or thermal demagnetization treatment. This was to prevent the acquisition in the laboratory of short-period viscous components that could mask the actual remanence obtained by the treatment. The hazards of adding viscous components to a specimen just after demagnetization in the laboratory, even when the apparatus itself is entirely non-inductive, have been noted by several authors (Roy et al., 1967) and were also observed at the beginning of the present study before magnetic shielding had been acquired. As expected, this problem was particularly serious in the case of specimens having appreciable components in the low-coercivity range, and in some cases where such components dominated the resultant moment, the direction of the latter was observed to follow the laboratory field through large angles in the time of a few hours or even less (e.g. KH 17b, KH 24cII).

The shielding cans were manufactured by Perfection Mica Co., Chicago, Ill. from three cylindrical cans of decreasing size, mounted coaxially (Fig. A5.1) and made of "Netic" (outer) and "Co-Netic" (middle and inner) material. Each can had a separate, removable cover. For  $n$  cans, the "shielding factor"  $S$  which measures the attenuation of a uniform external field by the can assembly is a function of the can radii, permeabilities, and thicknesses, and is proportional to the product of the  $n$  permeability values and also of

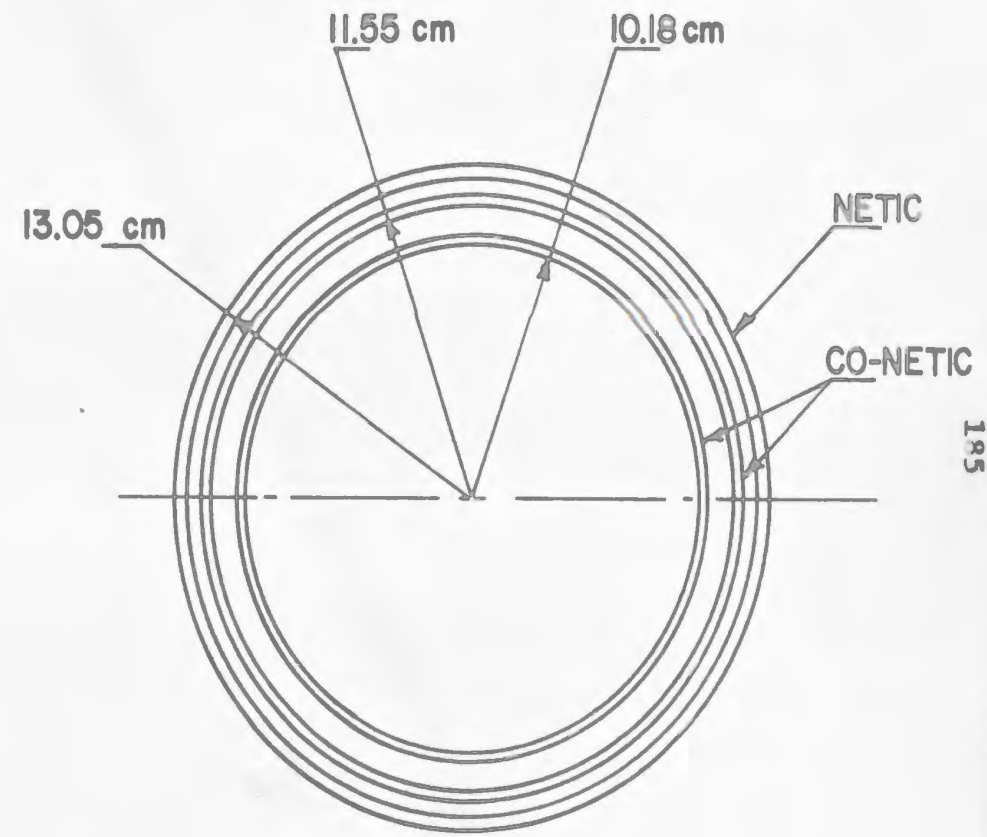
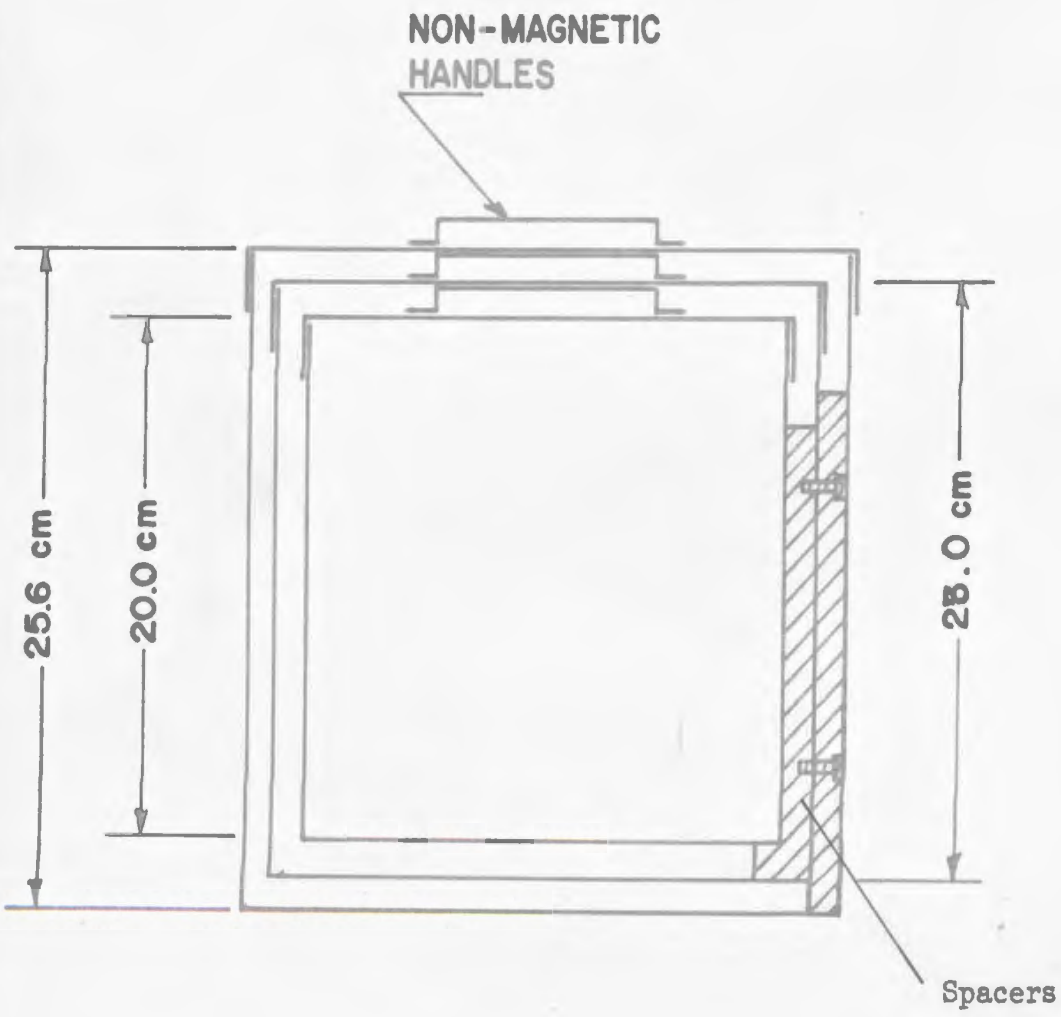


Fig A5.1. Cross section of three stage spherical shield

the  $n$  thicknesses, and inversely proportional to the product of the  $n$  radii. The shielding factor is given by

$$S = \frac{H_e}{H_i} = S_1 S_2 \left[ 1 - \left( \frac{R_2}{R_1} \right)^3 \right] S_3 \left[ 1 - \left( \frac{R_3}{R_2} \right)^3 \right] \dots S_n \left[ 1 - \left( \frac{R_n}{R_{n-1}} \right)^3 \right] \quad A5.1$$

and the "individual stage shielding factor"  $S_j$ , is given by

$$S_j = \frac{2\mu_j t_j}{3R_j} \quad (j = 1, 2, \dots, n) \quad (A5.2)$$

where for the  $j$ th shell,

$\mu_j$  = magnetic permeability (cgs units)

$t_j$  = thickness of the material

$R_j$  = radius of the shell

$H_e$  = uniform external field

$H_i$  = internal field within the inner most shell

The definitions of "shielding factor",  $S$  and  $S_j$ , above, are taken from Patton (1967), who made a critical study of magnetic shielding with emphasis on the reduction of disturbing fields to a low level within the working space used for paleomagnetic research.

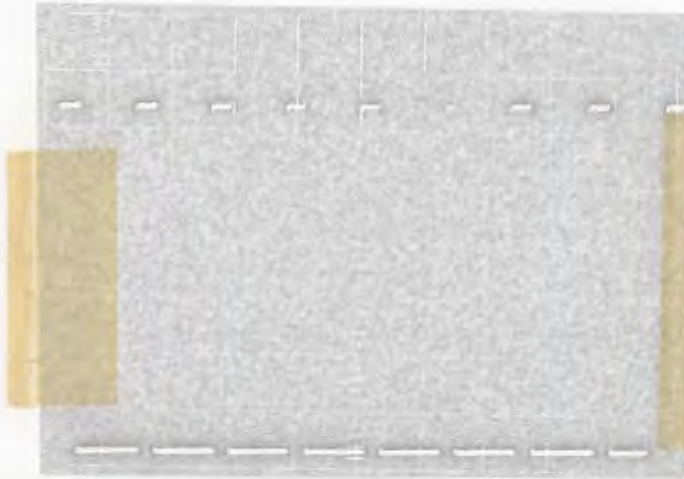
The field reduction obtained by the can assembly was estimated with the aid of the fluxgate elements described in Chapter 4, the total field ( $H_e$ ) in the region to be occupied by the can assembly being obtained first. The cans were then placed into the external field in such a position that the axis of the concentric shields was parallel to the direction of  $H_e$ , and the internal field ( $H_i$ ) was measured along the axis of the assembly, first with all cans being open, then after

successively closing the inner can, the inner and middle cans, and finally all three cans. In actual operation the lids fit closely upon the respective shields, but in order to admit the fluxgate leads into the assembly during  $H_i$  measurement the lids had to be raised somewhat; hence the attenuation achieved in actual operation may exceed slightly that obtained in the present calibration, with the lids imperfectly closed.

With only the inner can capped with a lid, inside fields ( $H_i$ ) ranging from  $10 \gamma$  to  $35 \gamma$  were obtained in three separate measurements [Figs. A5.2 - (b), (c), (d)] with two different fluxgate elements. The large difference in these values, which correspond to a range  $S = 1.4 \times 10^3$  to  $5.0 \times 10^3$  for various measurements, is probably due to the difficulty of (a) reproducing the fluxgate position in the inner can when the can is closed; (b) measuring the noise. The lowest field values obtained from the patterns in Figs. [A5.2 (e), (f) and (g), (h)] correspond to less than  $5\gamma$  and  $6\gamma$  respectively for the two fluxgate elements, and are here quoted as  $H_i \leq 5-6\gamma$ ; which corresponds to a range  $S = 0.8 \times 10^4$  to  $1.0 \times 10^4$ .

The theoretical "shielding factor" calculated from equation A5.1 and A5.2, using the known values of radius, thickness, and permeability given in Table A5.1, was  $S = 1.29 \times 10^5$ . Comparison with the estimated value of  $S$  from the above experiments ( $S \sim 1 \times 10^4$ ) shows the attenuation of which the three-stage shield is theoretically capable to be one order of magnitude greater than the experimentally estimated attenuation.

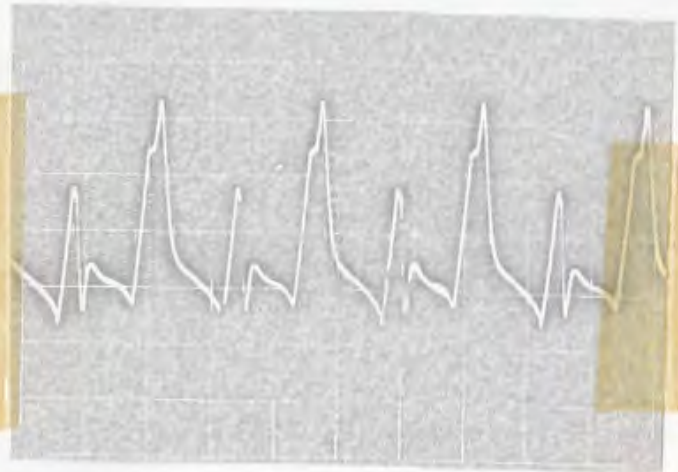
Figure A5.2. Oscilloscope patterns from fluxgate measurement of field attenuation by magnetic shielding assembly (all cases: 1 Volt =  $50\gamma$ )



(a) Total external field (no cans present: Probe 1)

$$H_e = 5 \times 10^4$$

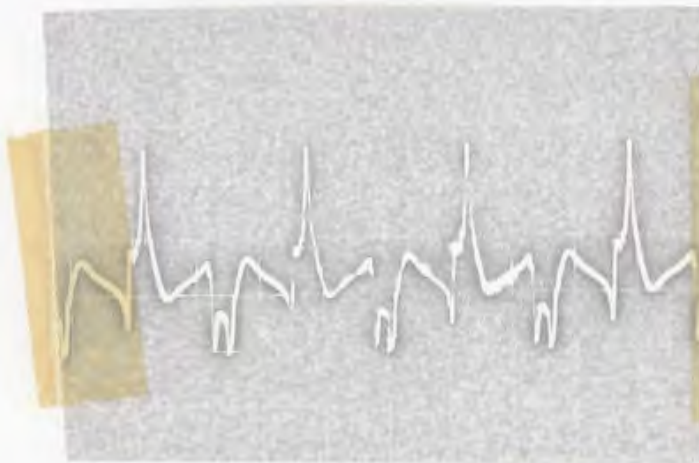
Scale: 0.1 V/cm



(b) Inside field, with inner lid attached only. (Probe 1)

Scale: 0.05 V/cm

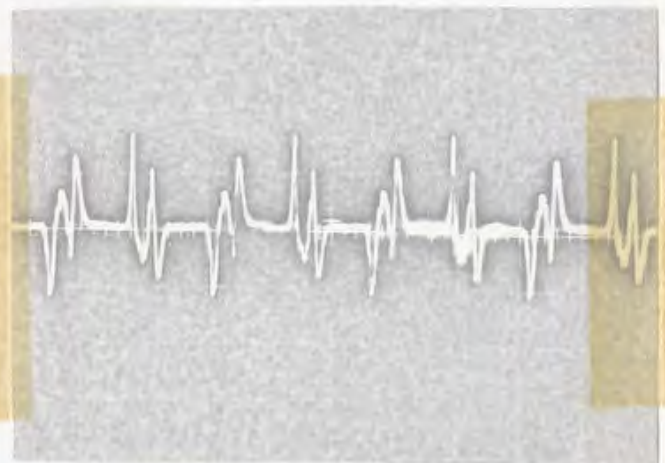
$$H_i = 10\gamma$$



(c) Inside field, with inner lid attached only (Probe 1)

Scale: 0.2 V/cm

$$H_i = 35\gamma$$

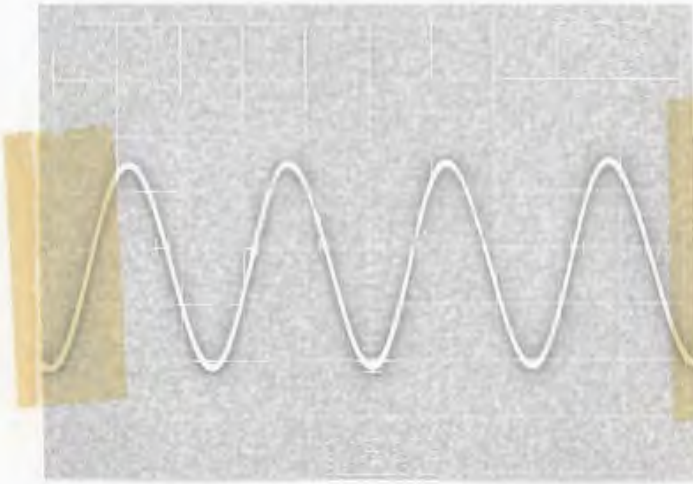


(d) Inside field, with inner lid attached only (Probe 2)

Scale: 0.2 V/cm

$$H_i = 30\gamma$$

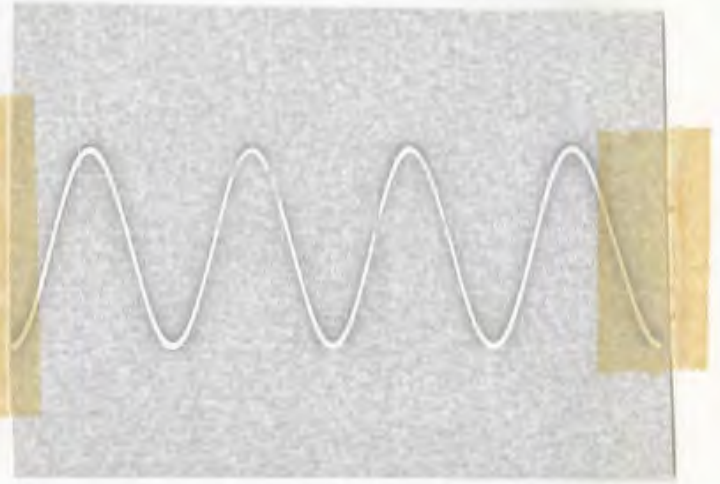
Figure A5.2. (Continued)



(e) Inside field, with inner and intermediate lids attached only (Probe 1)

Vertical scale: 0.01 V/cm

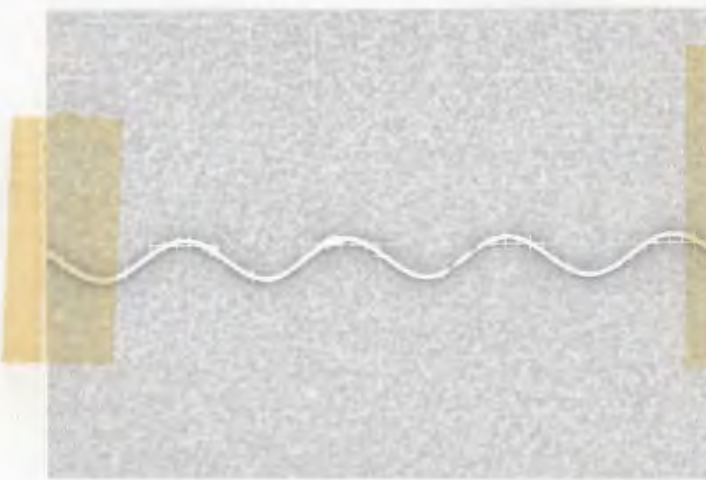
$$H_1 = 5\gamma$$



(f) Inside field, with all lids attached (Probe 1)

Vertical scale: 0.01 V/cm

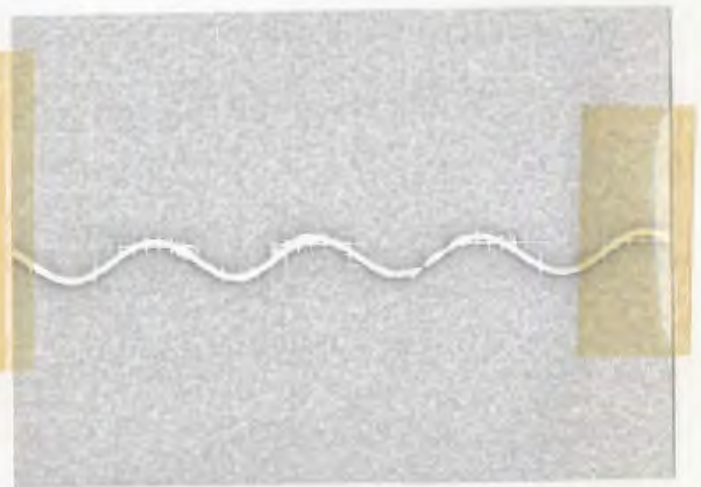
$$H_1 \leq 5\gamma$$



(g) Inside field, with inner and intermediate lids attached only (Probe 2)

Vertical scale: 0.2 V/cm

$$H_1 \leq 6\gamma$$



(h) Inside field, with all lids attached (Probe 2)

Vertical scale: 0.2 V/cm

$$H_1 \leq 6\gamma$$

TABLE A5.1

Dimensions and physical data of the  
cylindrical shields

Parameter	Inner (1)	Middle (2)	Outer (3)
Radius (cm)	10.05	11.55	13.05
Thickness (cm)	0.086	0.127	0.166
Permeability* (cgs units x 10 <sup>3</sup> )	23.8	23.8	6.67

\*The permeability values are quoted from the manual: "Netic and Co-Netic magnetic shielding manual": Manual 101-122; p.20, 32p.

ACKNOWLEDGEMENTS

I wish to acknowledge with thanks the help received from the following people in the course of this work:

Professor Ernst Deutsch, for his guidance, frequent help and suggestions, constructive criticism of the results, and constant encouragement, and for providing the rock samples; Drs. Sithapati Rao and Bruce May, for their encouragement and helpful suggestions, particularly during the installation and calibration of the oven;

Professor Marshall Kay of Columbia University, New York, for helpful, stimulating discussions, and for providing details of the Killary Harbour sampling; Dr. John Dewey of Cambridge University, for much useful geological information on western Ireland; Professor Norman Watkins of Florida State University, Tallahassee, who provided the polished-section analyses;

Mr. Ernest Kenney for his assistance during installation and calibration of the astatic magnetometer and the oven; Messrs. John Royle and Roy MacLellan of Technical Services Department for their help during the construction and calibration of the oven; Messrs. Richard Seary and Robert Kennedy, for considerable summer assistance in measuring and preparing rock specimens; Messrs. Wesley Drodge and Adrian Walsh, who prepared specimens and gave much general assistance; Mr. Viswasundara Rao, for his constant encouragement, for constructive criticism and helpful suggestions; Messrs. William Higgins and Ross Tucker, who carried out the photographic and drafting work for the thesis; Mrs. Lynda Strong, who typed the thesis.

Finally, I am much indebted to the Physics Department and Memorial University of Newfoundland for financial support since 1968, and to the Geological Survey of Canada and National Research Council of Canada (Grants 14-65 and A-1946 to Prof. E. R. Deutsch) for support during 1966-68.

REFERENCES

- As, J.A., and Zijderfeld, J.D.A., 1958, Magnetic cleaning of rocks in paleomagnetic research: *Geophys. J.*, 1, p. 308-319.
- Black, R.F., 1964, Paleomagnetic support of the theory of rotation of the western part of the island of Newfoundland: *Nature*, v. 202, no. 4936, p. 945-948.
- Blackett, P.M.S., 1956, *Lectures on rock magnetism: The Weizman Science press of Israel, Jerusalem.*
- Blackett, P.M.S., 1961, Comparison of ancient climates with the ancient latitudes deduced from rock magnetic measurements: *Proc. Roy. Soc., A*, v. 263, p. 1-30.
- Brynjolfsson, A., 1957, Studies of remanent magnetism and viscous magnetism in the basalts of Iceland: *Phil. Mag. Supp. Adv. Phys.*, v. 6, p. 247-254.
- Bullard, Edward, Everett, J.E., and Smith A.G., 1965, The fit of the continents around the Atlantic: *Phil. Trans. Roy. Soc. London, A*, v. 258, p. 41-51.
- Bucha, Vaclav, 1965, Results of the paleomagnetic research on rocks of Pre-Cambrian and lower Paleozoic age in Czechoslovakia: *Jour. Geomag. Goeelec.*, v. 17, no. 3-4, p. 435-444.
- Carey, S.W., 1958, The tectonic approach to continental drift, p. 177-355, in continental drift - a symposium: Hobert, Univ. Tasmania, 355 p.
- Chamalaun, F.H., 1963, Thermal demagnetization of red sediments: Ph.D. thesis, Univ. Durham, 227 p.
- Chamalaun, F.H., 1964, Origin of the Secondary magnetization of the Old Red Sandstone of the Anglo-Welsh Cuvette: *J. Geophy. Res.*, v. 69, p. 4327-4337.
- Chamalaun, F.H., and Creer, K.M., 1964, Thermal demagnetization studies on the Old Red Sandstone of the Anglo-Welsh Cuvette: *Jour. Geoph. Res.*, v. 69, no. 8, p. 1607-1616.
- Christie, A.M., 1951, Geology of the southern coast of Labrador from Forteau Bay to Cape Porcupine, Newfoundland: *Geol. Survey Can.*, Paper 51-13, 19 p.
- Cox, Allan, and Doell, Richard R., 1960, Review of paleomagnetism: *Geol. Soc. America Bull.*, v. 71, p. 645-768.
- Clifford, P.M., 1965, Paleozoic flood basalts in northern Newfoundland and Labrador: *Can. J. Earth Sci.*, V.2, p. 183-187.

- Cox, A., and Doell, R. R., 1961, Paleomagnetic evidence relevant to a change in the Earth's radius: *Nature*, v. 189, no. 4758, p. 47-
- Creer, K.M., 1959, A.C. demagnetization of unstable Keuper Marls: from S.W. England; *Geophy. J.*, v. 2, p. 261-275.
- Creer, K.M., 1967, Measuring methods with the astatic magnetometer p. 172-191; in Collinson et al., (eds), 1967, methods in paleomagnetism, Amsterdam, Elsevier Publ. Co., 609 p.
- Deutsch, E.R., Roy, J.L., and Murty, G.S., 1967, An improved astatic magnetometer for paleomagnetism: *Can. Jour. Earth Sci.*, v. 4, p. 1270-1273.
- Deutsch, E.R., Rao, P.S., 1966, unpublished field notes.
- Deutsch, E.R., 1969, Paleomagnetism and North Atlantic paleogeography *Amer. Assoc. Petrol.geol.* (in press).
- Dewey, John Frederick, 1963, The Lower Paleozoic stratigraphy of central Murrisk, County Mayo, Ireland, and the evolution of the south Mayo trough: *Quart. Jour. Geol. Soc. London*, v. 119, p. 313-344.
- Doell, R.R., and Cox, A., 1964, Analysis of alternating field demagnetization equipment: Contribution 1964 NATO conference on paleomagnetism, Newcastle, England.
- Douglas, G.V., 1953, Notes on localities visited on the Labrador coast in 1946 and 1947: *Geol. Surv. Can.*, paper 53-1.
- Du Bois, P.M., 1959, Paleomagnetism and the rotation of Newfoundland *Nature*, v. 184, no. 4688, p. B.A. 63-64.
- Eade, K., 1962, Geology, Battle Harbour-Cartwright map area, coast of Labrador, Newfoundland: *Geol. Surv. Can.*, Map 22-1962.
- Egyed, L., 1956, A new theory of the internal constitution of the Earth and its geological and geophysical consequences: *Acta Geol. Acad. Sci. Hung.*, v. 4, p. 43-83.
- Fisher, R.A., 1953, Dispersion on a sphere; *Proc. Roy. Soc. London*, A, v. 217, p. 295-306.
- Graham, J.W., 1949, The stability and significance of magnetism in sedimentary rocks: *Jour. Geoph. Res.*, v. 54, p. 131-167.
- Heezen, B.C., 1960, The rift in the ocean floor: *Scient. American*, v. 203, no. 4, p. 98-110.
- Hide, Raymond, 1967, Motions of the Earth's core and mantle, and variations of the main geomagnetic field: *Science*, v. 157, no. 3784, p. 55-56.

- Holmes, Arthur, 1965, Principles of physical geology: revised ed., London, Thomas Nelson, 1288 p.
- Irving, E., 1964, Paleomagnetism and its application to geological and geophysical problems: New York, John Wiley & Sons, Inc., 399 p.
- Irving, E., Stott, P.M., and Ward, M.A., 1961a, Demagnetization of igneous rocks by alternating magnetic fields: Phil. Mag., v. 6, p. 225-241.
- Irving, E., Robertson, W.A., Stott, P.M., Tarling, D.H., and Ward, M.A., 1961b, Treatment of partially stable sedimentary rocks showing planar distribution of directions of magnetization; J. Geophys. Res., v. 66, p. 1927-33.
- Irving, E., and Opdyke, N.D., 1965, The paleomagnetism of the Bloomsburg Red Beds and its possible application to the tectonic history of the Appalachians: Geophys. J. Roy. Astro. Soc., v. 9, no. 2, 3, p. 153-167.
- Johnson, E.A., Murphy, T., and Torreson, O.W., 1948, Pre-history of the Earth's magnetic field: Terr. Magn. Atmos. Elec., v. 53, p. 349-372.
- Jones, D.L., and McElhinny, M.W., 1967, Stratigraphic interpretation of paleomagnetic measurements on the Waterberg Red Beds of South Africa: Jour. Geophys. Res., v. 72, no. 16, p. 4171-4180.
- Khramov, A.N., Rodionov, V.P., and Komissarova, R.A., 1965, New data on the paleozoic history of the geomagnetic field in the U.S.S.R., p. 206-213 in The present and past of the geomagnetic field: Nauka Press, Moscow (Engl. Transl., Defence Research Board, Canada no. T460R, Oct. 1966).
- Koenigsberger, J.G., 1930, Grossenverhaltnis von remanentem zu induziertem Magnetismus in Gesteinen; Grosse und Richtung des remanenten Magnetismus: Z.F. Geophys. v. 6, p. 190-207.
- Larochelle, A., 1967, A reexamination of certain statistical methods in paleomagnetism: Geol. Surv. Can., paper 67-18.
- Larochelle, A., 1968, L'application de la statistique au paleomagnetisme: Geol. Surv. Can., paper 68-59, 19 p.
- Lin'kova, T.I., 1961, Laboratory studies of the natural remanent magnetization of direct and reverse magnetized Devonian rocks: Akad. Nauk. SSSR Izv. Geophys. Ser., p. 91-95.
- Maurain, C., 1901, Proprietes des depots electrolytiques de fer obtenus dans un champ magnetique: J. Physique, 10 (3rd ser.), p. 123-125.
- McElhinny, M.W., 1964, Statistical significance of the fold test in paleomagnetism: Geophys. J., v. 8, p. 338-340.

- McElhinny, M.W., 1966, An improved method for demagnetizing rocks in alternating magnetic fields: *Geophy. J. Roy. Ast. Soc.*, v. 10, p. 369-374.
- McElhinny, M.W. and Gough, D.I., 1963, The paleomagnetism of the Great dyke of Southern Rhodesia,: *Geophys. J.*, v. 7, p. 287-303.
- Melloni, M., 1853, L'aimantation des laves de l'Etna et l'orientation du champ terrestre en Sicile du XVII<sup>e</sup> au XVIII<sup>e</sup> siecle, *Ann. Phys.*, 4, 5 - 162.
- McKerrow, W.S. and Campbell, C.J., 1960, The stratigraphy and structure of the Lower Paleozoic rocks of north-west Galway: *Sci. Proc. Roy. Dublin Soc. Ser. A 1*, p. 27-51.
- McNish, A.G., and Johnson, E.A., 1938, Magnetization of unmetamorphosed varves and marine sediments: *Terr. Magn. Atmos. Elect.*, 53, p. 349-360.
- Murty, G.S., 1966, Design and calibration of an astatic magnetometer and the remanent magnetization of some Newfoundland rocks: M.Sc. Thesis, Memorial University of Newfoundland. 177 p.
- Nagata, T., 1961, Rock magnetism (second revised edition), Maruzen Co. Ltd., Tokyo, 350 p.
- Nairn, A.E.M., Frost, D.V. and Light, B.G., 1959, Paleomagnetism of certain rocks from Newfoundland: *Nature*, v. 183, no. 4661, p. 596-597.
- Nesbitt, Jill D., 1967, Paleomagnetic evidence for the Ordovician geomagnetic pole position: *Nature*, v. 216, no. 5110, p. 49-50.
- Opdyke, N.D., 1962, Paleoclimatology and continental drift, . in Runcorn, S.K. (ed), *Continental drift*: New York, Academic press, 338 p.
- Opdyke, N.D., 1964, The paleomagnetism of the Permian Red Beds of Southwest Tanganyika: *Jour. Geophy. Res.*, v. 69, no. 12, p. 2477-2486.
- Patton, B.J., 1967, Magnetic shielding p. 568-588: in Collinson et al., 1967 (eds), *methods in paleomagnetism*, Amsterdam, Elsevier Publ. Co., 609 p.
- Pearce, G.W., 1967, Design and calibration of apparatus for the alternating field demagnetization of rocks: M.Sc. Thesis, Memorial University of Newfoundland, 134 p.
- Petrova, G.N., 1961, Various laboratory methods of determining the geomagnetic stability of rocks: *Akad. Nauk. SSSR Izv. Geophy. Ser.* p. 1585-1598.

- Petrova, G.N. and Koroleva, V.A., 1959, Determination of magnetic stability of rocks under laboratory condition: Akad. Nauk. SSSR Izv. Geophy. Ser., p. 703-709.
- Rimbert, F., 1956, Sur la Desaimantation Action de Champs Magnetique Alternatifs, de la Magnetite et da Sesquioxyde de Ferr: Acad. Sci. (Paris); Comptes Rendus; Vol. 242, p. 890-893.
- Robertson, W.A., Roy, J.L. and Park, J.K., 1968, Magnetization of the Perry formation of New Brunswick and the rotation of Newfoundland: Can. Jour. Earth Sci., 5, p. 1175-1181.
- Rodionov, V.P., 1966, Dipole character of the geomagnetic field in the Late Cambrian and the Ordovician in the south of the Siberian platform: Geologiya i Geofizika, 1966, no. 1, p. 94-101 (Engl. Transl., Defence Research Board, Canada, no. T460R, Oct. 1966).
- Roy, J.L., 1963, The measurement of the magnetic properties of rocks specimens; Publ. Dominion Obs., Ottawa, no. 27, p. 420-439.
- Roy, J.L., N.D. Opdyke, and E. Irving, 1967, Further paleomagnetic results from the Bloomsburg formation: Jour. Geophy. Res., v. 72, no. 20, p. 5075-5086.
- Runcorn, S.K., 1965, Paleomagnetic comparisons between Europe and North America: Phil. Trans. Roy. Soc. London, A, v. 258, p. 1-11.
- Stanton, W.I., 1960, The Lower Paleozoic rocks of south-west Murrisk, Ireland: Quart. J. Geol. Soc. London. v. 116, p. 269-291.
- Stephens, M.A., 1964, The testing of unit vectors for randomness: Jour. Amer. Statis. Assoc., v. 59, no. 305, p. 160-167.
- Storetvedt, K.M., 1968, On remagnetization problems in paleomagnetism: Earth and Planetary Sci. Letters v. 4, p. 107-112.
- Thellier, E., 1938, Thesis: University of Paris.
- Thellier, E., and Rimbert, F., 1955, Sur l'utilisation en paleomagnetisme de la desaimantation par champs alternatifs: Comptes Rendus, Acad. Sci., Paris, v. 240, p. 1404-1406.
- Taylor, F.B., 1910, Bearing the Tertiary Mountain Belts on the origin of the Earth's plan. Bull. Geol. Soc. America; Vol. 21, p. 179-226.
- Vincenz, S.A., 1968, Phenomenon of partial self reversal in Keweenaw rocks: 1. Magnetization of Portage Lake lavas: Jour. Geophy. Res., v. 73, no. 8, p. 2729-2752.
- Wanless, R.K., Stevens, R.D., Lachance, G.R., and Rimsaite, R.Y.H., 1965, Age determinations and geological studies; Part 1-Isotopic ages, report 5: Geol. Surv. Canada: paper 64-17 (part 1), p. 111-112, 126, p.

- Ward, M.A., 1963, On detecting changes in the Earth's radius: *Geoph. Jour.*, v. 8, p. 217-225.
- Watkins, N.D., Haggerty, S.E., 1965, Some magnetic properties and the possible petrogenetic significance of oxidized zones in an Icelandic olivine basalt: *Nature* v. 206, no. 4986, p. 797-800.
- Watson, G.S., 1956, Analysis of dispersion on a sphere: *Mont. Notices Roy. Astro. Soc., Geophy. Suppl.*, v. 7, no. 4, p. 153.
- Wegener, Alfred, 1929, *Die Entstehung der Kontinente und Ozeane*: 4th revised ed., Braunschweig, F. Vieweg & Sons, 231 p. (Engl. Transl. by John Biram, 1966, *The origin of continents and oceans*: New York, Dover Publications, Inc., 246 p).
- Wells, John M., and Verhoogen, John, 1967, Late Paleozoic paleomagnetic poles and the opening of the Atlantic ocean: *Jour. Geoph. Res.*, v. 72, no. 6, p. 1777-1781.
- Wilson, J.T., 1966, Did the Atlantic close and then re-open?: *Nature*, v. 211, no. 5050, p. 676-681.
- Wilson, R.L., 1961, Paleomagnetism in Northern Ireland; Part I, the thermal demagnetization of natural magnetic moments in rocks: *Geoph. J. Roy. Astro. Soc.*, v. 5, no. 1, p. 45-58.
- Wilson, R.L., 1962, An instrument for measuring vector magnetization at high temperatures, *Geophy. J.*, v. 7, p. 125-130.
- Wilson, R.L. and Everitt, C.W.F., 1963, Thermal demagnetization of some Carboniferous lavas for paleomagnetic purposes: *Geophy. J.*, v. 8, p. 149-164.
- Wilson, R.L., Haggerty, S.E. and Watkins, N.D., 1968, Variation of paleomagnetic stability and other parameters in a vertical traverse of a Single Icelandic Lava: *Geophy. J. Roy. Astro. Soc.*, v. 16, p. 79-96.
- Wilson, R.L., Watkins, N.D., 1967, Correlation of Petrology and natural magnetic polarity in Columbia Plateau basalts: *Geophy. J. R. Astr. Soc.* v. 12, p. 405-424.







